AD-A117 979 HARRIS CORP MELBOURNE FL GOVERNMENT INFORMATION SYST--ETC F/G 9/5
FINITE ELEMENT ANALYSIS OF MICROELECTRONIC PACKAGES.(U)
MAY 82 J R SOUTHLAND, V R BEATTY F30602-81-C-0083
UNCLASSIFIED RADC-TR-82-133 NL

1 OF 3
AD A
117979

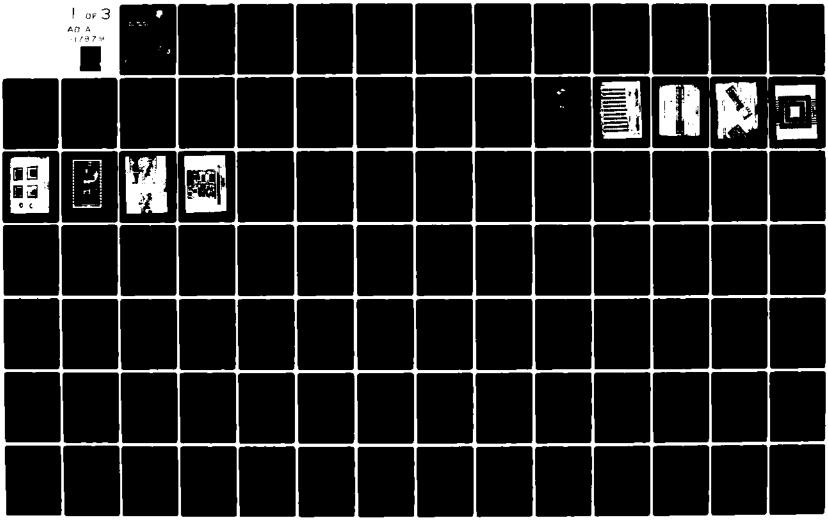

RADC-TR-82-133
Final Technical Report
May 1982

FINITE ELEMENT ANALYSIS OF MICROELECTRONIC PACKAGES

Harris Corporation

J.R. Southland, V.R. Beatty and W.J. Vitaliano

APPROVED FOR PUBLIC RELEASE; DISTRIBUTION UNLIMITED

ROME AIR DEVELOPMENT CENTER
Air Force Systems Command
Griffiss Air Force Base, NY 13441

This report has been reviewed by the RADC Public Affairs Office (PA) and is releasable to the National Technical Information Service (NTIS). At NTIS it will be releasable to the general public, including foreign nations.

RADC-TR-82-133 has been reviewed and is approved for publication.

APPROVED: William J. Bocchi

WILLIAM J. BOCCHI
Project Engineer

APPROVED: David C. Luke

DAVID C. LUKE, Colonel, USAF
Chief, Reliability & Compatibility Division

FOR THE COMMANDER: John P. Huss

JOHN P. HUSS
Acting Chief, Plans Office

UNCLASSIFIED

SECURITY CLASSIFICATION OF THIS PAGE (When Data Entered)

REPORT DOCUMENTATION PAGE		READ INSTRUCTIONS BEFORE COMPLETING FORM
1. REPORT NUMBER RADC-TR-82-133	2. GOVT ACCESSION NO. AD-A117979	3. RECIPIENT'S CATALOG NUMBER
4. TITLE (and Subtitle) FINITE ELEMENT ANALYSIS OF MICROELECTRONIC PACKAGES		5. TYPE OF REPORT & PERIOD COVERED Final Technical Report
		6. PERFORMING ORG. REPORT NUMBER N/A
7. AUTHOR(s) J. R. Southland V. R. Beatty W. J. Vitaliano		8. CONTRACT OR GRANT NUMBER(s) F30602-81-C-0083
9. PERFORMING ORGANIZATION NAME AND ADDRESS Harris Corporation Government Information Systems Division P O Box 37, Melbourne FL 32901		10. PROGRAM ELEMENT, PROJECT, TASK AREA & WORK UNIT NUMBERS 62702F 23380266
11. CONTROLLING OFFICE NAME AND ADDRESS Rome Air Development Center (RBES) Griffiss AFB NY 13441		12. REPORT DATE May 1982
		13. NUMBER OF PAGES 222
14. MONITORING AGENCY NAME & ADDRESS(if different from Controlling Office) Same		15. SECURITY CLASS. (of this report) UNCLASSIFIED
		15a. DECLASSIFICATION/DOWNGRADING SCHEDULE N/A

16. DISTRIBUTION STATEMENT (of this Report)

Approved for public release; distribution unlimited.

17. DISTRIBUTION STATEMENT (of the abstract entered in Block 20, if different from Report)

Same

18. SUPPLEMENTARY NOTES

RADC Project Engineer: William J. Bocchi (RBES)

19. KEY WORDS (Continue on reverse side if necessary and identify by block number)

Finite Element Analysis	Finite Element Computer Programs
Microelectronic Package Problems	Reliability improvements
Structural Analysis	Hybrid lid seal integrity
Stress Analysis	Cost Savings by Analysis
Heat Transfer Analysis	Exposing failure modes

20. ABSTRACT (Continue on reverse side if necessary and identify by block number)

New and innovative methods are being applied to the analysis of the mechanical integrity of microelectronic packages. This study resulted in 1) a summary of commercially available finite element computer programs for both structural and thermal analyses, 2) a categorization of microelectronic problems that can be evaluated using analytical techniques, 3) assessment of applicable analysis techniques, 4) cost comparisons of exposing failure modes by the use of computer analysis rather than

physical test, and 4) to provide engineers with a base of technical knowledge necessary for the application of the finite element technique to solve microelectronic reliability problems.

TABLE OF CONTENTS

TABLE OF CONTENTS - Continued

TABLE OF CONTENTS - Continued

LIST OF FIGURES

LIST OF FIGURES - Continued

LIST OF TABLES

ACKNOWLEDGEMENTS

This report is based on the contributions of both individual technologists and the microelectronic package industry.

We wish to express our appreciation to the following companies and individuals for their contributions, openness, and assistance during this program.

Tektronix Inc.
Martin Marietta
Circuit Technology Inc.
Airpax Inc.
Tekform Products Company
Isotronics
E-Systems
Litton Guidance & Control Systems
General Electric
General Dynamics
Microelectronics Engineering Corporation
AEL
RCA
Roger E. Settle

We also wish to recognize the technical contribution of:

Mr. Joseph Richiuso
Mr. Eric D. Yost
Mr. John W. Shipley

We would like to personally thank Mrs. Eunice Search for typing this final report. She deserves our special gratitude for providing typing support and patience during the many iterations.

William Bocchi, RADC, recognized the importance of this program to both the military and the industry and provided the leadership to initiate this program.

SUMMARY

This study was initiated to provide documentation and guidelines for the application of finite element analysis (FEA) to perform mechanical and thermal analyses of microelectronic packages. The documentation includes an investigation of the use of mechanical engineering analyses as a viable means of assessing the reliability of microelectronics devices. The guidelines show how to apply FEA to electronic devices.

In the finite element technique, a complex structure is modeled using an assemblage of finite elements (rods, beams, plates, or solids). During the finite element analysis values of a field quantity (for example, displacement) are estimated throughout the element by the use of interpolation functions. The stiffness matrix for each element is then obtained by applying one of several possible energy principles. The FEA computer program then obtains the stiffness matrix for the entire structure by properly assembling the stiffness matrices of all the elements using energy principles and/or constitutive laws. Inputting nodal forces and nodal boundary conditions results in an output of the field variable at each node.

The technical approach to this study was to: 1) perform a technical assessment to identify microelectronic package problems and computer programs, 2) evaluate the computer programs and perform sample calculations, 3) perform finite element analysis on a critical problem, and 4) instrument and test an empty hybrid package for comparison to FEA and closed-form analyses to assist in preparing guidelines for analysis.

This study has shown that although FEA is primarily a tool for designers of large complex structures, a great potential exists if applied to microelectronic packages. By using FEA for early warnings of potential failures, the

mechanical engineer can play a significant role in assuring or improving the reliability of microelectronic systems. The most frequent microelectronic package problems were hermeticity, broken or corroded internal wires, and broken wirebonds. The survey showed that most companies do not use FEA for microelectronic packages and that considerable cost savings can be realized by substituting FEA for MIL-STD-883 screening tests.

The computer program evaluation resulted in the following recommended programs for microelectronics package analysis: ABAQUS, ANSYS, NISA, and STARDYNE. STARDYNE was found to be the best program for analyzing the majority of microelectronic problems.

Recommended future work related to this report includes; understanding the sealing of large custom packages, inspection criteria for hermetic chip carrier solder joints, selective MIL-STD-883 qualification by analysis, work in nonlinear analysis, and a pre and postprocessor computer program study linked to CAD/CAM activities.

The reader is referred to the text of the report for a more detailed discussion of the study. Each section is concluded with a detailed summary, while a condensed section at the end of the report presents all of the conclusions and recommendations.

It is refreshing that RADC took the initiative to sponsor a study of this nature. It is only by the knowledge gained in this type of study that we can advance the state-of-the-art for mechnical design and analysis.

1.0 INTRODUCTION

The microelectronic package is one of the key elements in electronic ecuipment reliability a d cost. However, little information is available for assessing the overall acceptability of the various microelectronic packages in the early design stages. The intent of this study is to evaluate existing finite element computer programs to be used in assessing the reliability of microelectronic devices.

2.0 PROGRAM DESCRIPTION

2.1 Background

Finite element analysis (FEA) can be compared to a puzzle where the structure or picture is broken down into small non-uniform parts. With a puzzle, one must assemble the individual pieces to reconstruct the picture. In finite element analysis the structure is assembled using the rules of structural mechanics: ecuilibrium of forces and continuity of displacements.

FEA has been applied to large complex structures as a mechanical and structural analytical tool. These same FEA technicues can be applied to the evaluation of microelectronic packages for structural and thermal integrity when exposed to military specifications such as MIL-STD-883 and MIL-STD-810.

2.2 Program Objectives

The objective of the program was to evaluate new and innovative analytical methods to ensure the mechanical integrity of microelectronics packages used for Hybrid Integrated Circuits (HIC), Microwave Integrated Circuits (MIC), and Stripline Microwave Circuits (SMC). The mechanical computer analysis could be applicable to HIC, MIC, and SMC, as well as any microelectronic package. The data generated by computer analysis will be compared to the data generated by physical environmental testing of a particular hybrid package. The programs used for the analysis have adaptability to the various thermal and mechanical properties of the package types.

Below is a concise summary of the study objectives:

- o Investigate the feasibility of exposing failure modes by use of computer analyses of package types rather than physical testing.
- o Evaluate feasibility of reducing cost by performing FEA as an acceptable alternative to MIL-STD-883, Group D package evaluation.
- o Conduct a survey of commercially available finite element and thermal analysis programs.
- o Generate a set of guidelines documenting the practical use of some of these programs.
- o Compile a list of microelectronic problems that can be evaluated using mechanical analyses.
- o Perform a solution of a critical problem by the finite element method, compared to the closed-form method, with correlation to test results.

The next section outlines the program in chronological order of the various activities.

2.3 Technical Approach

Below, in outline form, is a brief description of the entire program.

Phase 1: Technical Assessment

- o Identify microelectronic package problems that could be solved by analytical methods.
- o Determine the extent to which mechanical and thermal analyses of microelectronic packages are performed by industry.

Phase 2: Analysis Methods

- o Compare and assess general purpose public domain finite element computer programs.
- o Compare finite element methods with closed-form methods.

- Perform sample finite element analyses on typical problems.

Phase 3: Critical Problem Analysis

- Select a critical problem and appropriate finite element computer program to show how a finite element analysis can solve a useful problem, how it compares with a closed-form solution, how it compares with test results, and as a demonstration of the application of the guidelines.

Phase 4: Correlation to Test Data

- Instrument and test an empty hybrid package
- Prepare guidelines for finite element analyses of microelectronic packages.

3.0 TECHNICAL ASSESSMENT (PHASE 1)

3.1 Introduction

A technical assessment was deemed necessary to determine which microelectronic package problems could be solved by analytical methods, and the extent to which mechanical and thermal analyses of microelectronics are performed by industry. Included in this survey was an assessment of computer programs, closed form techniques, and correlation to test data.

The technical assessment consisted of sending some 43 questionnaires to representative microelectronics manufacturers and users. Several government agencies were also polled. A copy of the questionnaire is presented as Table I. Other reference sources were: a) Report Bibliography from the Defense Technical Information Center, b) Shock and Vibration Information Center, c) personal references and contacts at other companies. The two most useful information sources for this study were the Shock and Vibration Information Center and the personal references. The questionnaire survey, in theory, should provide the most data; however, this was not the case. It is believed that for the survey to be effective, each company must be visited to obtain a meaningful response.

TABLE 1

QUESTIONNAIRE FOR FINITE ELEMENT ANALYSIS OF MICROELECTRONIC PACKAGES

	YES	NO
1. Do you utilize mechanical engineering analyses as a means of assessing the reliability of microelectronic devices?	___	___

If your answer is yes, please provide further data by filling in the appropriate blocks in the following table.

ANALYSIS VERSUS TEST

	Computer Analysis	Closed Form Analysis	Test Data
Structural and Dynamic			
Thermal			

2. What kinds of devices that have mechanical problems do you apply the above analysis or testing to?

3. The following matrix chart is to ascertain the relationship between package types and related problems. Please fill in where possible.

Related Problems

	Type of Microelectronic Package Problem	Hybrid Integrated Circuit	Microwave Integrated Circuit	Stripline Microwave Circuit	Other
Package Related	Lack of hermeticity				
	Die bond failure				
	Broken external lead				
	External lead corrosion				
	External lead fatigue				
	Solder reject				
Wire Related	Broken wire				
	Corroded wire				
	Shorted wire				
Wirebond Related	Broken bond				
	Intermetallic formation				
	Lifted bond				
	Misplaced bond				
	Multiple bond				
	Overbonded				

TABLE 1 (cont'd)

QUESTIONNAIRE FOR FINITE ELEMENT ANALYSIS OF MICROELECTRONIC PACKAGES (cont'd)

4. Comment on the impact of MIL-STD-883 on your end product.

5. Are there any outstanding problems in the design, fabrication, test or utilization practices for microcircuit packages?

6. General comment - please discuss any problem that has not been addressed above.

3.2 Field Survey

The search for microelectronic package data (and finite element analysis of the same) was fairly successful. As in any search, it was not all inclusive; however, it is felt that the results represent actual trends in package problems and analysis. Below is a brief description of each search area and the pertinent results.

3.2.1 Questionnaire Survey

Forty-three (43) questionnaires (see Table 1 for Questionnaire form) were sent to various hybrid manufacturers, users, and package suppliers. Fourteen (14) responded by returning the completed forms. This is an average-to-above-average response for this type of survey. Table 2 presents a summary of the survey results. Note that several respondents did not complete all sections of the questionnaire.

From Table 2 it is seen that the number-one package related problem is lack of hermeticity, the number-one wire problem is a broken or corroded wire, and the number-one wirebond problem is broken bonds.

One purpose of this study is to determine which microelectronic problems can be analyzed using FEA or closed-form solutions, and now is an opportune time to discuss this topic as well as to describe microelectronic packages.

A definition of a microelectronic package is very difficult, since it encompasses many types of parts and components. It would, however, be useful to give a list of some of the containers used to package microelectronic packages, they are;

Flatpack Package (Figure 1)
Metal Plug-In Package (Figure 2)
"TO" Transistor Outline (Figure 3)
Dual-in-line-package (DIP) (Figure 4)
Microwave Flat Package (Figure 5)
Multiple Cavity Package (Figure 6)
Leaded Chip Carrier (Figure 7)
Leadless Chip Carrier (Figure 8)

Table 2. Summary of Survey Results

1. Use of mechanical engineering analysis

	Computer Analysis	Closed-Form Analysis	Test Data
Structural and Dynamic	4	3	5
Thermal	6	3	7

2. Devices that the above analysis or test data are applied to for solving mechanical problems.

   Hybrids, DIPS, Flatpacks, and any special modules

3. The following matrix chart is to ascertain the relationship between package types and related problems.

Related Problems

Type of Microelectronic Package Problem	Hybrid Integrated Circuit	Microwave Integrated Circuit	Stripline Microwave Circuit	Other
Lack of Hermeticity	8	3	2	1
Die bond failure	4	1	-	-
Broken external lead	3	1	1	-
External lead corrosion	5	3	3	2
External lead fatigue	4	1	1	-
Solder Reject	3	1	1	-
Broken wire	3	2	2	1
Corroded wire	3	2	2	1
Shortened wire	2	2	2	1
Broken bond	6	2	1	1
Intermetallic formation	5	2	2	1
Lifted bond	3	2	1	1
Misplaced bond	4	2	1	1
Multiple bonds	2	2	2	2
Overbonded	3	1	-	-

4. Impact of MIL-STD-883 on end product
   - o Makes for more reliable product
   - o For large packages (2" x 2") Method 1014 seal test at 30 PSIG minimum bomb pressure may cause breakage of feed-through glass beads
   - o Some use 883 as a general specification and use internal spec's with more realistic testing
   - o MIL-STD-883 is more expensive than the above approach
   - o No destructive analysis required

Table 2. Summary of Survey Results (Continued)

5. Outstanding problems in the design, fabrication, test, or utilization practices for microcircuit packages
   - o Need better knowledge on the sealing of large custom packages
   - o There exsits a basic lack of knowledge on fracture failures of brittle materials used in packages such as glasses and ceramics
   - o Meniscus crack criteria needs to be established

6. General Comments -
   - o Long lead times for finished hybrid products.
   - o Large packages usually have more difficulty in sealing than smaller ones.
   - o Need to develop a criteria for inspecting mounted hermetic chip carriers (leaded or leadless).
   - o The industry may be approaching the position to have to pay for, and receive rights to test lot samples for seal integrity.

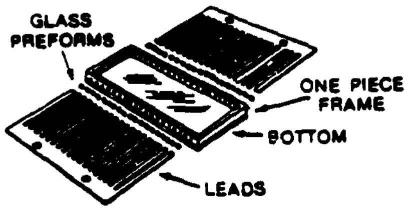

FIGURE 1 FLATPACK PACKAGE

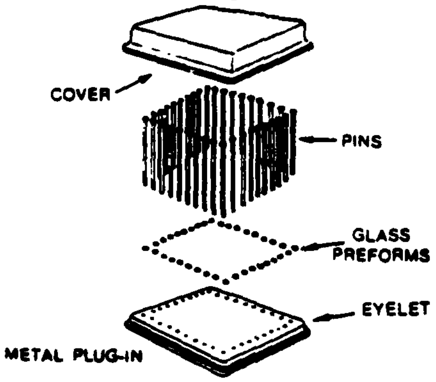

FIGURE 2 METAL PLUG-IN PACKAGE

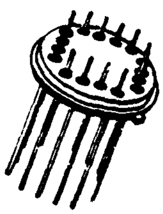

FIGURE 3 "TO" TRANSISTOR OUTLINE

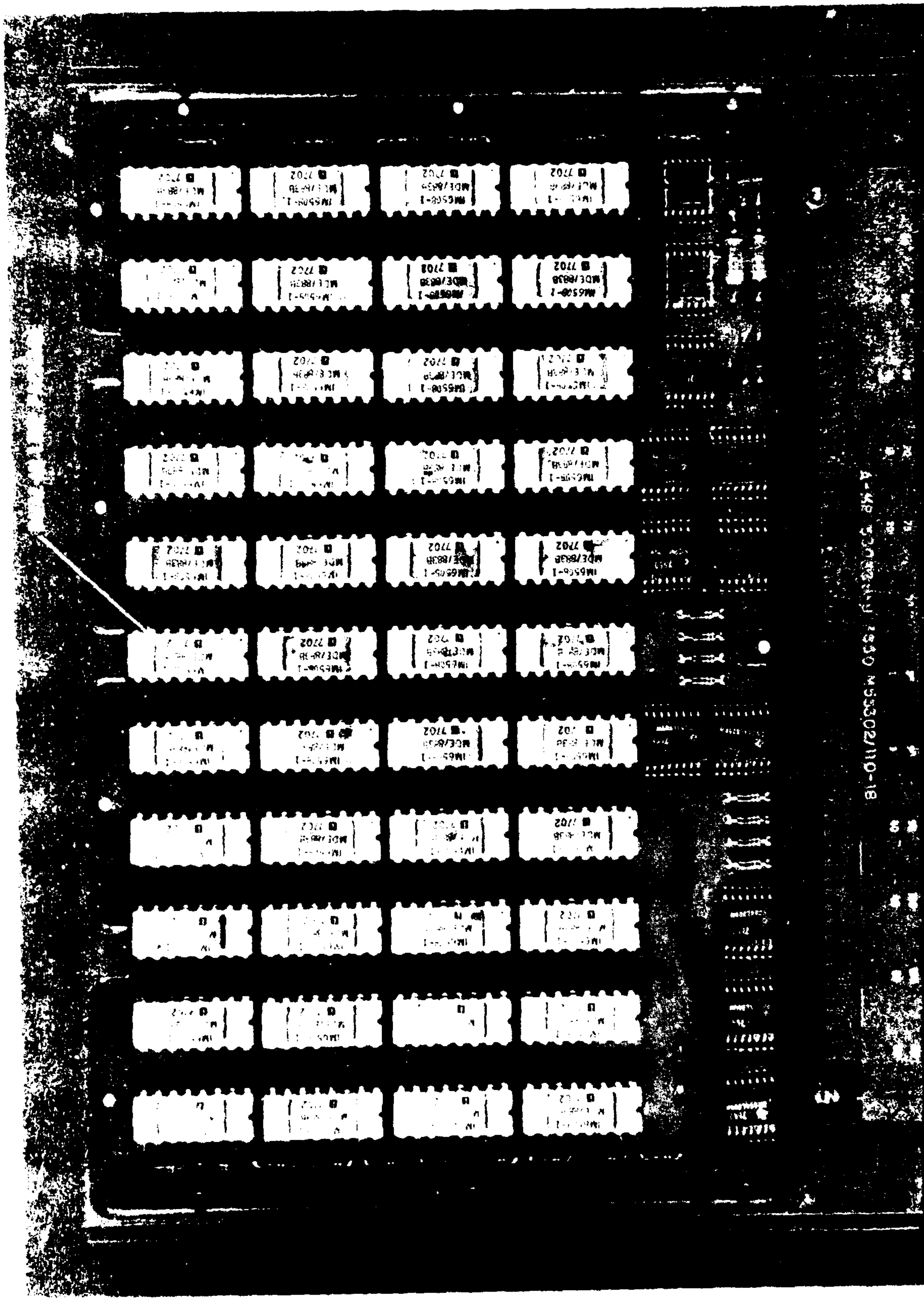

Figure 4. Dual-in-Line Packages Mounted to a Printed Circuit Board

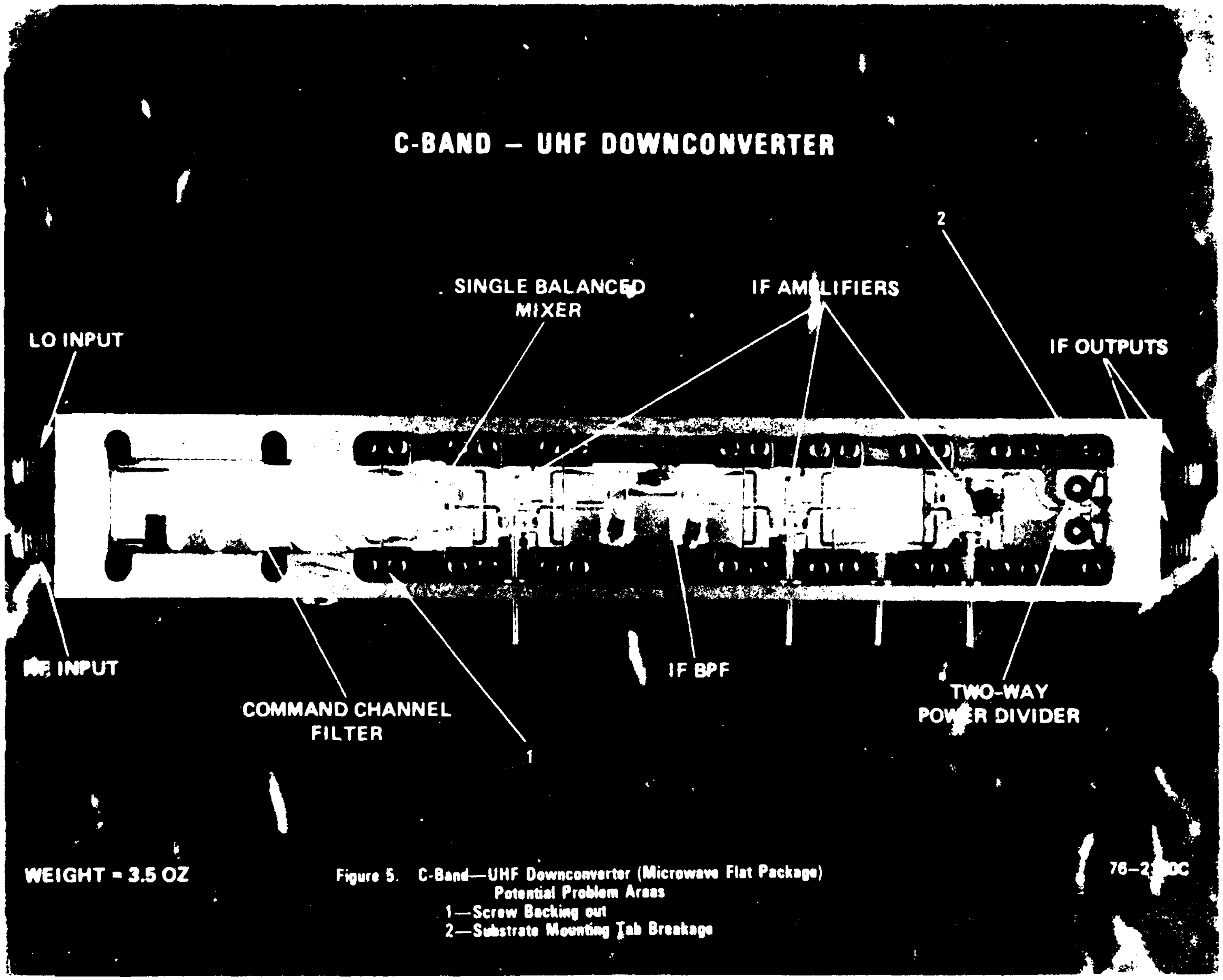

Figure 5. C-Band—UHF Downconverter (Microwave Flat Package)
Potential Problem Areas
1—Screw Backing out
2—Substrate Mounting Tab Breakage

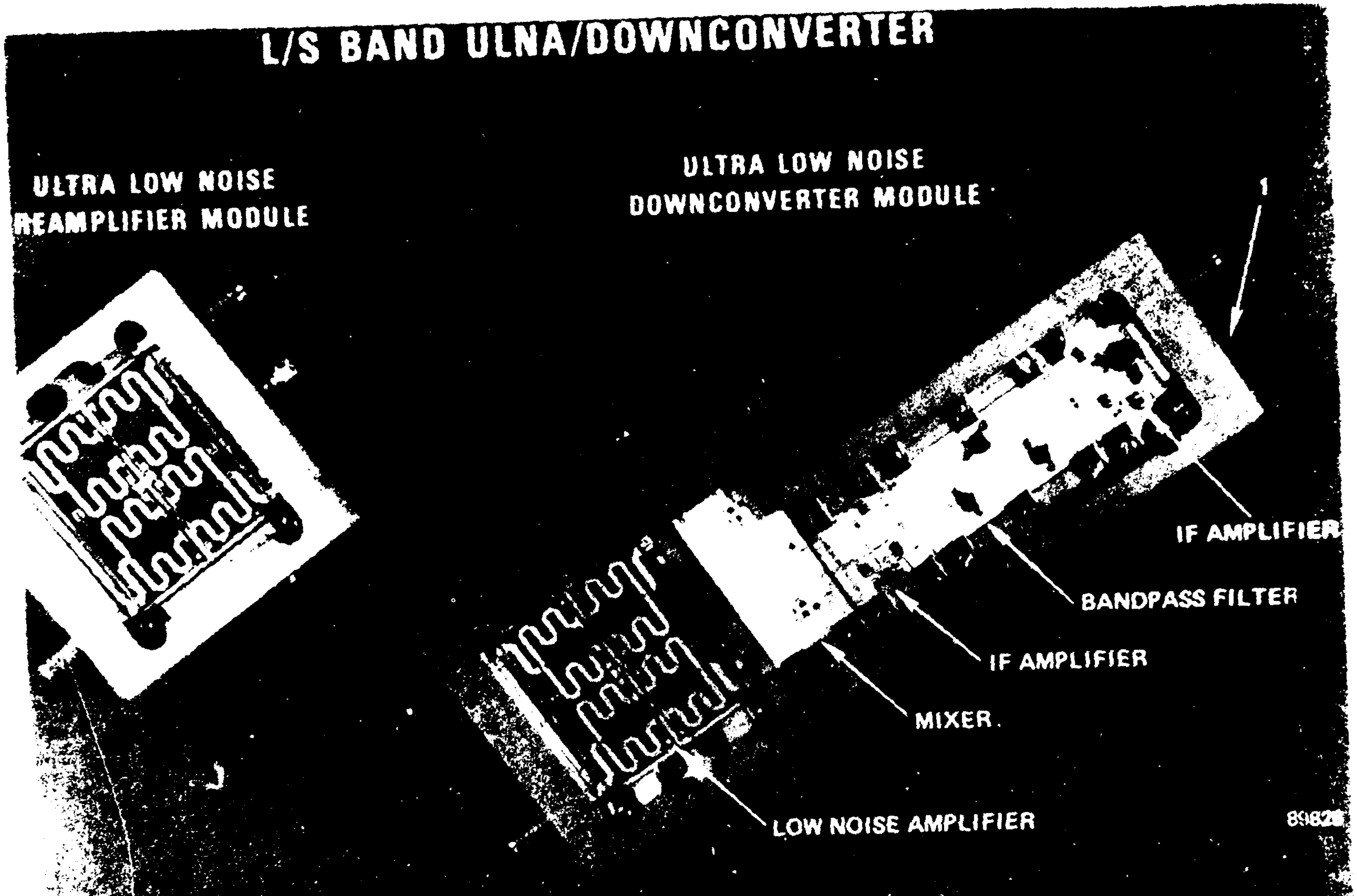

Figure 6. L/S Band U1na/Downconverter (Multiple Cavity Package)
Potential Problem Area
1—Feed Thru Connector Breakage

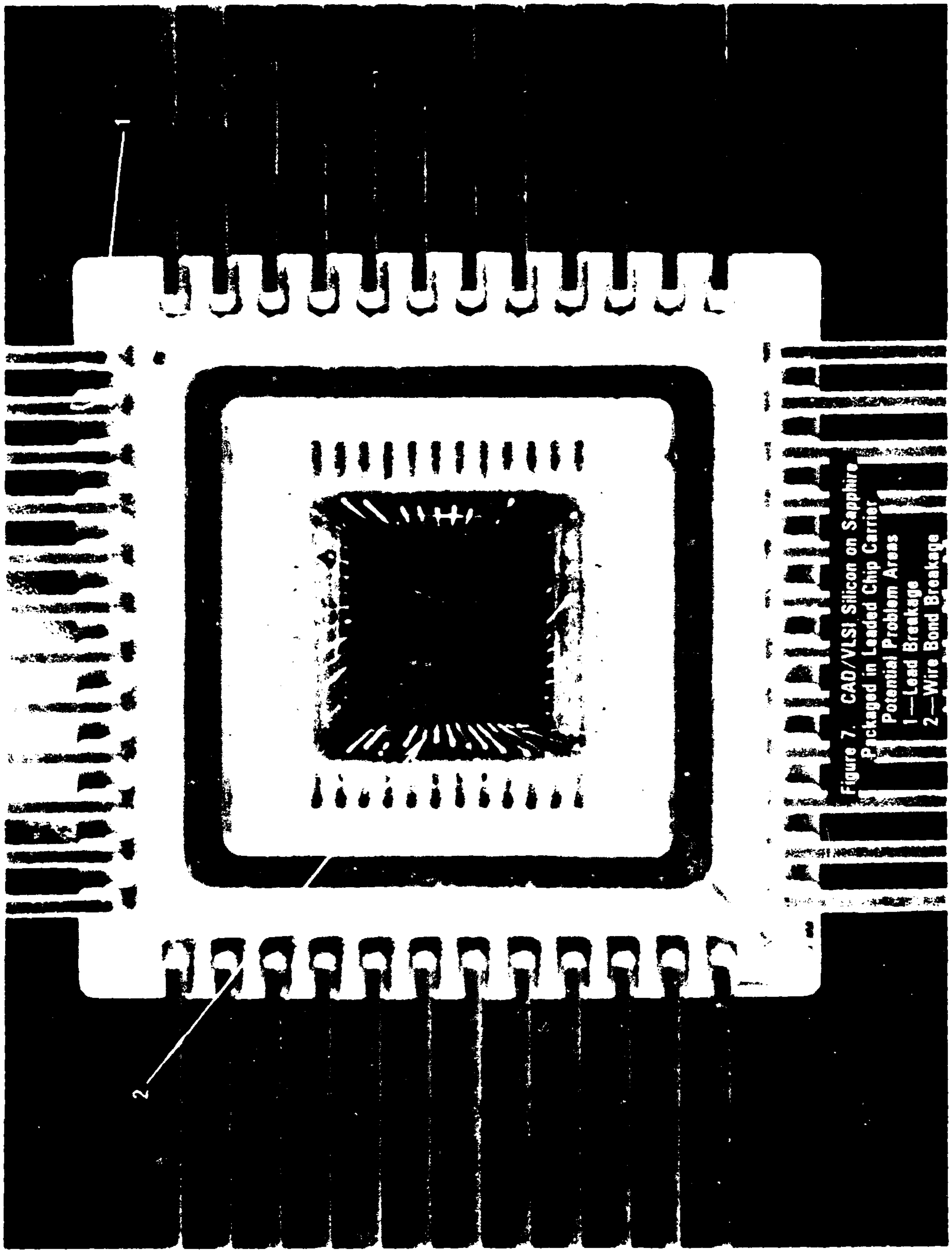

Figure 7. CAD/VLSI Silicon on Sapphire Packaged in Leaded Chip Carrier
Potential Problem Areas
1—Lead Breakage
2—Wire Bond Breakage

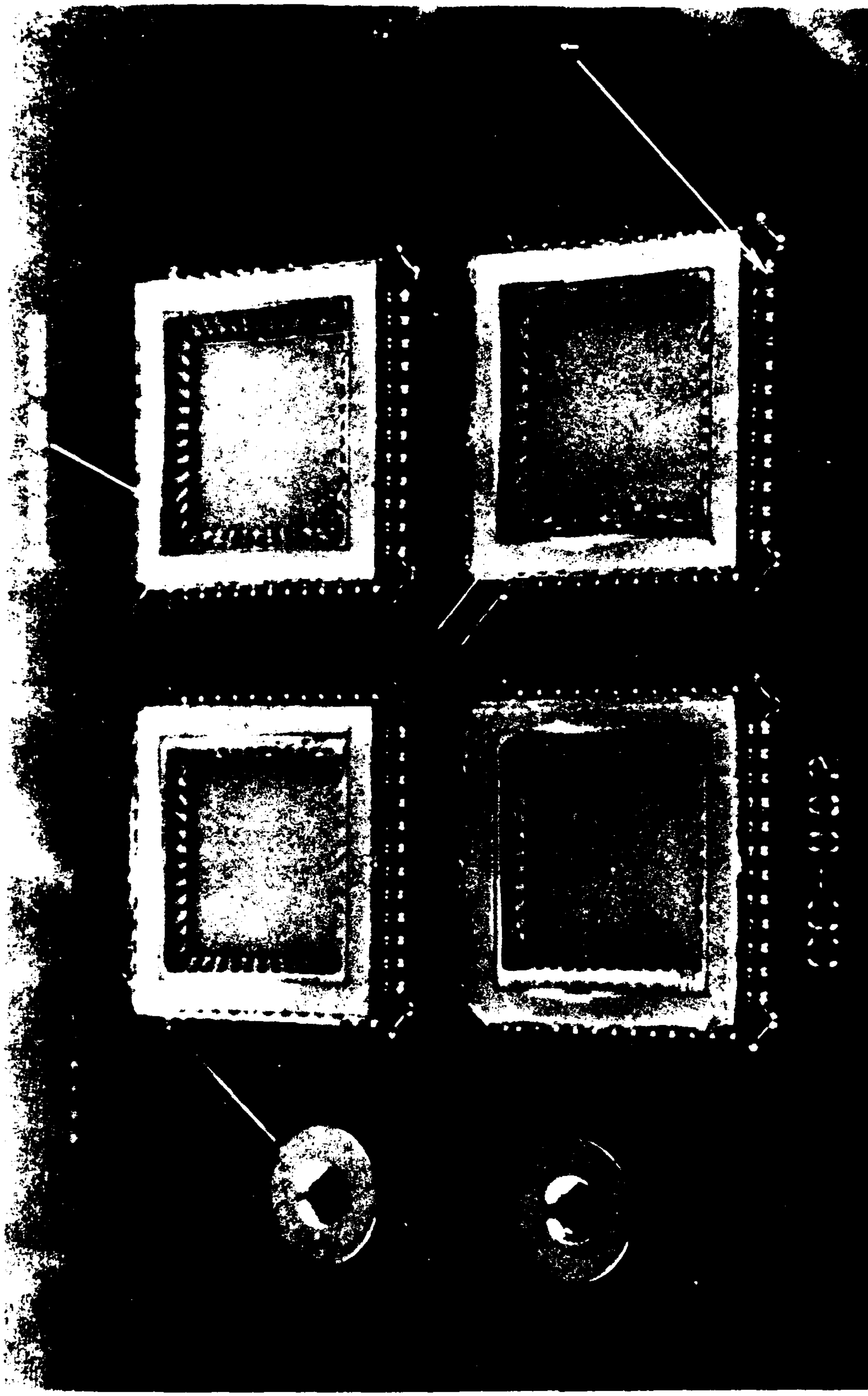

Figure 8. Leadless Chip Carrier Without Substrate Circuitry
Potential Problem Area
1—Solder Joint Cracking Due to Extreme Temperature Cycling or Vibration and Shock

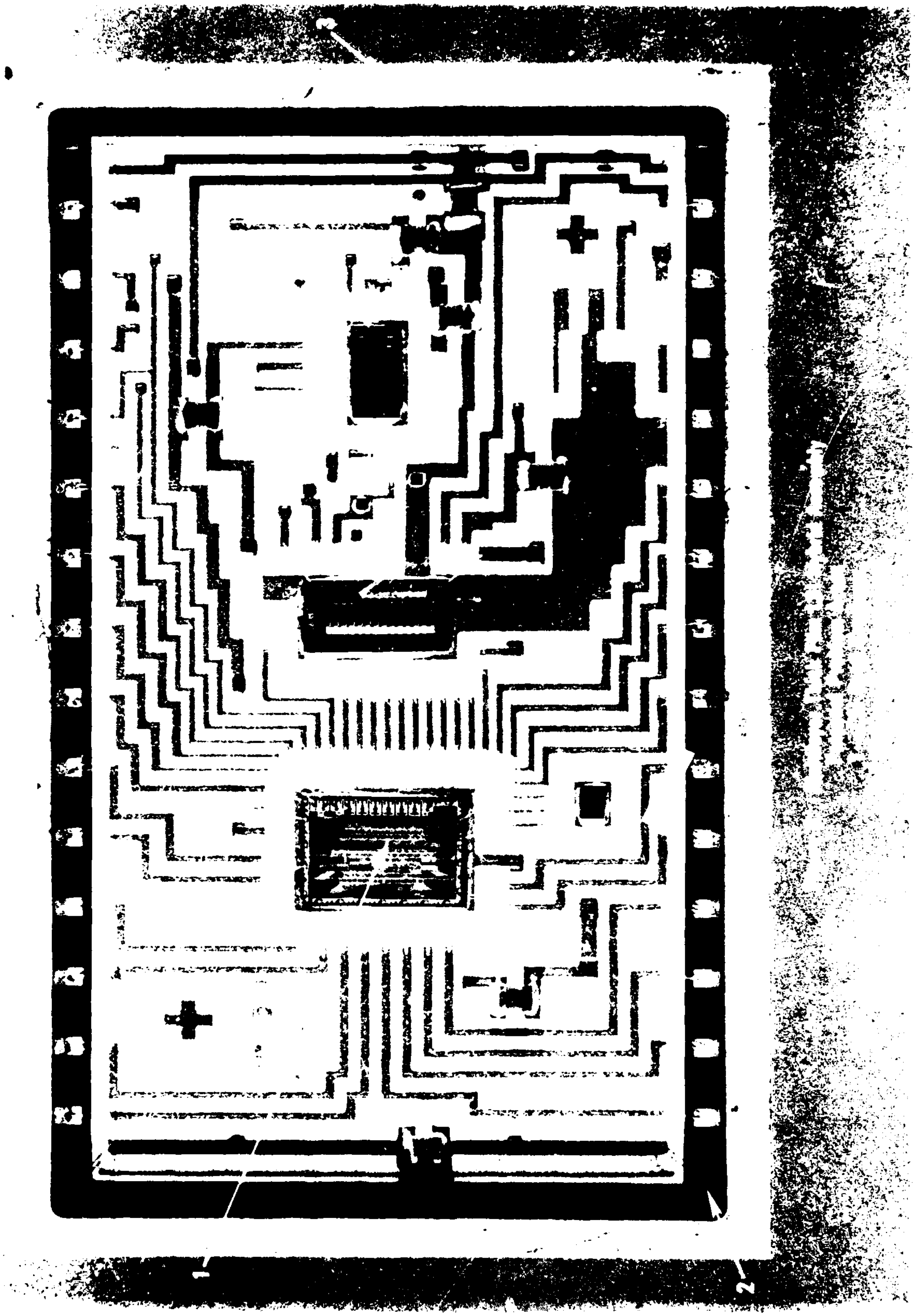
1
2

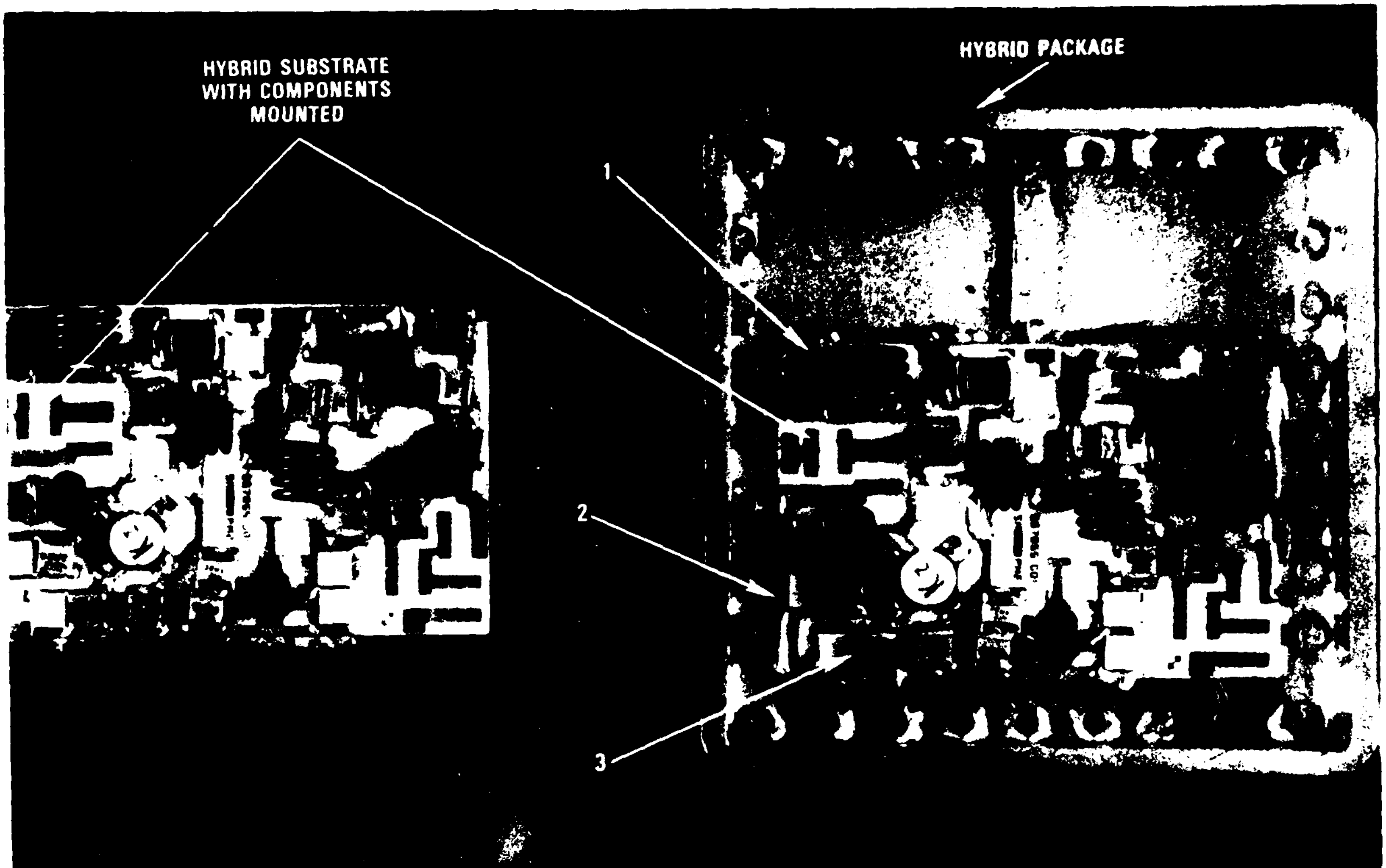

Figure 10. RF Hybrid Multiplier
Potential Problem Areas
1—Breakage of Air Wound Inductors
2—Chip Capacitor Bond Joint Breakage
3—Chip Resistor Bond Joint Breakage

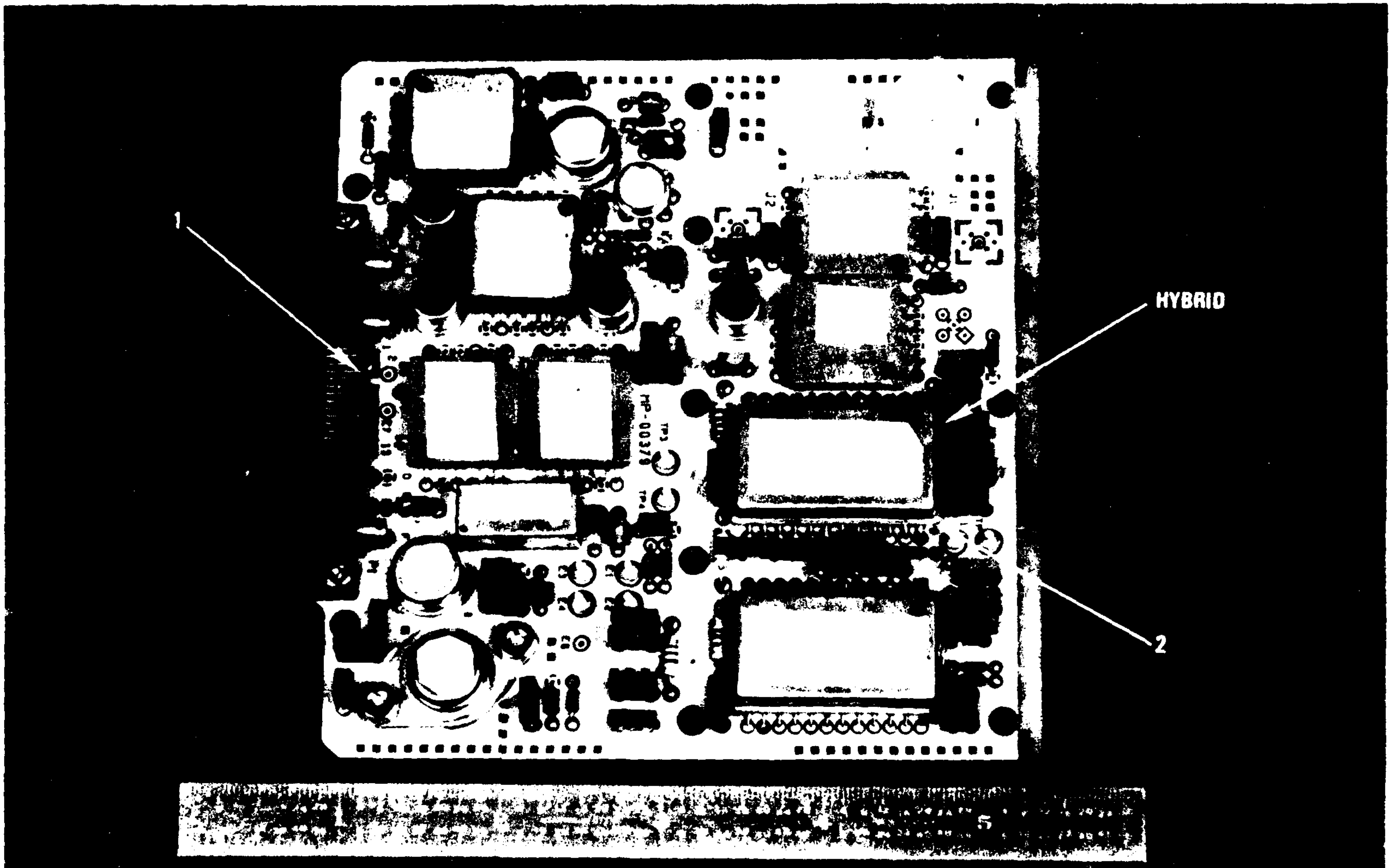

Figure 11. Hybrid Printed Circuit Board
Potential Problem Areas
1—Connector Pin Breakage
2—Hybrid Lead Breakage

These packages are used to package Hybrid Integration Circuits (HIC), Microwave Integrated Circuits (MIC), and Stripline Microwave Circuits (SMC), or any other microelectronic circuits, such as Large Scale Integration (LSI) or Very High Speed Integrated Cricuits (VHSIC). Figures 9, 10, and 11 present other examples of microelectronic packages.

Below is a direct quote from [9] which further describes microelectronic packaging.

> "Microelectronic packaging protects and supports electronic devices and circuits and provides connections to the other parts of the system. The protection function avoids mechanical, electrical, chemical, contamination, and photo-optical damage, degeneration, and causes of malfunction. Hybrid microelectronic circuits and subsystem packages support the substrates; the substrate contains the circuit elements, (semiconductor devices or IC chips, deposited or chip resistors and capacitors, and attached inductors), as well as deposited and bonded interconnection wires. The connections to other parts of the system include electrical leads, heat removal paths, and mounting functions. At present, in order to meet the demands of VLSI, the emphasis is on packages with higher densities while maintaining performance, reliability, and low cost."

In discussing microelectronic packages, it becomes necessary to discuss microelectronic packaging on the Printed Circuit Board (PCB) level. This is required since this is one level of potential failure. Failures can occur during part screening or qualification testing. Failures can also occur at the integrated assembly qualification testing (i.e., microelectronics packages mounted to PCB's which are in-turn secured to an electronic housing assembly). Failures may also occur during field service. So it is seen that one must be able to assess potential failures at any cycle in the life of a microelectronic package. FEA can be applied to any or all of these potential failures where dynamic, static, or thermal stresses are imposed. Below is a condensed list of microelectronic packages potential problem areas, some of these are indicated in Figures 1 through 11.

- o Lack of hermeticity - This can occur when the lead glass-to-metal seal fails, when the lid seal fails, or when leakage occurs through any seal or connector.
- o Die bond failure - When the die (or chip) bond is stressed beyond its allowable strength, a bond failure will occur. This can result from thermal shock, thermal stress, or static and dynamic loading (see Figure 9).
- o Broken external lead - When the external lead is stressed beyond its endurance or ultimate strength, a failure will occur. This can be accelerated if scratches or nicks are present from an improper lead bending process.
- o External lead corrosion - If proper lead plating is not specified, then lead corrosion can result in lead failure.
- o Wire bond and wire failures - The wire bond is the connection between the chip or die and the external lead of the package. An example is given in Figure 7. These wires are usually 0.001" diameter gold or aluminum. Wire bond failures occur from improper bonding techniques, over-stress conditions, and corrosion. Wire failures generally result from corroded wire or an over-stress condition.

- Microwave package failures - These packages are typically very rugged and, therefore, structural or lead failures are rare. Figures 5 and 6 show some of the expected failures. They are: substrate tie-down screws backing out due to improper torque or over-stress, substrate mounting tab breakage due to over-stress and feed-through connector breakage due to thermal stress build-up.
- Leadless chip carrier solder joint failures - this is probably one of the most discussed, analyzed, and tested areas in the microelectronics area over the past four years. Figure 8 presents empty leadless chip carriers mounted to a polyimide substrate. Solder joint failures result from a difference in coefficient of thermal expansion between the ceramic leadless chip carrier and the polyimide or G-10 substrate.
- Air wound inductor breakage - Figure 10 presents an RF hybrid multiplier with air wound inductors. At certain dynamic levels, these inductors will either physically break or will be out of the electrical specification for which they were intended.
- Connector lead breakage or connector wear - While a connector is not a microelectronic package, it is a part of the overall packaging concept and a connector failure will cause system failure the same as a package failure will. Figure 11 shows a connector mounted to a PCB populated with hybrids. Two failures generally occur in the connector; they are: 1) lead breakage, due to excessive relative motion between the connector and PCB, and 2) connector pin wear from extended or high vibration levels

causing intermittents in the system operation. A third connector failure should be mentioned although it is unique to a particular design. There have been reports of the connector solder joints cracking or pins breaking due to a mismatch in the coefficient of thermal expansion between the connector body and the PCB.

3.2.2 Shock and Vibration Information Center

The Shock and Vibration Bulletin Index was reviewed for applicable material to be used for this study. The first pass-through resulted in no obvious references. At this point it was decided to inspect each paper from 1978 to 1980. This resulted in eight excellent references for FEA or closed-form analysis compared to test data. It was concluded that a review of the reference titles would not necessarily indicate whether a paper discussed FEA. It should be noted, however, that no references were found on microelectronic FEA. This does not mean that these articles do not exist; however, there are probably not many such articles. Many analysts, the authors included, perform such analyses on a daily basis, but do not present the results at every symposium. Reference [1] presents the dynamic analysis of a torpedo shell modeled with plate and beam elements. NASTRAN was used as the Finite Element Computer Program.

Overall, there was very excellent agreement between the FEA solution and the test, showing once again that a properly constructed finite element model will give accurate results. This fact was repeated over and over again throughout this search.

Reference [2] is another example of FEA applied to large structures (helicopters) with test data comparisons. The results were excellent over most of the frequency range, but at higher frequencies the accuracy deteriorated. The authors believe that this reduction in accuracy was due to modeling assumptions rather than the models themselves or the FEA. This shows that one must understand all the analytical assumptions and their effects on the final results.

Reference [3] is a different application of FEA. It compares the FEA and an exact solution. The FEA uses the STAGS USA (Underwater Shock Analysis) Code. The FEA agrees favorably with the exact method when calculating the transient response of an elastic cylindrical shell immersed in an acoustic media that is engulfed by a plane wave.

Transient analysis of multicomponent structures impacting rigid barriers is given by Reference [4]. Separate analyses are performed on each component considering distortion and failure of joints, multiple impacts, and elastic-plastic material behavior. Comparison of analytical results to test data demonstrates the applicability and accuracy of the models. Next, the total structure is analyzed by generating a new model which consists of the structure and the individual component models. The overall results give good correlation between analysis and test. (The program used was SUPER, a three-dimensional general purpose finite element structural analysis code.)

In Reference [5], closed-form equations are developed for comparison with test results. Resonant frequency results are excellent, giving credence to the fact that closed-form equations, if properly used, can provide accurate answers.

The author of Reference [6] compared three different closed-form approximation techniques to find an easy, low cost method of evaluating vibration response characteristics for airborne optical packages. The author states, "a finite element analysis of the simply supported beam was conducted in order to determine the accuracy of the various analytical techniques presented here". The results show that one method, the generalized coordinates solution, gave very good estimates of the first four modes. It is important to note that the FEA, and not a test, is used as the check here. It is also important to realize that, at times, a closed-form solution can provide acceptable answers at a reduced cost.

Reference [7] is an excellent application of FEA, namely damping predictions. The authors used MSC/NASTRAN and reported good results.

Reference [8] is an excellent discussion on the STAGS USA code. The authors say that this code is conditionally acceptable for the response of submerged shells to shock loadings but improvements are needed. They have no hesitation in recommending this program.

The following was learned from References [1] through [8]:

- o FEA modeling, with proper assumptions, results in excellent correlation to test data.
- o FEA has been applied to many problems but there are not many reports on microelectronic package analysis.
- o Closed-form solutions can result in accurate, cost-effective solutions.
- o FEA analysis is sometimes used as a standard in evaluating closed-form solutions in lieu of test data.

3.2.3 Personal References

Personal references include personal libraries, personal contacts, and personal experience in the FEA and microelectronic package areas. Since the number of personal references is so great, Table 3 was generated to summarize the findings.

A special note is needed to discuss Reference [9], one of the most significant sources of information on microelectronic package problems. This book was discovered in a personal library, and, after being reviewed, many interesting articles were ordered for this study. These articles discussed bonding problems and analysis, glass-to-metal-seal data, hermeticity, package design, thermal design, fabrication techniques, repair/rework, types of packages, reliability, (bond failure, circuitry failure, encapsulation failure, contamination and cleaning), coatings, substrates, and much more.

Ref. NO.	FEM Analysis		Test Data		Closed Form Analysis		Microelectronic Package Data	REMARKS
	Thermal	Structural	Thermal	Structural	Thermal	Structural		
10		x						This appears to be a good ref. for FEM analysis on bond joints.
11		x						A good theoretical ref. for thermal stress analysis.
12		x				x		Closed form versus Fem bond analysis, good correlation.
13							x	A general discussion on the control of thermal stresses due to CTE differences.
14							x	Discussion on matching CTE's for silicon substrates,polyimide/Kevlar.
15		x		x				FEM analysis compared to test data for bond joints, both good and poor correlation.
16						x		Bond joint closed form analysis appears to be an excellent article.
17			x					Thermal design and analysis of a hybrid system, good analysis to test correlation.
18								Has a fortran transient computer program, finite difference, good data.
19								Finite difference thermal analysis is used to understand thermal shock. Test results for semi conductor pkgs., is a good application of thermal analysis.
20							x	Glass-to-metal-seal evaluation, general discussion.
21							x	Glass-to-metal-seal discussion.

TABLE 3 - Discussion of References

Ref. No.	FEM Analysis		Test Data		Closed Form Analysis		Microelectronic Package Data	REMARKS
	Thermal	Structural	Thermal	Structural	Thermal	Structural		
22							x	Reliability of microcircuit interconnections, FEM can not be used for material corrosion problem discussed here.
23							x	Reliability can be improved by reducing the number of electrical joints, using more stable substrate materials, provide greater resistance to mechanical stresses. They also recommend high temperature operational testing for burning.
24							x	Glass-to-metal-seal information.
25							x	Glass-to-metal-seal information.
26							x	Glass-to-metal-seal information.
27							x	The adhesion promoter is very important for moisture protection and at elevated temperatures parylene cracked.
28							x	Good article on parylene coating for microcircuits.
29		x		x		x		A good selection of FEM and closed form analysis with test data.
30							x	Appears to be a good article looking at thermal fatigue of bonded joints.
31				x		x		Test and analysis data, good correlation.
32							x	Hybrid substrate bonding specification.
33		x		x		x		A good ref. for thermal fatigue in bonded joints, good test to analysis correlation.

TABLE 3 (cont'd)

Ref. No.	FEM Analysis		Test Data		Closed Form Analysis		Microelectronic Package Data	REMARKS
	Thermal	Structural	Thermal	Structural	Thermal	Structural		
34						x		Good data.
35						x		Old data,not all of it is valid.
36						x		Appears to be valuable data.
37		x		x		x		Good source of bond joint analysis and test for static & fatigue loadings.
38						x		Appears to be a good article.
39						x		A good reference for bond joint analysis.
40		x		x				Good correlation for non linear analysis, bond joint.
41				x		x		Good correlation, presents guide-lines for designing bond joints.
42							x	Four out of thirty were concerned with analytical methods for sealing, good response from questionnaire (also made many visits) the top persistant failure modes in hybrid microcircuits were in descending order; wire bonds, defective semi-conductor devices, contamination, moisture related, & leaky packages.
43							x	Good source of hybrid articles.
44							x	See para. 3.2-3 for detailed write-up.
45			x				x	Test data compared to finite diff-erence analysis, good correlation
46							x	Good reference for lead corrosion.
47	x		x					Appear to be an excellent comparison between FEM & test,good correlation.

TABLE 3 (cont'd)

Ref. No.	FEM Analysis Thermal	FEM Analysis Structural	Test Data Thermal	Test Data Structural	Closed Form Analysis Thermal	Closed Form Analysis Structural	Microelectronic Package Data	REMARKS
48							x	Thermal design criteria for substrates.
49	x							Thermal analysis of integrated circuit packages.
50			x				x	Thermal analysis versus test data for chip carriers, good correlation.
51								A good reference article.
52							x	An excellent survey of DIP and flatpack mfg., problems which can be related to hybrids, #1 problem was lack of hermeticity with die bond failure #2.
53		x						A good reference on isoparametric finite elements.
54							x	A good source of microcircuit pkg., problems.
55							x	An excellent reference on surface treatment for bonding surfaces.
56							x	A very good source of state-of-the-art packaging problems.
57	x	x						An excellent collection of FEM applications & evaluations, this reference is discussed in detail in the text.

TABLE 3 (cont'd)

Reference [44] is deserving of some attention since it has some very pertinent data for microelectronic packages. Shown below is a list of information gained:

- o Commercial houses are claiming lower cost and higher reliability than military houses (pages 6 and 7).
- o Die rework and testing account for 75% of hybrid cost (page 21).
- o Specification relaxation can reduce hybrid cost 10% (may be an application for computer analysis).
- o Recommendations were made for deletion of the following tests (page 29):
  Thermal cycling
  Mechanical shock
  SEM Inspection
  Lead bond testing
  Centrifuge
  Die shear test
- o Only 67% of those who responded to the survey used thermal analysis. No mention was made of stress and dynamics which means they ignore it or use engineering judgement (page 37).

Reference [57] is a collection of many FEA articles and is also deserving of some special discussion. Below are discussions on pertinent papers:

(1) Paper 5, Volume 1 "Practical Aspects of the Finite Element Method," Hoggenmacher, G.G., and Lahey, R.S. The important conclusions or considerations are listed below:

- o The accuracy of some membrane elements may deteriorate at higher aspect ratios. An arbitrary system of elements covering a given region may not result in useful data; sound judgment is needed.

- Model integrity can be verified by
  1. Line-by-line check of the input data
  2. Computer plots to detect ill-shaped structures
  3. A "common sense" review to detect unreasonable results
  4. Equilibrium checks on all nodes
  5. Constraint compatibility check
- The key point is to understand the limitations of the elements you are using in order to achieve the best possible model. Then apply all possible checking techniques.

(2) Paper [9], "Utilization of Isoparametric Shell Elements in Solution of Practical Problems," Citipitioglu, E., Nicholas, V.T., and Ecer, A. This is an excellent article on the practical usage of isoparametric shell elements: both middle surface shell (MSS) and solid type shell (STS). Instructive examples are presented which show the pitfalls in using these element types. One example presented is the comparison between analysis and experiment for a steel wheelwell from the front end of an automobile. The wheelwell was stamped from 0.033 inch thick steel into a complex geometric configuration. The thickness variation caused by the stamping process varied from 0.030 to 0.035 inches. There were thirty-nine holes of different sizes with many types of ribs. The results for the first natural frequency are summarized below:

Number of Elements in Model:	78	142	204	289	520
% Error:	+145%	+94%	+51%	21%	7%

This example demonstrates the analysis by an iterative modeling method. Basically, a coarse model is chosen initially, and then it is systematically improved.

Many other interesting articles are presented in Reference [57], some of the more pertinent ones are listed below:

Paper 11: "Higher Order Versus Lower Order Elements; Economics and Accuracy," MacNeal, R.H.

Paper 12: "Element Evaluation - A Set of Assessment Points and Standard Tests," Robinson, J.

Paper 16: "Thin Shell Isoparametric Elements," Berkovic, M.

Paper 19: "Overview and Evaluation of Some Versatile General Purpose Finite Element Computer Programs," Frederikson, B., Mackerle, J.

3.3 Trips

Two trips were made for the survey portion of this study. One trip was a conference with a large representation of microelectronic package manufacturers and users. The other trip was to a microelectronic package manufacturer. Many key points were learned on these trips; the results are summarized below based on these two trips and the experience of the many companies polled.

- Most companies do not use FEA to assess the structural and thermal integrity of microelectronic packages. Most large companies use the finite element method for analysis of structures.
- FEA for microelectronic packages has great potential.
- Very few recommend the "full blown" screening in MIL-STD-883. Most utilize an abbreviated version that has worked for them.
- Each company has their own preference for finite element computer programs, but the most widely used are STARDYNE, ANSYS, and NASTRAN.

3.4 Analysis and Test Cost Comparison for Qualification Verification

The purpose here was two-fold; 1) to determine which typical microelectronic military environmental tests can be replaced by finite element analysis and 2) the relative cost comparisons between closed-form analysis, finite element analysis and testing.

3.4.1 Finite Element Analysis Applied to Microelectronic Package Qualification Verification

The purpose here was to determine which, if any, military-specified test environments for electronic packages might lend themselves to a structural or thermal analysis prior to a test being performed on an actual piece of hardware. Obviously, schedules and budgets could benefit from the use of analysis to detect design shortcomings prior to expensive and time consuming test sequences. Therefore, the test methods of four different military specified tests were reviewed to determine the possibility of supplementing the test secuences with either a finite element analysis (structural or thermal) or a finite difference analysis (thermal only).

The four military test sequences which were reviewed included MIL-STD-883 (Test Methods and Procedures for Microelectronics), MIL-STD-810 (Environmental Test Methods), MIL-STD-202 (Test Methods for Electronic and Electrical Component Parts), and MIL-M-38510 (Digital Microcircuits). For each of these four test sequences, the test methods which could be suitable for a finite element and/or finite difference analysis were noted.

3.4.1.1 Applicable Test Methods

Tables 4 through 7 indicate the test methods suitable for analysis from each of the four military specifications considered. Also inlcuded is a brief description of the type of analysis which might be used to simulate the various test methods.

MIL-STD-883

Table 4 summarizes those test methods of MIL-STD-883B which were considered suitable for analysis:

Table 4. MIL-STD-883B Test Methods

Method No.	Description	Applicable Analyses
1010.2	Temperature Cycling	Thermal, thermal stress
1011.2	Thermal Shock	Thermal, thermal stress
1012	Thermal Characteristics	Thermal
1015.2	Burn-In Test	Thermal
1016	Life/Reliability Tests	Thermal
2001.2	Constant Acceleration	Static stress
2002.2	Mechanical Shock	Dynamic stress (shock)
2004.2	Lead Integrity	Static stress, static nonlinear stress
2005.1	Vibration Fatigue	Dynamic stress (sinusoidal)
2007.1	Vibration, Variable Frequency	Dynamic stress (sinusoidal)
2011.2	Bond Strength	Static stress, static nonlinear stress
2019.1	Die Shear Strength	Static stress

As shown in Table 4, twelve of the test methods in MIL-STD-883 were considered suitable for structural and thermal analysis. Methods 1010.2 and 1011.2 could use a finite element heat transfer program to define component temperatures, which could, in turn, be used to define the loading for a thermal stress analysis of the same system. Methods 1012, 1015.2, and 1016 could use either a finite element heat transfer program, or a finite difference program, to solve for specific component temperatures based on the boundary conditions specified in the test methods. In each of the above-mentioned cases, analysis could be used to predict a failure or to spot a marginal design (excessive junction temperatures, excessively large thermal stresses, etc.) prior to the test sequence.

From a structural point of view, test methods 2001.2, 2004.2, 2011.2, and 2019.1 could be analyzed using the static analysis capabilities of a finite element program.

Methods 2001.2 and 2019.1 would be relatively straight-forward statics-type problems; however, methods 2004.2 and 2011.2 would require the program to have nonlinear analysis capabilities. These nonlinear capabilities would be required in order to satisfactorily analyze the lead bending of method 2004.2 (large deflection theory with plastic deformation), and to analyze the various bonds of method 2011.2 (a common bond, solder, tends to plastically relieve itself at stresses exceeding about 500 psi).

Similarly, test methods 2002.2, 2005.1, and 2007.1 could be analyzed using a structural finite element program with dynamic analysis capabilities. For both the shock and the sinusoidal vibration environments, the finite element program would be used to calculate the system's natural frequencies, and to then calculate the dynamic response stresses based on user-provided transmissibility assumptions.

Using the stresses calculated by the finite element analyses of the various mechanical tests, marginal or inadequate designs could be spotted (excessively large stresses or unsatisfactory fatigue coefficients) prior to expensive testing sequences.

MIL-STD-810

Table 5 summarizes those test methods of MIL-STD-810C which were considered suitable for analysis.

As shown in Table 5, thirteen of the test methods in MIL-STD-810 were considered suitable for structural and thermal analysis. Methods 500.1, 504.1, 517.2, and 518.1 would require a combination of "static" structural analysis (differential pressure/venting analysis), heat transfer analysis (varying convective and conductive characteristics), and thermal stress analysis. Methods 501.1, 502.1, 503.1, and 505.1 would similarly require a heat transfer analysis and a thermal stress analysis to determine the effects of the specified thermal loads.

Table 5. MIL-STD-810C Test Methods

Method No.	Description	Applicable Analyses
500.1	Low Pressure (Altitude)	Static stress, thermal
501.1	High Temperature	Thermal, thermal stress
502.1	Low Temperature	Thermal, thermal stress
503.1	Temperature Shock	Thermal, thermal stress
504.1	Temperature-Altitude	Static stress, thermal, thermal stress
505.1	Solar Radiation	Thermal, thermal stress
513.2	Acceleration	Static stress
514.2	Vibration	Dynamic stress (sine & random)
515.2	Acoustical Noise	Dynamic stress
516.2	Shock	Dynamic stress (shock)
517.2	Space Simulation	Static stress, thermal, thermal stress
518.1	Temperature-Humidity-Altitude	Static stress, thermal, thermal stress
519.2	Aircraft Gunfire Vibration	Vibration (sine superimposed over random)

From a structural viewpoint, method 513.2 would require a static analysis, while methods 514.2, 515.2, 516.2, and 519.2 would all require some type of dynamic stress analysis (either sinusoidal or random vibration, acoustical noise, or shock). For method 519.2, it would be necessary to use super-position to determine the effects of the combined sinusoidal and random vibration environment.

MIL-STD-202

Table 6 summarizes those test methods of MIL-STD-202E which were considered suitable for analysis.

Twelve of the test methods in MIL-STD-202 were considered suitable for structural and thermal analysis. Method 105C would require a static stress analysis to account for the behavior of any pressurized assemblies, and a heat transfer analysis to account for the varying convective and conductive characteristics. Methods 107D, 108A and 210A would all require a combined heat transfer and thermal stress analysis to determine the effects of the specified thermal loads.

Table 6. MIL-STD-202E Test Methods

Method No.	Description	Applicable Analyses
105C	Barometric Pressure (reduced)	Static stress, thermal
107D	Thermal Shock	Thermal, thermal stress
108A	Life (at elevated ambient temp)	Thermal, thermal stress
201A	Vibration	Dynamic stress (sinusoidal)
203B	Random Drop	Dynamic stress (repeated shock)
204C	Vibration, High Frequency	Dynamic stress (sinusoidal)
207A	High Impact Shock	Dynamic stress (shock)
210A	Resistance to Soldering Heat	Thermal, thermal stress
211A	Terminal Strength	Static stress, static nonlinear stress
212A	Acceleration	Static stress
213B	Shock (specified pulse)	Dynamic stress (shock)
214	Random Vibration	Dynamic stress (random)

From a structural point of view, methods 201A, 203B, 204C, 207A, 213B, and 214 would all require some type of dynamic stress analysis -- either sine vibration, random vibration, or a specified shock or series of shocks. Finally, methods 211A and 212A would require a static stress analysis to determine the resulting stresses. However, it would be necessary to use a nonlinear program for method 211A: the "Terminal Strength" method involves the plastic deformation of terminal leads.

MIL-M-38510

Table 7 summarizes the test procedures of MIL-M-38510 which were considered suitable for analysis:

Table 7. MIL-M-38510 Test Procedures

Description	Applicable Analyses
Stabilization Bake	Thermal, thermal stress
Temperature Cycling and/or Shock	Thermal, thermal stress
Constant Acceleration	Static stress
Bond Strength	Static stress, non-linear static stress, thermal stress
Lead Integrity	Static stress, non-linear static stress,
Steady State Life Tests	Thermal
Die Shear Strength Test	Static stress
Barometric Pressure	Static stress, thermal
Intermittent Life	Thermal

Nine of the test procedures in MIL-M-38510 were considered suitable for structural and thermal analysis. The "Stabilization Bake" and the "Temperature Cycling and/or Shock" tests would require a combined heat transfer and thermal stress analysis to determine the effects of the specified thermal loads. In addition, the "Steady State Life Tests" (accelerated and normal tests), the "Intermittent Life", and the "Barometric

Pressure" methods would all require a heat transfer analysis of the system.

From a structural viewpoint, the "Constant Acceleration", the "Bond Strength", the "Lead Integrity", the "Die Shear Strength Test", and the "Barometric Pressure" methods could all benefit from a static stress analysis. Also, it would be necessary to use a nonlinear program to analyze the stresses in the "Bond Strength" and "Lead Integrity" methods (solder bonds plastically relieve themselves, and leads are plastically deformed in these tests).

3.4.2 "Front-End" Analysis Cost Savings

The purpose of this section is to compare the relative costs of closed-form analysis and finite element analysis supplementing qualification testing of microelectronic packages. Obviously not all qualification tests can be replaced; however, based on the previous discussion, let us assume that the following tests can be replaced by analysis; shock (0.6 to 11.0 msec, up to 100 G's), acceleration (up to 30,000 G's), variable frequency vibration (20 to 70 G's), f tigue vibration (20 G's to 50 G's), and random vibration (up to 50 Grms). With this in mind, the following assumptions are given for an example in cost savings:

1. Hybrid cost - $500/each
2. A military program has a requirement for 1,000 hybrids per MIL-STD-883.
3. Compliance to MIL-STD-883, on a recent Harris program with 11 hybrid types, required 23% more nondeliverable hybrids to be used for 5008 testing. Therefore, 23% will be assumed for this example as the number of extra hybrids for MIL-STD-883 compliance.
4. 230 hybrids are required for the full compliance to MIL-STD-883. Part of this number of test samples is required for dynamic testing, let it be assumed that 100 hybrids can be deleted if

analysis is substituted for dynamic testing. This is only an assumption and will vary with each individual program. Therefore, a cost reduction of $100 x $500 or $50,000 would be saved if analysis was used to supplement the tests. Below are typical current costs for testing and analysis based on engineering experience at many different companies.

5. Dynamic Testing cost is $3,200
6. Finite element analysis cost is $7,000
7. Closed-form analysis cost is $3,000

Table 8 presents a summary of the cost comparisons between analysis and test. It is seen that a substantial amount can be realized based on a company's overhead structure. The savings for this hypothetical case is $46,200 for finite element analyses and $50,200 for closed-form analysis. Now this is, of course, assuming that all of the dynamic tests are deleted which is not recommended. What is recommended is to perform an analysis using finite element analysis, and develop a relative comparison of resulting stress levels for each dynamic test. Then the worst case tests can be selected and the equipment subjected to these tests. It is estimated that this procedure would result in a real cost savings of roughly $25,000 to $30,000, not an insignificant amount. Additional cost savings can be realized by using pre and postprocessor software programs, and by utilizing Computer Aided Design/Computer Aided Manufacturing (CAD/CAM) techniques.

Table 8. Cost Comparison for Analysis and Test of a Hybrid Component

Dynamic Testing Compliant to MIL-STD-883	Finite Element Analysis Substituted for Dyanmic Testing	Closed-Form Analysis Substituted for Dynamic Testing
$53,200	$7,000	$3,000

3.4.3 Summary

The previously discussed tables list those test methods of MIL-STD-883, MIL-STD-810, MIL-STD-202, and MIL-M-38510 which we consider to be suitable for a finite element structural or thermal analysis, or for a finite difference thermal analysis. It is believed that the use of analysis in conjunction with testing will benefit schedules and budgets; design shortcomings may be identified and solved prior to expensive testing sequences. It has been shown, by use of an example, that cost savings from $25,000 to $50,200 can be realized by substituting analysis for dynamic testing per MIL-STD-883 on hybrids.

3.5 General Summary for Techical Assessment (Phase 1)

The more germane findings for the technical assessment are presented below:

- o Although FEA is primarily a tool for designers of large complex structures, a great potential exists if applied to microelectronic packages.
- o By using FEA for early warnings of potential failures the mechanical engineer can play a significant role in assuring or improving the reliability of microelectronic systems.
- o The survey showed that the areas giving microelectronic packages the most problems were hermeticity, broken or corroded internal wires, and broken wirebonds.
- o FEA can provide accurate answers if proper assumptions are made and if one understands the finite element theory.
- o Commercial hybrid houses claim lower cost and higher reliability than similar products produced at military hybrid houses.
- o Most companies do not use FEA to assess the structural and thermal integrity of microelectronic packages.

- The "full blown" screening in MIL-STD-883 is not recommended by most of the companies polled. Instead, an abbreviated version that works for them is utilized.
- Closed-form solutions can result in accurate, cost-effective solutions.
- Considerable cost savings can be realized by substituting FEA for MIL-STD-883 screening tests. An example, showed cost savings from $25,000 to $50,000 for a lot of 1000 hybrids with 11 hybrid types.

4.0 ANALYSIS METHODS (PHASE 2)

4.1 Introduction

This phase of the study consisted of taking the information gained in Phase 1 in the form of programs, closed-form solutions, test data, and problems, and deciding which to use. The computer programs studied were those most pertinent to the microelectronic problems. Sample problems were then developed for evaluating these computer programs.

The topic of general purpose programs has been one of considerable interest since the power of the finite element first became recognized. The capabilities of today's programs are numerous and varied -- many programs have identical capabilities in several areas of analysis. Several programs provide excellent ability to solve problems in a limited area of structural mechanics, whereas others provide the ability to solve problems in many areas of structural mechanics. This makes the evaluation of general purpose programs a very difficult task. There are so many parameters involved that it is almost impossible to do a parameter study with all parameters included. Furthermore, many of the parameters involved are of a "subjective" nature and are difficult to quantify [69]. Therefore, the selection of a general purpose finite element program requires the user to identify his analysis needs -- it also usually involves some degree of personal preference. It is important that the user not restrict himself to selecting one program -- this is especially true if the user has wide-ranging analysis needs.

4.2 Criteria for Program Selection

Listed below are the requirements for program selection [58]. An ideal program with analysis capabilities in all areas would possess all the requirements below. However, no program has "complete" analytical abilities. A good program would, however, possess most of these requirements:

1. It should have proven capability for both linear static and linear dynamic response, including computation of natural frequencies. Desirable capabilities include (a) nonlinear static response, (b) nonlinear dynamic response, (c) stability (buckling), both static and dynamic, (d) thermal loading, and (e) heat transfer analysis.
2. A good library of planar and three-dimensional elements should be available. It should include:
    a. One-dimensional straight elements for axial loading,
    b. One-dimensional straight and curved elements, capable of resisting forces and moments in three dimensions,
    c. Plate and shell elements of various shapes, both for membrane and/or bending loading,
    d. Three-dimensional elements of various shapes and numbers of nodes,
    e. Axisymmetric elements and axisymmetric thin and thick shell elements, and

f. Geometrically nonlinear elements, such as gaps and tension-only or compression-only elements.

3. The capability for handling linear and nonlinear materials.
4. It should provide accurate answers.
5. It should solve problems quickly, with a minimum cost.
6. It should be readily available and have well-documented User's, Examples, and Theoretical Manuals.
7. Competent technical assistance must be available, either from the host computer center, from the program developers, or from the user's group.

The above-mentioned list of program attributes are necessary for program(s) performing the entire gamut of finite element analyses. For the specific case of finite element analysis of electronics equipment and microelectronics, in particular, the following program prerequisites are offered. The structural loadings should include statically applied forces, thermal loadings, sinusoidal vibration, random vibration, shock loading, and other generalized transient dynamic loadings. Therefore, a program must have capabilities for solving linear statics and dynamics problems with a wide variety of loading conditions.

When temperature distributions are necessary for a thermal stress analysis, steady state and transient heat transfer analyses become desirable program capabilities. Finally, many electronics equipment and materials (i.e., solder) exhibit nonlinear behavior. This makes the ability to solve nonlinear statics and dynamics problems a desirable program attribute. The area of nonlinear material behavior (especially that of solder) is a promising area for future work and needs more investigation. Typically, microelectronics problems involve models of the small-to-medium size range. This precludes the necessity for solving large models with huge numbers of elements.

4.3 Preliminary List of Programs Reviewed

Reviews of the majority of well-known programs available in the United States and Europe were completed. Below is the initial list of 21 programs that were reviewed during this study. Obviously, the best way to evaluate a program is to use it constantly over a long period of time. This would involve a substantial effort, and was considered beyond the scope of this study. Based on their capabilities, 12 programs from this initial list were then eliminated from further consideration and an interim list of nine programs was made. This interim list included most of the widely known general purpose programs. The programs in the interim list were reviewed in detail and five of these programs were then eliminated, forming a final matrix of four programs. The programs in the final matrix were further reviewed, including benchmark computer runs of these programs.

The programs reviewed are available on a wide variety of computer network systems. This general sense of wide availability makes it relatively easy for the analyst to use the program of his choice. Program capabilities are constantly being upgraded and increased. This makes it virtually impossible to easily compare program capabilities. Therefore, the program comparisons were based on available information that was current at the time of this writing.

The initial list of programs is shown below:

1. ABAQUS
2. ADINA
3. ANSYS
4. ASKA
5. COSA
6. EASE2

7. FINITE
8. MARC-CDC
9. MINIELAS
10. NASTRAN
11. NISA
12. NONSAP
13. PISCES
14. SAP IV
15. SESAM-69
16. SPAR
17. STAGS
18. STARDYNE
19. STRUDL II
20. STRUDL DYNAL
21. TEXGAP 3-D

4.4 Development of Interim Program List

The following is a list of the 12 programs eliminated from further consideration after reviewing the original 21 programs. After each program is a brief synopsis of program capabilities, along with reasons for that program's elimination from further consideration:

1. ASKA - This is a fairly large program that can perform both linear and nonlinear analyses [69]. It was developed in Germany [58] and has capabilities in dynamics analysis. It has an extensive element library, good mesh generation, and is especially effective with substructuring. However, it is a very large system requiring considerable user experience [58]. It is not readily available in the United States. A recent study [78] has further evaluated this program.

ASKA does not appear on any major computer network in the U.S. It appears not to have random vibration capabilities. This would make this program undesirable for microelectronic analysis.

2. COSA - This program appears to have been developed in Germany. It has a good element library and appears suitable for dynamic analysis. Very little information was available on this program [58]. Performing only dynamic analysis makes this program's use very limited for microelectronic analysis.

3. EASE2 - This is a program limited to linear statics and dynamics analysis [59]. It seems to be well-suited to large problems. Little information was found on this program. It does not possess heat transfer capabilities. However, it appears to have limited dynamic analysis features. A recent study [79] revealed that EASE2 does not have random vibration capabilities. It is, therefore, not a desirable program for microelectronics analysis.

4. MINIELAS - This is part of the ELAS system [58] and is limited to dynamic analysis. It is a special-purpose program designed for only random vibration analysis. It, therefore, has very limited capabilities and is not well suited for microelectronic analysis.

5. NONSAP - This program is limited to static and dynamic analysis of shell structures [58]. It is the forefunner of the ADINA program, to be

discussed later. Since microelectronic packages are not shell structures, this program is not suitable.

6. PISCES - This is a program that solves linear and nonlinear problems. It is especially strong where nonlinear materials are being analyzed [58]. However, it employs the finite difference method of analysis, rather than the finite element method. The finite difference method employs nodes, as does the finite element method. However, the finite difference method requires all the information concerning node connectivity (i.e., stiffness) to be fully defined. The finite element method uses model geometry, element properties, and material properties to compute these stiffnesses. The result is that structural analysis via finite elements is generally cheaper than that done with finite differences [79]. Structural analysis with finite differences has very limited applications and would not be cost-effective when analyzing microelectronics.

7. SESAM-69 - It was developed in Norway [58] and has applications primarily designed for super elements. It has limited nonlinear and dynamics capabilities [69]. This program has recently been evaluated [78]. It appears to be a specialty-type program with strong fracture mechanics capabilities. It does not appear to have random vibration capabilities, nor can prescribed accelerations be applied. This would make this program undesirable

for microelectronic analysis. A more current version of this program is SESAM-80.

8. SPAR - This is a series of small interactive programs for linear static and dynamic analysis [60]. It appears to have limited capabilities and does not compare well with the larger general purpose programs. Since this program concentrates on beam-like structures, it is unsuitable for microelectronic analysis.

9. STAGS - This program is limited to linear and nonlinear shell analysis [60]. It is similar to ANSYS [61] and is a good program for this limited application. It is also a finite difference program. The finite difference comments relating to the PISCES program also apply to STAGS. Since STAGS concentrates on shell structures, it is not suitable for microelectronic analysis.

10. STRUDL II - This is a program developed for the civil engineering community [62]. It has limited element properties and loadings with poor mesh generation capability [58]. It was a very popular program in the building industry. However, further developments on the program were stopped, due to lack of support. Mc Donnell-Douglas has developed and marketed its own version, and its use appears to be declining [58]. Since this program concentrates on civil engineering structures (especially frameworks [79]), it is not suitable for microelectronic analysis.

11. STRUDL DYNAL - This is the proprietary version of STRUDL II with emphasis on dynamic analysis [58]. All the previous comments on STRUDL II apply here, except that its capabilities have been improved by Mc Donnell-Douglas. However, it suffers from several deficiencies, including no transient analysis capability using direct integration. This makes STRUDL DYNAL unsuitable.

12. TEXGAP 3-D - This program was developed by the Air Force and is limited to linear and nonlinear statics analysis [61]. It has an element library oriented towards continuum analysis. It is a good program for performing thermal stress analysis. This program appears to be excellent when solving statics-only problems. Since this program cannot solve dynamics problems, its use would be very limited when performing microelectronics analysis.

4.5 Interim Program List

Below is the interim list of nine programs:

1. ABAQUS
2. ADINA
3. ANSYS
4. FINITE
5. MARC-CDC
6. NASTRAN
7. NISA
8. SAP IV
9. STARDYNE

The above programs were then reviewed in detail and five were eliminated from further consideration, forming a final matrix of four programs. These eliminated programs are summarized below, along with reasons for their elimination. The capabilities of the interim list of nine programs are considered "very good." This made it difficult to eliminate five of these programs from further consideration. The analyst should consider using one of the five eliminated programs when his specific analysis needs correspond with the specific strengths of one of these programs. For certain, specific, uncommon problems, the five eliminated programs possess capabilities that are considered "excellent" when performing microelectronic analysis.

1. ADINA - This is a program that performs linear and nonlinear static, dynamic, and heat transfer analysis [71]. It is particularly suited to nonlinear problems involving large displacements, large strains, and nonlinear materials [69]. However, it has a limited element library; it is difficult to obtain technical support; and is not especially user-oriented [68]. A recent study [72,73] of ADINA revealed the following: (1) it has well-written users and theoretical manuals, (2) it is easy for the user to add newly developed elements or materials, (3) it is efficient in handling simpler, linear problems, (4) it is relatively machine-independent, (5) it can be used for large problems, (6) it is well-suited as a research tool, (7) it has poor data generation and error checking features, (8) it has trouble with complex structures due to a limited element library, (9) its method for handling large deformation problems is incomplete; (10) it cannot handle the situation where load-deformation response exhibits softening behavior and then suddenly becomes stiffened, and (11) it is

difficult to determine the optimum time increment when solving nonlinear dynamics problems.

When considering microelectronics nonlinear problems (solder behavior, bottoming out, nonlinear springs, etc.), the ADINA program had deficiencies as noted by comments (7) through (11) above. Based on the findings of Dr. Chang [68,72,73] it was felt that ABAQUS was a more suitable program for nonlinear microelectronic analysis than ADINA.

2. FINITE - This is a program similar to STRUDL and is, therefore, oriented towards civil engineering problems. It solves both linear and nonlinear statics problems. Its dynamics capabilities are still being developed. It has a good element library and seems best equipped at solving nonlinear problems. However, elements for geometric nonlinearities are not yet available. Its strengths are in material nonlinear problems and in substructuring [70] and appears to be a good program when solving these types of problems. When geometric nonlinear elements and a dynamic analysis capability are added, it may become a good multi-purpose program. Until then, it is not considered a useful program for microelectronic analysis.

3. MARC-CDC - This program offers the most advanced technology for nonlinear static analysis [58,69]. Although it does have linear static and dynamic capabilities [64], it should be used primarily as a nonlinear analysis program. It has a good element library for one and two-dimensional problems. It

has a limited library, however, of three-dimensional elements [58,66,67]. Its dynamic capabilities are limited [58,64,69]. Some users reported the program was not easy to use and poorly documented [58,64,65,78], however, improvements have been made in recent versions. Agreement of results as calculated by MARC-CDC with experimental results indicates that a high degree of confidence can be placed in a MARC analysis [64]. When the dynamic capabilities are brought on a par with the static capabilities, the program may become a powerful tool for nonlinear dynamics analysis. Until then, MARC should only be used for solving those nonlinear microelectronic problems that cannot be handled by ABAQUS, ADINA, or ANSYS.

4. NASTRAN - This is probably the largest general purpose program available [63,64]. Three versions [78] of NASTRAN are available: (1) COSMIC, a version distributed by NASA, (2) a version distributed by Sperry-Univac, and (3) MSC, a version distributed by McNeal-Schwendler Corporation. It has been the subject of more discussion than any other program. Part of the reason for NASTRAN's popularity could be because use of this program has been required on many NASA and nuclear power contracts. It provides a wide base of analysis capabilities with emphasis on aerospace problems. This program, however, requires extensive user experience [58,64]. It is basically a linear program, capable of static, dynamic, buckling, heat transfer, hydro-elastic, and aeroelastic analysis [61,63]. Its documenta-

tion is extensive, but its size is likely to scare the potential user [58,64,65]. It is expensive for solving smaller problems [58], and is, therefore, better suited for larger problems. NASTRAN is not considered a user-oriented program [78]. Its use should be limited to large problems, or those involving special capabilities, such as aeroelasticity. It does not do a good job of solving sinusoidal and random vibration response problems [61].

Concerning microelectronic analysis, the following reasons are given explaining why NASTRAN is not a suitable package. It is difficult to use and requires a lot of experience for effective use. This makes NASTRAN hard to use for the inexperienced analyst or the experienced analyst not familiar with NASTRAN. Microelectronic problems are typically of the small-to-medium size range. NASTRAN is not cost effective in solving smaller problems. Its wide-ranging capabilities make it difficult for the user to locate the portion of the program suited to his needs (bigger is not necessarily better for finite element software). Microelectronics packages nearly always experience sinusoidal or random vibration, and NASTRAN is not particularly effective when solving these problems.

5. SAP IV - A more current version of this program is SAP VI. However, applicable information was obtained only for the SAP IV version. This program performs linear static and dynamic analysis. Users report that it is easy to use [58,64,68]. It is

the _only_ program that is simple enough that users have tried to modify it to suit their needs [58,64]. It is therefore useful for research-type problems requiring considerable interface with user routines. However, it has limited dynamic capabilities [58]. These limited capabilities include no Guyan reduction, only one method of eigenvalue extraction (subspace iteration), only one value of damping can be used for transient analysis, and centrifugal loadings are not available. SAP IV does not appear to have heat transfer analysis capabilities. It is most useful when applied to small or medium-sized linear problems. When compared with other programs, STARDYNE was ranked first while SAP IV was ranked third in order of preference when consideration to solving small-to-medium range dynamics problems was given [58]. Due to its limited dynamics capabilities and its comparison with other programs solving small-to-medium range dynamics problems, SAP IV was found to be a less desirable program than STARDYNE for microelectronic analysis.

The five programs that have just been eliminated from the interim program list are all very good general purpose programs within the limitations already discussed. Their use should only include problems that address these program's strengths.

4.6 Final Program List

Below is the 1st of the four programs that remain, along with a brief description of each program's _primary_ functions:

1. ABAQUS - nonlinear statics and dynamics analysis
2. ANSYS - general purpose (linear and nonlinear statics and dynamics and heat transfer analysis)

3. NISA - general purpose (linear and nonlinear statics and dynamics and heat transfer analysis)
4. STARDYNE - linear statics and dynamics analysis

The following is a detailed summary of each program's capabilities, strengths, and weaknesses.

1. ABAQUS - This program [74] performs linear and nonlinear static, dynamic, and heat transfer analysis. It is best suited for nonlinear problems encountered in static and dynamic analysis. It can solve the three types of nonlinear problems: (1) material nonlinearities, (2) geometric nonlinearities, and (3) large displacements and rotations. It has a good element library including axisymmetric elements. It has a full range of material models including viscoelastic, elastic-plastic, creep, and volumetric swelling. It has the capability of following a static analysis with a dynamic analysis (and vice versa), such as in the dynamic response of preloaded structures. It can solve linear or nonlinear heat transfer problems and can provide temperatures for loading a thermal stress analysis model.

   Dr. Chang [68] had the following comments about ABAQUS: (1) it is the best program for nonlinear problems, (2) it has a hotline which provides excellent technical support, (3) it is easier to use than ANSYS, (4) it has a better element library than ADINA, and (5) it is user-oriented and is easier to use than ADINA. Dr. Chang is currently doing a study on ABAQUS. His interim report was not yet available at the time of this writing.

The user manual appears to be well-written with good example problems. Slight difficulty was noted in interpreting program commands. Free format input makes data generation simple. It appears that ABAQUS is a user-oriented program. Its use should be limited to nonlinear microelectronics behavior such as solder behavior, bottoming out, or nonlinear springs.

2. ANSYS - This program [75] is a large general purpose package that provides linear and nonlinear static and dynamic and heat transfer analysis. It is used heavily in the nuclear industry. It performs linear and nonlinear elastic analysis of structures subjected to static loads as well as transient and harmonic dynamic excitations. It does not perform random vibration response analysis. The program considers the nonlinear effects of plasticity, creep, swelling, and large deformations. Transient and steady state heat transfer analyses consider conduction, convection, and radiation effects. Coupled thermal-electric and wave motion analysis capabilities are available. ANSYS also predicts steady state and transient fluid flow in one-dimensional networks. Temperatures obtained from thermal analyses can be input as loadings for static stress analyses.

It is considered a versatile program [58] with a wide variety of engineering applications possible. Its strength is its comprehensive element library. It appears to have the most complete library of heat transfer elements available. It has excellent node and element generation capabilities.

It has a well-written user's manual and an excellent, thorough examples manual. It is relatively user-oriented, and excellent technical support is available. ANSYS will be best utilized for microelectronics problems involving heat transfer solutions as inputs for thermal stress calculations. We have used the axisymmetric elements for microelectronics thermal stress analysis [81] and found the program to be excellent.

3. NISA - This program [76] is a large general purpose program that provides linear and nonlinear static and dynamic and heat transfer analysis. It has an extensive element library including isoparametric linear, parbolic, cubic, linear parabolic, linear parabolic cubic, etc. for plane stress and plain strain problems. Additional elements include axisymmetric (with symmetric or unsymmetric loading), general shells, laminated composite or sandwich shells, thick shells, solids, beams, spars, springs, mass elements and rigid elements. A unique program feature is its treatment of composite and sandwich structures. It has good node and element generation capabilities [58].

NISA can solve nonlinear problems involving geometric or material nonlinearity or both. Dynamic analysis capabilities include eigenvalue/eigenvector extraction, transient analysis, shock spectrum analysis, harmonic analysis, and random vibration analysis. Heat transfer capabilities include steady state and transient problems involving conduction, convection, and radiation. Temperatures obtained from thermal analyses can be input as loadings to static stress analyses. A recent study [79] found NISA to be the best program for analyzing tactical shelters.

It appears to have a well-written user's manual and seems to be a user-oriented program. An extensive examples and verification manual is available with several good example problems illustrated. Good technical support is available. NISA appears well-suited for solving the myriad of microelectronics problems. Its only apparent limitations are in solving highly nonlinear problems.

4. <u>STARDYNE</u> - This program [77] performs linear static and dynamic analysis. It has limited nonlinear static and dynamic capabilities. Nonlinear problem applications are limited to geometric nonlinearities such as gaps and bottoming out of adjacent structures. It has a strong ability, however to solve dynamics problems. The program has a simple, yet good, element library with enough elements to describe most structures under static or dynamic loading. The same model can be used for static and dynamic analysis, saving time, eliminating errors, and saving computer costs.

Dynamic analysis capabilities include eigenvalue/eigenvector extraction, transient analysis, shock analysis, harmonic analysis, random vibration analysis, and shock spectrum analysis.

It is considered to have the best ability for solving sinusoidal vibration response and random vibraton response problems [61]. It has a very efficient method for extracting natural frequencies and mode shapes [69]. It was rated the best general purpose program for solving small to medium-sized dynamics problems [58]. STARDYNE does not have heat transfer capabilities. However, it is capable of performing thermal stress analysis.

The program's strengths are its simplicity, its efficient solution of dynamics problems, and the fact that it is extremely user-oriented. The user's manual is well-written and provides a simplified tool for learning the program. There is an excellent learner's manual, examples manual, and theoretical manual available. STARDYNE is one of few programs that can be learned by simply reading the user's manual.

Since STARDYNE is particularly adept at solving small-to-medium range statics and dynamics problems, it is probably the best program for performing the majority of microelectronics finite element analyses. The writers have used STARDYNE for solving general electronics packaging and microelectronics packaging problems [81], and have found the program to be excellent.

4.7 Comparison of Final Program Capabilities

To compare program capabilities, tables of parameters were made in the following areas:

1. Types of Analysis
2. Material Properties
3. Element Library

4. Types of Loading
5. Data Input and Output
6. Documentation

These program capabilities are summarized in Tables 9 through 14 which follow.

4.8 General Summary of Analysis Methods (Phase 2)

1. A review of 21 general purpose finite element programs resulted in an interim list of nine programs. Five programs - ADINA, FINITE, MARC-CDC, NASTRAN, and SAP IV - were then eliminated from further consideration. These five programs were rated "very good"; however, their use should only include those unique microelectronic problems that address specific program strengths.

2. The four recommended programs are ABAQUS, ANSYS, NISA, and STARDYNE. These recommended programs will best be utilized when performing the following types of microelectronic analyses:
   a. ABAQUS - nonlinear statics and dynamics. Nonlinear effects may include material nonlinearities such as a solder creep, geometric nonlinearities, such as a substrate bottoming out on a module, and large displacement nonlinearities, such as a hybrid lead bending under load.
   b. ANSYS - linear and nonlinear statics and dynamics and heat transfer. ANSYS is best suited for heat transfer analysis where generated temperatures can be used as inputs for a thermal stress analysis such as required

Table 9. Types of Analysis

CAPABILITY	ABAQUS	ANSYS	NISA	STARDYNE
	PROGRAM			
Linear Statics	X	X	X	X
Thermal Stress	X	X	X	X
Nonlinear Statics	X	X	X	X
Geometric	X	X	X	X
Material	X	X	X	
Large Deflection	X	X	X	
Linear Dynamics	X	X	X	X
Modal Extraction	X	X	X	X
Transient		X	X	X
Harmonic		X	X	X
Random Vibration			X	X
Shock Spectra			X	X
Nonlinear Dynamics	X	X	X	X
Transient	X	X	X	X
Geometric	X	X	X	X
Material	X	X	X	
Large Deflection	X	X	X	
Buckling	X	X		
Linear Heat Transfer	X	X	X	
Nonlinear Heat Transfer	X	X	X	
Fluid Flow		X		

Table 10. Material Properties

CAPABILITY	PROGRAM ABAQUS	ANSYS	NISA	STARDYNE
Linear Elastic	X	X	X	X
Isotropic	X	X	X	X
Anisotropic	X	X	X	X
Orthotropic		X	X	X
Temperature-Dependent		X	X	
Plastic	X	X	X	
Viscoelastic	X	X		
Creep	X	X		
Swelling	X	X		
Sandwich		X	X	X
Composite			X	

Table 11. Element Library

CAPABILITY	PROGRAM			
	ABAQUS	ANSYS	NISA	STARDYNE
Bar Element	X	X	X	X
Beam Element	X	X	X	X
Membrane Plate Element	X	X	X	X
Bending Plate Element	X	X	X	X
Thin Shell Element	X	X	X	X
Thick Shell Element		X	X	
Isoparametric 8 Node Solid	X	X	X	X
Isoparametric 20 Node Solid	X	X	X	
Axisymmetric Shell Element		X	X	
Axisymmetric Solid Element	X	X	X	
Pipe Element		X		X
Gap Element	X	X	X	X
Friction Element	X	X		
Spring, Mass, Damper Elements		X	X	X

Table 12. Types of Loading

CAPABILITY	PROGRAM ABAQUS	ANSYS	NISA	STARDYNE
Point Loads	X	X	X	X
Line Loads	X	X		X
Surface Loads	X	X	X	X
Volume Loads	X	X		X
Thermal Loading	X	X	X	X
Centrifugal Loads	X	X	X	X
Axisymmetric Loads	X	X	X	
Prescribed Displacements	X	X	X	X
Elastic Foundation		X		
Time Dependent	X	X	X	X
Deformation Dependent		X		
Contact	X	X	X	
Friction	X	X	X	

Table 13. Data Input and Output

CAPABILITY	ABAQUS	ANSYS	NISA	STARDYNE
Input				
Node Generation	X	X	X	X
Element Generation	X	X	X	X
Load Generation	X	X	X	X
Interactive Graphics	X	X	X	X
Restart Capability	X	X	X	X
Free Format Input	X	X	X	
Plot Routines	X	X	X	X
Data Input Check	X	X	X	X
Output				
Numerical Results	X	X	X	X
Graphical Results	X	X	X	X
Plotting				
Deformed, Undeformed	X	X	X	X
Temperature, Stress Contours	X	X	X	X
Dynamic Response	X	X	X	X

Table 14. Documentation

CAPABILITY	PROGRAM			
	ABAQUS	ANSYS	NISA	STARDYNE
User's Manual	X	X	X	X
Programmer's Manual				X
Theoretical Manual		X		X
Sample Problems Manual	X	X	X	X
Verification Manual		X	X	
Technical Support Available	X	X	X	X

when analyzing bonded MIC or stripline substrates.

c. NISA - linear and nonlinear statics and dynamics and heat transfer. NISA is best suited for analyzing composite or sandwich structures such as a circuit board with layered copper circuit runs.

d. STARDYNE - linear statics and dynamics. STARDYNE is best suited for analyzing dynamics problems such as circuit board response and hybrid lead dynamic stresses due to random or sinusoidal vibration.

3. STARDYNE is the best program for analyzing the majority of microelectronic problems.

4. The area of nonlinear analysis - particularly solder material effects - is a promising area for future work and should be investigated.

5.0 SAMPLE PROBLEM ANALYSIS (PHASE 2)

5.1 Introduction

This section of the report will discuss each of the four sample problems. The finite element models used for each problem will be explained, and the results from the different finite element programs will be compared with each other, and also with the theoretically correct results.

The sample problems were chosen using the following criteria: (1) they must represent typical analysis problems associated with microelectronic packaging, and (2) they should be simple enough that a theoretically "correct" answer is available for comparison. Consistent with these criteria, four problems were chosen from the general categories of linear statics, linear dynamics, linear steady-state heat transfer, and nonlinear statics.

Theoretically correct answers were only available for the problems of the first three categories mentioned above. The analysis approach was to determine program accuracy by comparing computed and theoretical answers, and to note any program idiosyncrasies. Noting the simplicity of these problems, the approach was not to determine "blanket" conclusions about a specific program's ability to solve a specific class of problems. Instead, it was desirable to note any situation where a program's solution was radically different from the other's.

The NISA program is capable of solving all the above types of problems. However, it was not available on either the Control Data Cybernet or the Harris computer networks. Therefore, NISA was not evaluated using sample problems. Of the remaining three programs, all can solve each of the above problems (with the exception of STARDYNE, which cannot solve heat transfer problems). Below is a description of the various sample problems.

5.2 Sample Problem Descriptions

Each of the sample problems is described in the following paragraphs; detailed discussions of these problems will follow in Sections 5.3 through 5.6.

5.2.1 Linear Statics Problem

Hybrid designs are frequently assessed by applying a uniform external pressure to the package. Therefore, it follows that the design engineer may need to determine the stresses and deflections in the hybrid lid due to the pressure loading. Theoretically, this is the classic problem of a plate bending under static loading. As a first (and possibly conservative) approximation, the engineer may assume the lid has four simply supported edges.

To compare the finite element solution to the theoretically correct answer, only the deflections will be considered. The finite element model was purposely made with a relatively coarse grid, and the stresses obtained with this model will reflect this coarseness. This problem is physically described in Figure 12.

5.2.2 Linear Dynamics Problem

Many microelectronic packages are mounted to printed circuit boards. Since most electronics equipment is evaluated by dynamic testing, it is desirable to determine the dynamic characteristics of a particular package. If the package is mounted to a circuit board, the first step in this process is to determine the board's natural frequencies and mode shapes.

For this problem, the first four natural frequencies of the circuit board will be calculated and compared to the theoretically correct solutions (note that for most situations, it is the first few low-frequency modes that represent the greatest damage potential to the system). In addition to the natural frequencies, the corresponding mode shapes will also be described.

This problem is shown pictorially in Figure 13; it represents a 0.50 lb., G-10 epoxy/fiberglass printed circuit board.

5.2.3 Heat Transfer Problem

Pin fins are commonly used in electronics applications to remove heat from temperature-sensitive areas. It is commonly desired to determine the effectiveness of a particular

Material: KOVAR
Young's Modulus = 20×10^6 psi.
Poisson's Ratio = 0.3

Loading: Uniform exterior pressure of 30 psi.

Support: All four edges simply supported

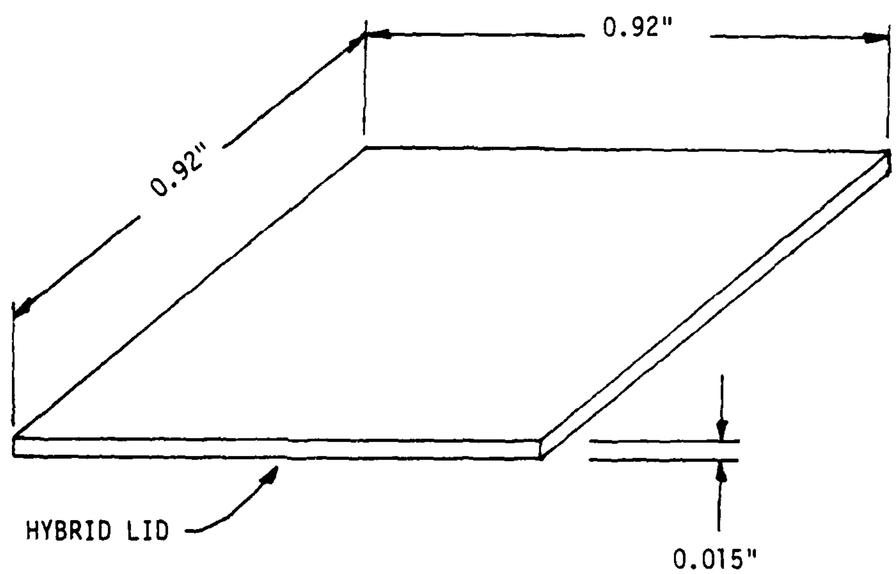

Figure 12. Linear Statics Problem

Material: G-10 EPOXY FIBERGLASS
Young's Modulus = 2.5×10^6 psi
Poisson's Ratio = 0.12
Total Weight = 0.50 lb.

Support: All four edges simply supported

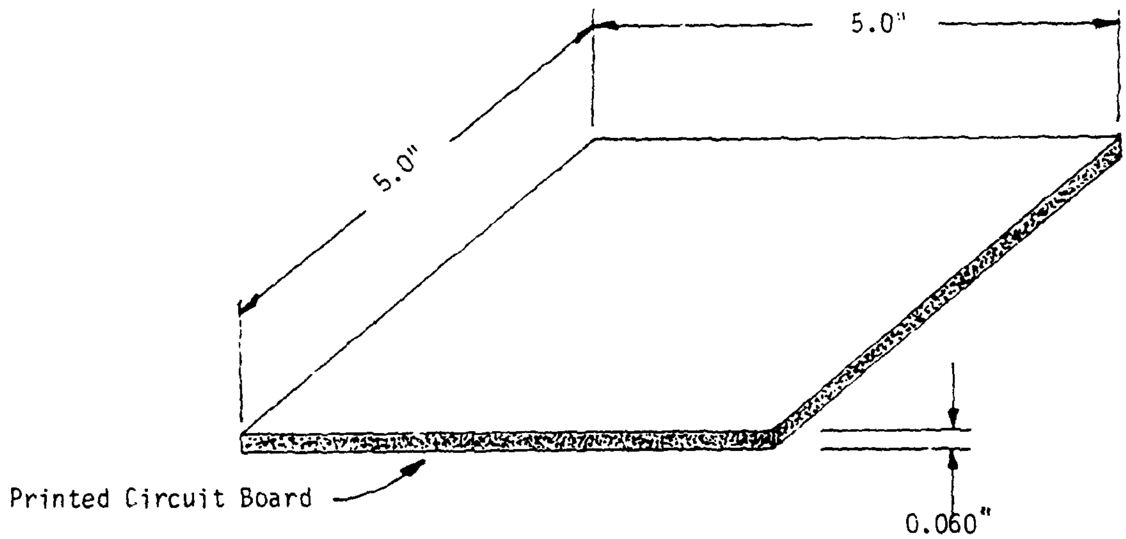

Figure 13. Linear Dynamics Problem

pin fin design; i.e., it is desired to know the heat flux allowed by a particular fin design.

Theoretically, this problem is that of a one-dimensional bar with both conductive and convective heat transfer capabilities. We will calculate both the heat flux and the temperature distribution of the fin, and the solution will be compared to the theoretically correct results. The particular fin used for this problem is described in Figure 14.

5.2.4 Nonlinear Statics Problem

This problem is concerned with a typical design where a substrate is mounted in a module. The substrate is attached to the module with four screws (one per substrate corner), and it is mounted to small bosses in the module such that the substrate is supported off the module floor.

This problem is considered to be nonlinear because it exhibits different responses depending upon the direction of loading. For instance, in the event of an upward load (produced by a downward acceleration of the module), the substrate is restrained by the four mounting screws only. However, in the case of a downward load, it is possible that the center of the substrate may deflect enough to contact the module floor. Thus, should the substrate-to-module gap be closed, the boundary conditions must consider the effect of the module floor in addition to the four mounting screws.

From a static standpoint, the most likely environment to produce the above-discussed responses is a constant acceleration. The 20,000g acceleration chosen for this problem is consistent with that found in MIL-STD-883B, Method 2001.2, Test Condition D. The substrate is physically described in Figure 15.

MATERIAL 6061-T6 Aluminum

Conductivity = 96 Btu/hr ft°F

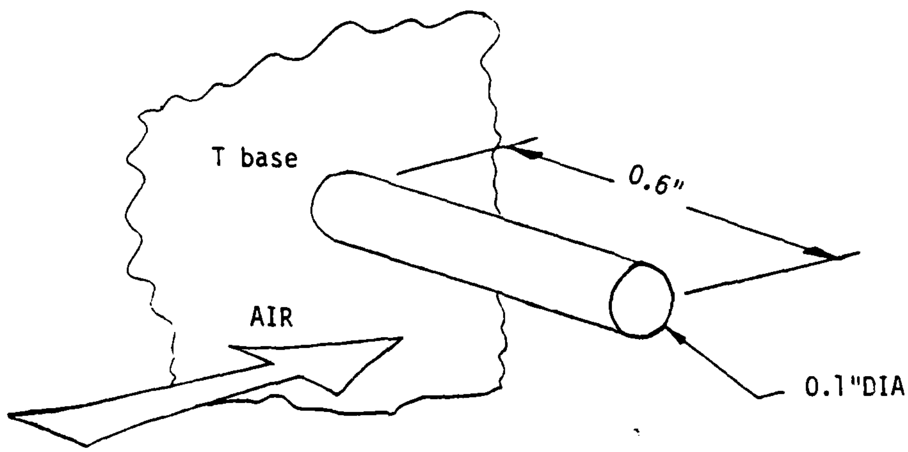

AIR FLOW

Flow Speed = 200 fpm
Flow Temperature = 131°F
Heat Transfer Coefficient = 12.7 Btu/hr·ft^2·°F (For both the circumferential surface area and the end surface area)

IMPOSED BOUNDARY CONDITION

Constant base temperature = 176°F

Figure 14. Heat Transfer Problem

Material: 771 ALUMINA
Young's Modulus = 43×10^6 psi
Poisson's Ratio = 0.3
Weight Density = 0.14 lb/in^3

Loading: Constant acceleration of 20,000 g's in either direction perpendicular to the substrate

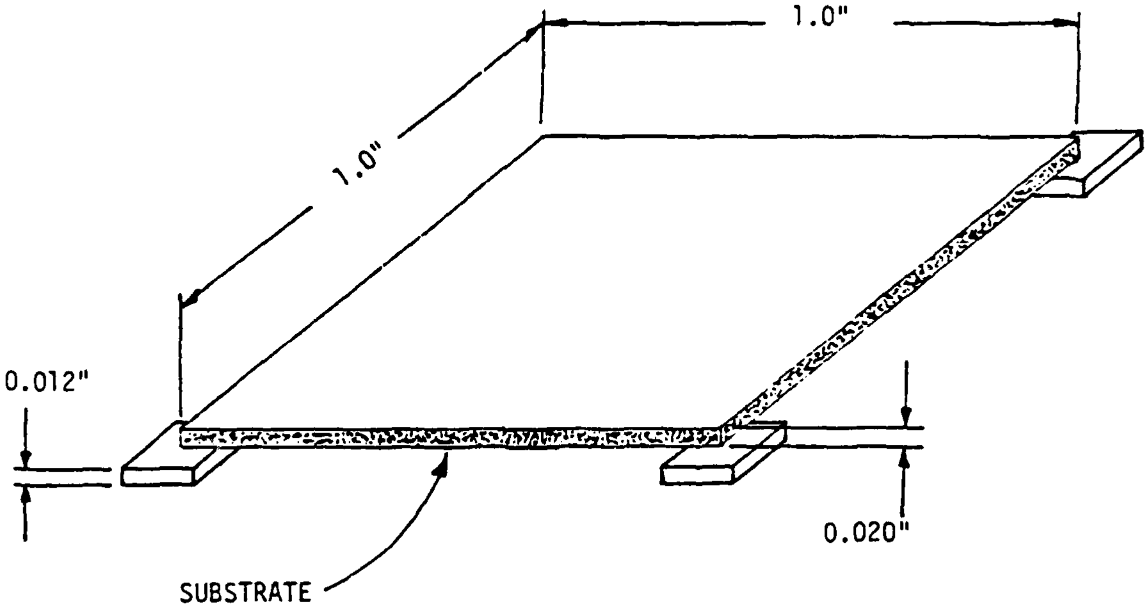

Support: Fixed support at all four corners

Displacement Restraints:
1) Upward load - none
2) Downward load - vertical translational restraint if gap is closed

Figure 15. Nonlinear Statics Problem

5.3 Sample Problem #1 - Linear Statics

The linear statics sample problem involved the determination of the deflection for a hybrid lid due to a 30 psi pressure loading. This problem was solved using the following finite element programs: (1) STARDYNE, (2) ANSYS, and (3) ABAQUS. Due to the symmetry of the chosen hybrid lid, a "cuarter" model was used without any loss of accuracy; this model is shown in Figure 16.

As shown in Figure 16, the cuarter model for the hybrid lid consists of sixteen nodes and nine cuadrilateral plate elements. The boundary conditions for the four edges of the model were grouped into two classifications: Those necessary to represent the simply-supported edges, and those necessary to provide continuity along the two lines of symmetry. Edge 1-2-3-4 and edge 1-5-9-13 were allowed to rotate about the X-axis and the Y-axis respectively; all other degrees-of-freedom (DOF) were assumed to be fully restrained for these nodes. Also, due to the hybrid lid symmetry, edge 4-8-12-16 was not allowed to translate in the X-direction, nor was it allowed to rotate about the Y-axis (the slope of edge 4-8-12-16 in the X-direction is constrained to be zero by symmetry). Similarly, edge 13-14-15-16 was restrained against Y-direction translations and X-axis rotations. These edge restraints resulted in node 16 being free only to translate in the Z-direction since it is located at the intersection of the two lines of symmetry.

In addition to the boundary conditions listed above, one additional restraint was recuired to prevent any nodal rotations about the axis perpendicular to the plane of the lid. STARDYNE utilizes a plate element which has 5 DOF (degrees of freedom) per node; there is no stiffness associated with rotations about an axis perpendicular to the plate. Therefore, when using STARDYNE, it is necessary to restrain this rotational DOF to prevent singularity problems from arising during the

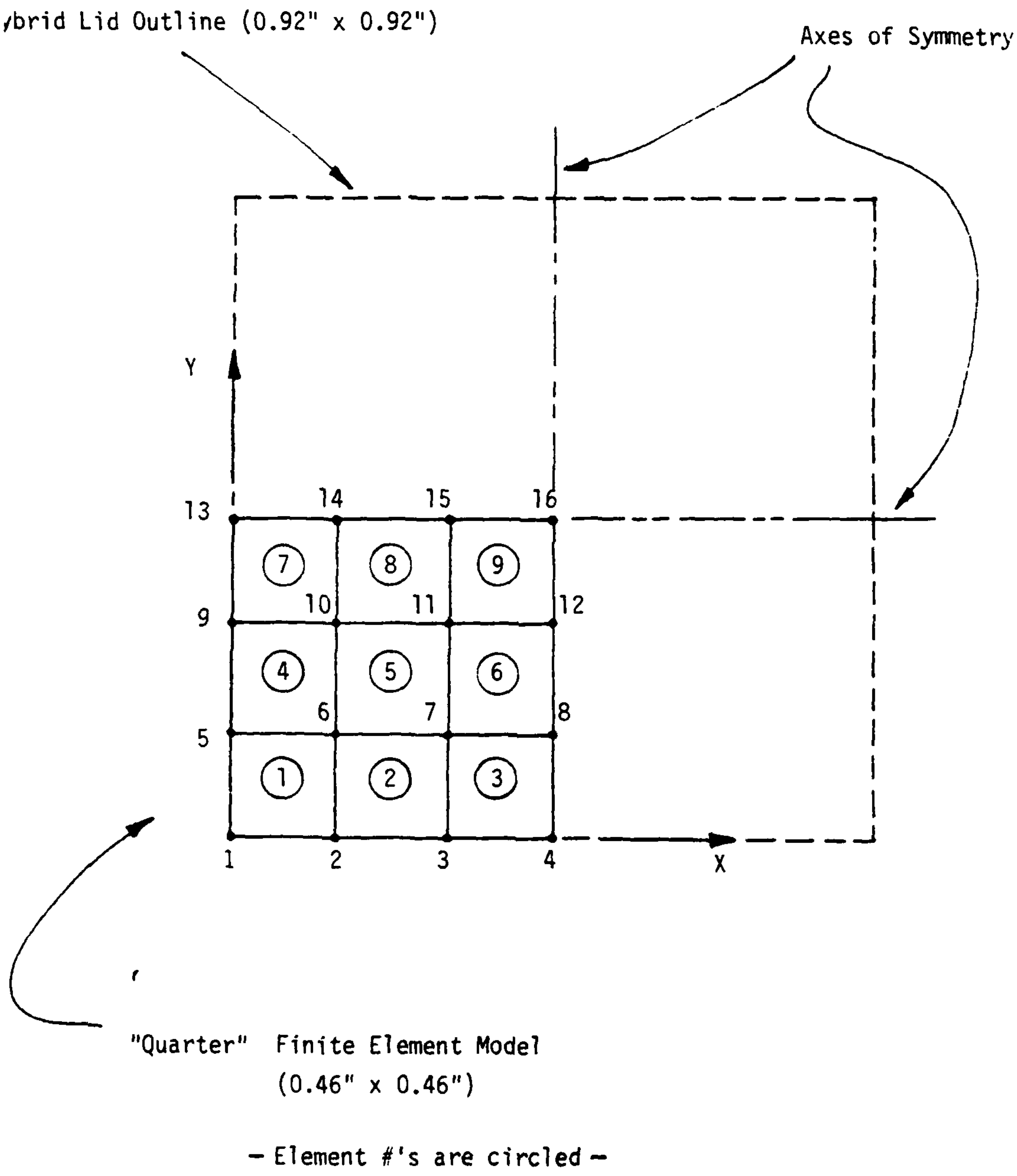

Figure 16. Hybrid Lid Finite Element Model

matrix solution. Similarly, the plate elements of ABAQUS have only 5 DOF per node, and the rotational DOF about the normal axis must be restrained (ABAQUS will automatically restrain this DOF if necessary). On the other hand, ANSYS provides an option for including a small rotational stiffness for rotations normal to the plane of the plate. However, as discussed in the ANSYS manual, this rotational stiffness is usually the least important of all stiffness components for the element and may be safely neglected. Therefore, to keep the finite element model of the lid consistent for each of the three programs, rotations about an axis perpendicular to the plane of the lid were restrained for all solutions.

The remaining physical and material properties reouired for this analysis are shown below in Table 15.

Table 15. Physical and Material Properties

Physical Dimensions	0.92" x 0.92" x 0.015"
Plate Type	Bending and Membrane
Material	Kovar
Young's Modulus	20×10^6 psi
Poisson's Ratio	0.3
Loading	30 psi Pressure

As shown in Table 15, the plates used for this finite element model had both bending stiffness and membrane stiffness. In each case, the ouadrilateral plate element which was used had four nodes per element. The element used for the STARDYNE analysis was the "QUAD" element, the element used for the ANSYS analysis was the "STIF43" element, and the element used for the ABAQUS analysis was the "S4R" element. Although both ANSYS and ABAQUS offer 8-node-per-element quadrilateral plate elements, the more simple 4-node-per-element plate elements were used in order to provide a valid comparison with STARDYNE's 4-node quadrilateral element.

A listing of the required input for each of the three finite element programs is shown in Figures 17 through 19. Both STARDYNE and ANSYS require a fixed format input, while ABAQUS has a free format option. For a complete understanding of these listings, refer to the appropriate user manual [82], [83],[84].

The nodes and elements for this model were generated more rapidly by ANSYS than by STARDYNE or ABAQUS. The "second level generation" capability of ANSYS was used for generating the model's elements and nodes (ANSYS also provides "third level generation" capability for three-dimensional gridworks). For example, nodes 1 through 4 were defined by specifying the locations of node 1 and node 4, and then telling the program to generate a total of four equally spaced nodes along the defined line. Next, the remaining twelve nodes were defined by telling the program to repeat the nodal set of nodes 1-4 an additional three times, incrementing the Y-coordinate by 0.1533" each time. Similarly, elements 1-3 were generated by copying element 1 twice, and then repeating the element set 1-3 twice.

STARDYNE has less node and element generation capability than ANSYS, although for this problem the difference was not great. STARDYNE allowed second level generation of the nodes using its NODEGRD option, but this program is limited to first level generation of elements (three separate commands were required to generate elements 1-3, 4-6, and 7-9).

ABAQUS has the least amount of generation capability among the three programs of interest; ABAQUS provides first level generation of nodes and elements only. However, this should not be considered a significant limitation of the program. For many structures analyzed with finite elements, the geometry is too complex to lend itself to a large amount of node or element generation. It is only for large, repetitive, "gridwork-type" models that generation can save the analyst a significant amount of time and effort.

5.3.1 Results for Sample Problem #1

Table 16 shows the computed transverse deflections for each of the nine nodes with an unrestrained z-translational DOF. The deflection at node 16 is the maximum deflection at the center of the hybrid lid.

Table 16. Deflections of a Hybrid Lid (inches)

Node	STARDYNE	ANSYS	ABAQUS	Theoretical
6	.003779	.003960	.003772	-
7	.006337	.006620	.006383	-
8	.007224	.007540	.007289	-
10	.006337	.006620	.006383	-
11	.010679	.011149	.010857	-
12	.012194	.012726	.012426	-
14	.007224	.007540	.007289	-
15	.012194	.012726	.012426	-
16	.013931	.014538	.014239	.014137
Dev*	-1.457%	+2.837%	+0.722%	

*Percent deviation of the computed deflection for node 16 from the theoretical maximum deflection at the center of the lid

As shown in the above table, the computed values of the maximum lid deflection are all within 3% of the theoretical solution. The theoretical solution was that found in the 5th edition of Formulas for Stress and Strain by R. J. Roark [85]. The solution is detailed on page 83.

```
                                      *** STARDYNE 3.0      INPUT ***
          /------------------------------- CARD  IMAGE  --------------------------------------/
          1  4   8  12  16  20  24  28  32  36  40  44  48  52  56  60  64  68  72  76  80
          *  *   *   *   *   *   *   *   *   *   *   *   *   *   *   *   *   *   *   *   *
CARD NO   ***********************************************************************************   CARD TYP
       2   RADC SAMPLE PROBLEM 1 ... HYBRID LID UNDER UNIFORM PRESSURE   (STARDYNE)                  RADC
       3  MATLG        1 KOVAR          20.E6        .3       .302                                  MATLG
       4  END                                                                                       END
       5  NODEGRD1     1   4                                   .46                                  NODEG
       6  NODEGRD2    13  16   4                  .46          .46      .46                         NODEG
       7  END                                                                                       END
       8  RESTG        1         111111                                                             RESTG
       9               2   3      11 11                                                             RESTG
      10               4         111 11                                                             RESTG
      11               5   9   41 11 1                                                              RESTG
      12              13         1111 1                                                             RESTG
      13               6   7          1                                                             RESTG
      14              10  11          1                                                             RESTG
      15               8  12   41    11                                                             RESTG
      16              14  15      1 1 1                                                             RESTG
      17              16         11 111                                                             RESTG
      18  END                                                                                       END
      19  QUAD8        1   3   1       2       6       5       1   1    .015      2                 QUAD8
      20               4   6   5       6      10       9                                            QUAD8
      21               7   9   9      10      14      13                                            QUAD8
      22  END                                                                                       END
      23  ENDGEOM                                                                                   ENDGE
      24   HYBRID LID UNDER 30 PSI UNIFORM PRESSURE                                                  HYBR
      25  STATIC                            1                                                       STATI
      26   HYBRID LID UNDER 30 PSI UNIFORM PRESSURE                                                  HYBR
      27  QPRS         1   9   1      30.                                                           QPRS
      28  END                                                                                       END
      29  END CASE                                                                                  END C
      30  ALL DONE                                                                                  ALL D
      31  OUTPUT           1                       2                                                OUTPU
      32  ENDMODEL                                                                                  ENDMO
```

Figure 17. STARDYNE Input Listing for Problem #1

```
**********  ANSYS INPUT DATA LISTING (TAPE18)  **********

     6     12    18    24    30    36    42    48    54    60    66    72    78
     V     V     V     V     V     V     V     V     V     V     V     V     V
RADC SAMPLE PROBLEM 1 ... HYBRID LID UNDER UNIFORM PRESSURE   (ANSY  )
J.R. SOUTHLAND    0      0
   0  0 00 0 0 0 1 0 0   099          0   0                         0 0  0
          70          70                                 0            0 0 0
  1 43010  0
 -1
     -2                                                            3  4  3
     1     2     6     5                       1     1    0 0    3  1  1
        .015                                       0
     -1
     4-2 4 4          0.15333333333        0
     1 0 0            0          0         0
     4 0 1          .46          0         0
     -1
  EX   1   0       20.E6
  EY   1   0       20.E6
NUXY   1   0          .3
ALPX   1   0          0
ALPY   1   0          0
DENS   1   0        .302
  END
  1  0  1  1
                                                                           0
     1   UX           0                        UY    UZ  ROTX  ROTY  ROTZ
     2   UY           0                 3   1  UZ  ROTY  ROTZ
     4   UX           0                        UY    UZ  ROTY  ROTZ
     5   UX           0                 9   4  UZ  ROTX  ROTZ
    13   UX           0                        UY    UZ  ROTX  ROTZ
     8   UX           0                12   4 ROTY ROTZ
    14   UY           0                15     ROTX ROTZ
    16   UX           0                        UY  ROTX  ROTY  ROTZ
    -1
    -1
     1     1        30.                 9   1
    -1
END
FINISH
```

Figure 18. ANSYS Input Listing for Problem #1

A B A Q U S   I N P U T   E C H O

P A G E   1

```
        5    10   15   20   25   30   35   40   45   50   55   60   65   70   75
-----------------------------------------------------------------------------------
*HEADING
 RADC SAMPLE PROBLEM 1 ... HYBRID LID UNDER UNIFORM PRESSURE    (ABAQUS)
*NODE
    1         0.0         0.0         0.0
    4         .46         0.0         0.0
   13         0.0         .46         0.0
   16         .46         .46         0.0
*NGEN
    1,13,4
    4,16,4
    1,4
    5,8
    9,12
   13,16
*ELEMENT, TYPE=S4R
    1,1,2,6,5
*ELGEN, ELSET=ALL
    1,3,4,3
    1,3
    4,3
    7,3
*SHELL SECTION, ELSET=ALL
      .015
*MATERIAL, ELSET=ALL
*ELASTIC, TYPE=ISO
     20.E6        0.3
*BOUNDARY
1,1,5
2,2,3
2,5,6
3,2,3
3,5,6
4,1,3
4,5,6
5,1
5,3,4
5,6
9,1
9,3,4
9,6
13,1,4
13,6
8,1
8,5,6
12,1
12,5,6
14,2
14,4
14,6
15,2
```

Figure 19. ABAQUS Input Listing for Problem #1

P A G E   2

```
      5    10    15    20    25    30    35    40    45    50    55    60    65    70    75
-------------------------------------------------------------------------------------------
15,4
15,6
16,1,2
16,4,6
*STEP, LINEAR=NEW
APPLIED PRESSURE OF 30 PSI ON THE HYBRID LID
*STATIC, PTOL=3
*DLOAD
  ALL     P        30.
*PRINT
*EL PRINT
*NODE PRINT
*END STEP
-------------------------------------------------------------------------------------------
      5    10    15    20    25    30    35    40    45    50    55    60    65    70    75
-------------------------------------------------------------------------------------------
```

Figure 19. ABAQUS Input Listing for Problem #1 (continued)

$$y_{max} = \frac{-\alpha q b^4}{Et^3}$$

where:

α	=	0.0444 for a/b = 1.0
q	=	30 psi pressure
b	=	0.92"
E	=	20 x 10^6 psi
t	=	0.015"

The results shown in Table 16 indicate that ABAQUS most closely approached the value of the theoretically-correct maximum deflection, followed closely by STARDYNE and ANSYS.

A second comparison which could be made between each of the three numerical solutions concerned the deflection shapes of the deformed lid. The deflection shapes presented in Table 17 are based on the maximum deflection for each solution being normalized to a value of 1.0.

As shown in Table 17, the deflection shapes are all very similar. STARDYNE and ANSYS have the least deviation between their deflection shapes; the largest deviation between their normalized values is 0.516% at node 6. The deviations between ABAQUS and both STARDYNE and ANSYS are only slightly larger.

Table 17. Deflection Shape of a Hybrid Lid

Node	STARDYNE	ANSYS	ABAQUS
6	0.2713	0.2724	0.2649
7	0.4549	0.4554	0.4483
8	0.5186	0.5186	0.5119
10	0.4549	0.4554	0.4483
11	0.7666	0.7669	0.7625
12	0.8753	0.8754	0.8727

AD-A117 979 HARRIS CORP MELBOURNE FL GOVERNMENT INFORMATION SYST--ETC F/G 9/5
FINITE ELEMENT ANALYSIS OF MICROELECTRONIC PACKAGES.(U)
MAY 82 J R SOUTHLAND, V R BEATTY F30602-81-C-0083
UNCLASSIFIED RADC-TR-82-133 NL

2 OF 3
AD A
117979

Table 17. Deflection shape of a Hybrid Lid - Continued

14	0.5186	0.5186	0.5119
15	0.8753	0.8754	0.8727
16	1.0000	1.0000	1.0000

Finally, a comparison was made between the calculated values for the maximum stress in the plate. Although the model was relatively coarse, it was felt that a comparison of the stress values between the three programs would be valid, regardless of how closely these values approached the theoretically correct stress. The maximum bending stress which occurred at the center of the lid (plate #9) is summarized below for each finite element program.

Table 18. Maximum Hybrid Lid Stress

Solution	Stress (psi)	Deviation (%)
STARDYNE	29,980	-7.57%
ANSYS	30,595	-5.67%
ABAQUS	30,780	-5.10%
Theoretical	32,434	-

The theoretical solution shown in Table 18 was once again taken from Roark's Formulas for Stress and Strain [85]. The ecuation is:

$$\max = \frac{\beta \, c \, b^2}{t^2}$$

where β = 0.2874 for a/b = 1.0

c = 30 psi pressure

b = 0.92"

t = 0.015"

As shown in Table 18, all of the computed maximum stresses were within 8% of the theoretically correct value. It should be noted that the maximum stress occurred at the center of plate #9 in the outer fibers of the plate surface. However, the theoretical solution shows the maximum stress at the center of the hybrid lid (node 16). A finer element grid would have allowed the finite element programs to calculate stresses similar to the theoretical answer; however, for most structural analyses, the numbers shown in Table 18 would be completely adequate.

This completes the discussion of the first sample problem. The next section of this report will deal with Sample Problem #2: the calculation of natural frequencies and mode shapes for a printed circuit board.

5.4 Sample Problem #2 - Linear Dynamics

This problem involved the determination of the first four natural frequencies (and the corresponding mode shapes) for a printed circuit board. The problem was solved using the following finite element programs: (1) STARDYNE, (2) ANSYS, and (3) ABAQUS. The finite element model of the circuit board is shown in Figure 20.

It should be noted that, although the finite element model was symmetric about a pair of axes parallel to the X-Y axes passing through node 13, a "quarter" model was not used for this solution. The reason for not using a quarter model was that we desired to calculate the first four natural frequencies of the system; the quarter model would only allow us to accurately determine the natural frequencies for modes with shapes symmetric about the central axes (in this case, only the first natural frequency would have been correct).

The boundary conditions for this model were similar to those chosen for the first sample problem; all four edges

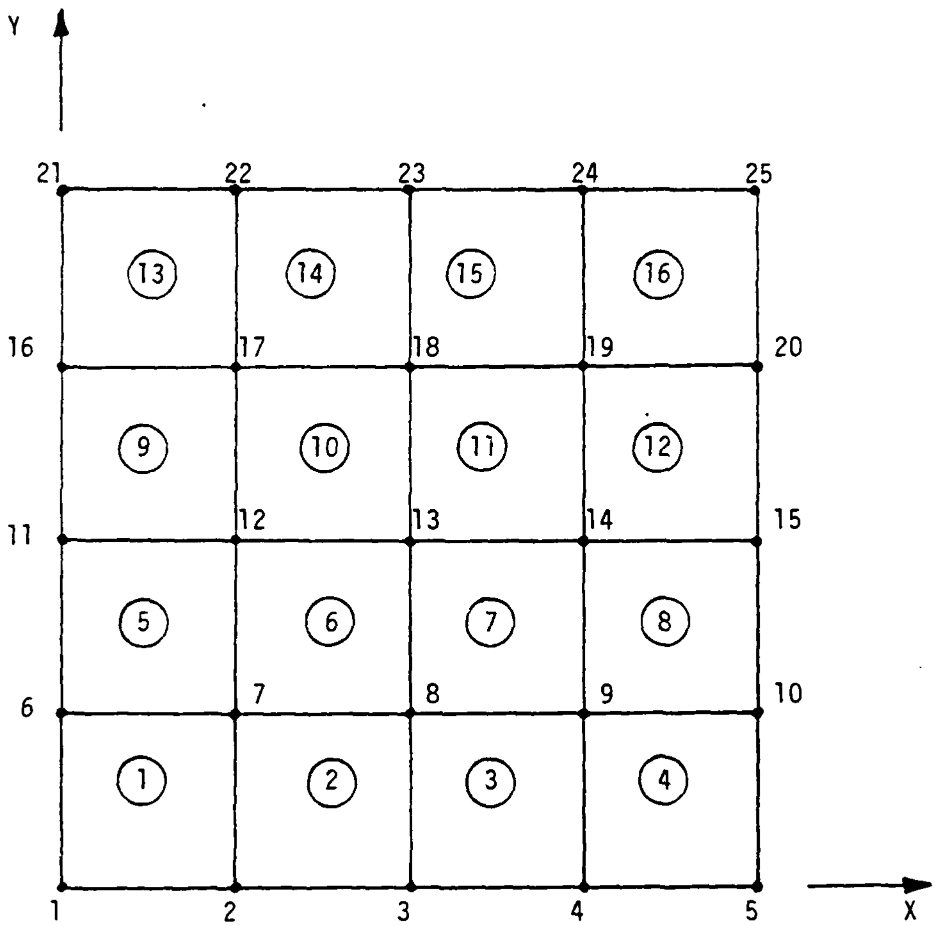

Figure 20. Printed Circuit Board Finite Element Model

were assumed to be simply supported, or hinged, along their length. Also, all nodal rotations perpendicular to the PC board were restrained for the reasons discussed in the description of the first sample problem. Other physical and material parameters are summarized in Table 19.

Table 19. Physical and Material Properties

Physical Dimensions	5.0" x 5.0" x 0.060"
Plate Type	Bending and Membrane
Material	G-10
Young's Modulus	2.5 x 10^6 psi
Poisson's Ratio	0.12
Weight	0.5 lb

As shown in Table 19, the plates used for this analysis had both bending stiffness and membrane stiffness. For each solution, 4-node cuadrilateral plates were used to model the PC board ("QUAD" elements for STARDYNE, "STIF43" elements for ANSYS, and "S4R" elements for ABAQUS).

Also shown in Table 19 is the weight of the PC board. This weight represents the sum of the G-10 weight and the weights of the individual components mounted to the board.

For this analysis, it was assumed that the components were fairly evenly distributed about the board, thus allowing us to include their weight into the calculation for the overall PC board density. It was also assumed that the components did not affect the overall stiffness of the board. For PC boards with large, heavy components, neither of these assumptions would be realistic, and a more detailed finite element model would be reouired. Also, for multilayer circuit boards with several layers of copper, it would be necessary to calculate an "equivalent" Young's Modulus for the copper/G-10 composite.

A listing of the required input for each of the three finite element programs is shown in Figures 21-23. Note that both STARDYNE and ANSYS require a fixed format input, while ABAQUS allows a free format input. Also, note that STARDYNE requests a weight density, while ANSYS and ABAQUS both request a mass density.

5.4.1 Results for Sample Problem #2

The following Table 20 shows the first four natural frequencies as computed by each program. Also, the theoretically correct natural frequencies are included for comparison purposes. These values were calculated using the equations in the reference Formulas for Natural Frequency and Mode Shape [86]; these equations are summarized below:

$$f_{ij} = \frac{\lambda^2_{ij}}{2\pi a^2} \left[\frac{Eh^3}{12\gamma(1-\nu^2)} \right]^{\frac{1}{2}}$$

$$\lambda^2_{ij} = \pi^2 \left[i^2 + j^2 \left(\frac{a}{b}\right)^2 \right]$$

For mode 1, $i = 1$, $j = 1$
For mode 2, $i = 2$, $j = 1$ Defined by Blevins,
For mode 3, $i = 1$, $j = 2$ Table 11-4 [86]
For mode 4, $i = 2$, $j = 2$

where:
a = length of plate = 5.0"
b = width of plate = 5.0"
E = Young's Modulus = 2.5×10^6 psi
h = plate thickness = 0.060"
= mass/unit area = 5.17081×10^{-5} lbf-sec^2/in^3
= Poisson's Ratio = 0.12

```
                                   *** STARDYNE 3.0      INPUT ***
          /------------------------------  CARD  IMAGE  ------------------------------/
          1   4   8  12  16  20  24  28  32  36  40  44  48  52  56  60  64  68  72  76  80
          *   *   *   *   *   *   *   *   *   *   *   *   *   *   *   *   *   *   *   *   *
CARD NO   ********************************************************************************   CARD TYPE
      2    RADC SAMPLE PROBLEM 2 ... PC BOARD VIBRATION    (STARDYNE)                          RADC
      3   MATLG       1 G-10          2.5E6        .12       .333                              MATLG
      4   END                                                                                  END
      5   NODEGR01    1   5                                  5.                                NODEG
      6   NODEGR02   21  25   5                  5.          5.      5.                        NODEG
      7   END                                                                                  END
      8   RESTG       1   5  4111111                                                           RESTG
      9               2   4     11 11                                                          RESTG
     10               6  16  51 11 1                                                           RESTG
     11              10  20  51 11 1                                                           RESTG
     12              21  25  4111111                                                           RESTG
     13              22  24     11 11                                                          RESTG
     14               7   9         1                                                          RESTG
     15              12  14         1                                                          RESTG
     16              17  19         1                                                          RESTG
     17   END                                                                                  END
     18   QUAD8       1   4   1       2       7       6       1   1      .06         2         QUAD8
     19               5   8   6       7      12      11                                        QUAD8
     20               9  12  11      12      17      16                                        QUAD8
     21              13  16  16      17      22      21                                        QUAD8
     22   END                                                                                  END
     23   ENDGEOM                                                                              ENDGE
     24    NATURAL  FREQUENCIES AND MODE SHAPES OF A PC BOARD                                  NATU
     25   DYNAMIC                 0       0                  4                                 DYNAM
     26   ENDMODEL                                                                             ENDMO
```

Figure 21. STARDYNE Input Listing for Problem #2

```
*********** ANSYS INPUT DATA LISTING (TAPE18) ***********

     6     12    18    24    30    36    42    48    54    60    66    72    78
     V     V     V     V     V     V     V     V     V     V     V     V     V
RADC SAMPLE PROBLEM 2 ... PC BOARD VIBRATION   (ANSYS)
J.R. SOUTHLAND    0      0
   0  2 00 0       0     099 0 4-1 0    0    0                           0 0  0
                        70                                     0          0 0 0
  1 43010  0
 -1
    -2                                                                4  5  4
     1     2     7     6                             1     1     0 0  4  1  1
          .06                                              0
    -1
     5-2 5 5           0         1.25          0
     1 0 0             0            0          0
     5 0 1             5.           0          0
    -1
   EX    1    0      2.5E6
   EY    1    0      2.5E6
 NUXY    1    0        .12
 ALPX    1    0          0
 ALPY    1    0          0
 DENS    1    08.6180124E-4
  END
     2   UX                               4    1  ROTX
    22   UX                              24    1  ROTX
     6   UY                              16    5  ROTY
    10   UY                              20    5  ROTY
     7   UX                               9    1    UY    UZ  ROTX  ROTY
    12   UX                              14    1    UY    UZ  ROTX  ROTY
    17   UX                              19    1    UY    UZ  ROTX  ROTY
    -1
  1  0  1  1

     1  ALL            0                  5    4
     2   UY            0                  4    1    UZ  ROTY  ROTZ
     6   UX            0                 16    5    UZ  ROTX  ROTZ
    10   UX            0                 20    5    UZ  ROTX  ROTZ
    21  ALL            0                 25    4
    22   UY            0                 24    1    UZ  ROTY  ROTZ
     7 ROTZ            0                  9    1
    12 ROTZ            0                 14    1
    17 ROTZ            0                 19    1
    -1
    -1
    -1
 END
 FINISH
```

Figure 22. ANSYS Input Listing for Problem #2

A B A Q U S   I N P U T   E C H O

P A G E   1

```
     5    10    15    20    25    30    35    40    45    50    55    60    65    70    75
-------------------------------------------------------------------------------------------
*HEADING
 RADC SAMPLE PROBLEM 2 ... PC BOARD VIBRATION
*NODE, NSET=CORN
1,0,0,0
5,5,0,0
21,0,5,0
25,5,5,0
*NGEN, NSET=EDGE
1,5,1
21,25,1
*NGEN, NSET=SIDE
1,21,5
5,25,5
*NGEN, NSET=MID
6,10,1
11,15,1
16,20,1
*ELEMENT, TYPE=S4R
1,1,2,7,6
*ELGEN, ELSET=PCB
1,4,1,1
1,4,5,4
2,4,5,4
3,4,5,4
4,4,5,4
*SHELL SECTION, ELSET=PCB
.060
*MATERIAL, ELSET=PCB
*DENSITY
8.61801E-4
*ELASTIC, TYPE=ISO
2.5E6,.12
*BOUNDARY
EDGE,2,3
EDGE,5,6
SIDE,1
SIDE,3,4
SIDE,6
*STEP, LINEAR=NEW
NATURAL FREQUENCIES AND MODE SHAPES OF A PC BOARD
*FREQUENCY
5,2000
*PRINT
*END STEP
-------------------------------------------------------------------------------------------
     5    10    15    20    25    30    35    40    45    50    55    60    65    70    75
-------------------------------------------------------------------------------------------
```

Figure 23.   ABAQUS Input Listing for Problem #2

As indicated in Table 20, STARDYNE appears to most accurately predict the first four natural frequencies. ANSYS is the second most accurate of the three, with ABAQUS being the least accurate. The percent deviation of each program from the theoretical solution is summarized in Table 21.

Table 20. Natural Frequencies of PC Board (Hz)

Mode	STARDYNE*	ANSYS	ABAQUS	Theoretical
1	120.0	115.1	124.2	118.1
2	300.4	285.5	377.2	295.2
3	300.4	285.5	377.2	295.2
4	484.7	438.8	572.6	472.4

*Lanczos Method; other options are Householder-QR Method or Inverse Iteration Method

Table 21. Deviation from Theoretical Frequencies

Mode	STARDYNE	ANSYS	ABAQUS
1	+1.61%	-2.54%	+5.17%
2	+1.76%	-3.29%	+27.78%
3	+1.76%	-3.29%	+27.78%
4	+2.60%	-7.11%	+21.21%
Average	+1.93%	-4.06%	+20.49%

At this point, it would be timely to make two points concerning idiosyncrasies of both ANSYS and ABAQUS. First, when ANSYS is requested to determine natural frequencies, it will compute as many natural frequencies as there are DOF in the structure. For instance, the model of the PC board had 69 active DOF; 69 frequencies were thus calculated, regardless of the fact that we were interested in only the first four frequencies. The only way to reduce the number of calculated frecuencies is to compose a list of "master degrees of freedom"; these are the DOF considered to be the most significant contributors to the structural behavior. These master DOF must be carefully selected in order to ensure an accurate modal analysis. For our analysis of the PC board, all 69 DOF were allowed to contribute to the modal analysis, thus remaining consistent with the STARDYNE and ABAQUS solutions.

Secondly, ABAQUS requires that more natural frecuencies be recuested than the actual number which are of interest to the analyst. Unfortunately, this is not indicated in the manual. The first time that the ABAQUS model was run, four natural frecuencies were recuested. The first three frecuencies were the same as those indicated in Table 20; however, the fourth frecuency was computed to be 1293.9 Hz. Since no obvious errors could be found in the model, ABAQUS' customer service was consulted. They volunteered to build and run their own PC board model with ABAQUS to determine the source of the problem. After several iterations it was determined that there were no model errors, but that, instead, the last eigenvalue calculated by ABAQUS was not an accurate solution. In order to determine four natural frequencies accurately, it was necessary to recuest a solution of five or more frequencies. As a general rule of thumb, it was suggested that the analyst should always recuest two or three more natural frequencies than those in which be has an interest when using the modal analysis option of ABAQUS.

As a footnote to the above discussion of the modal analysis option of ABAQUS, it is of interest to note that STARDYNE automatically calculates more natural frecuencies than recuested (how many more is a function of the original number of frecuencies requested). These additional frecuencies are then presented to the analyst as "approximate" eigenvalues, without their corresponding mode shapes. For example, in this PC board analysis, four frequencies were requested. STARDYNE then calculated four natural frequencies and mode shapes, and "estimated" two additional natural frequencies. In this way, STARDYNE ensures the accuracy of the requested eigenvalues and eigenvectors.

Returning to the discussion of the PC board results, the next comparison which could be made between the programs concerns the computed mode shapes. Table 22 summarizes the normalized mode shapes for each of the three programs. Note that the tabulated values represent normalized deflections in the transverse direction. Also notice that only modes 1 and 4 were calculated to have the same normalized shape by all three programs; differences do exist among the calculated shapes for modes 2 and 3.

As shown in Figures 24 through 27, the mode shapes calculated by each of the three programs are basically the same. The magnitudes shown in Table 22 indicate that differences do exist between the programs for modes 2 and 3; however, the sketches of the mode shapes reveal that the basic shape descriptions are the same. It is interesting to note that mode 2 and mode 3 are the same mode, except for being rotated 90° around the PC board from each other.

In summary of Sample Problem #2, STARDYNE was the most accurate program for determining the first four natural frequencies. It also had the most direct, user-oriented procedures for requesting these frequencies -- no idosyncrasies were apparent as was the case for both ANSYS and ABAQUS.

5.5 Sample Problem #3 - Heat Transfer

The heat transfer sample problem involved the calculation of the temperature distribution and heat flux of a 0.6" long by 0.1" diameter aluminum pin fin. The base of the fin was assumed to be held at a constant temperature of 176°F,

Table 22. PC Board Normalized Mode Shapes

Mode	Node	STARDYNE	ANSYS	ABAQUS
1	7	0.500	0.500	0.500
	8	0.707	0.707	0.707
	9	0.500	0.500	0.500
	12	0.707	0.707	0.707
	13	1.000	1.000	1.000
	14	0.707	0.707	0.707
	17	0.500	0.500	0.500
	18	0.707	0.707	0.707
	19	0.500	0.500	0.500
2	7	-0.414	-0.706	0.496
	8	0.414	0.002	1.000
	9	1.000	0.706	0.918
	12	-1.000	-1.000	-0.298
	13	0.000	0.000	0.000
	14	1.000	1.000	0.298
	17	-1.000	-0.706	-0.918
	18	-0.414	-0.002	-1.000
	19	0.414	0.706	0.496
3	7	1.000	-0.706	0.327
	8	1.000	-1.000	0.938
	9	0.414	-0.706	1.000
	12	0.414	-0.002	-0.476
	13	0.000	0.000	0.000
	14	-0.414	0.002	0.476
	17	-0.414	0.706	-1.000
	18	-1.000	1.000	-0.938
	19	-1.000	0.706	-0.327
4	7	-1.000	-1.000	-1.000
	8	0.000	0.000	0.000
	9	1.000	1.000	1.000
	12	0.000	0.000	0.000
	13	0.000	0.000	0.000
	14	0.000	0.000	0.000
	17	1.000	1.000	1.000
	18	0.000	0.000	0.000
	19	-1.000	-1.000	-1.000

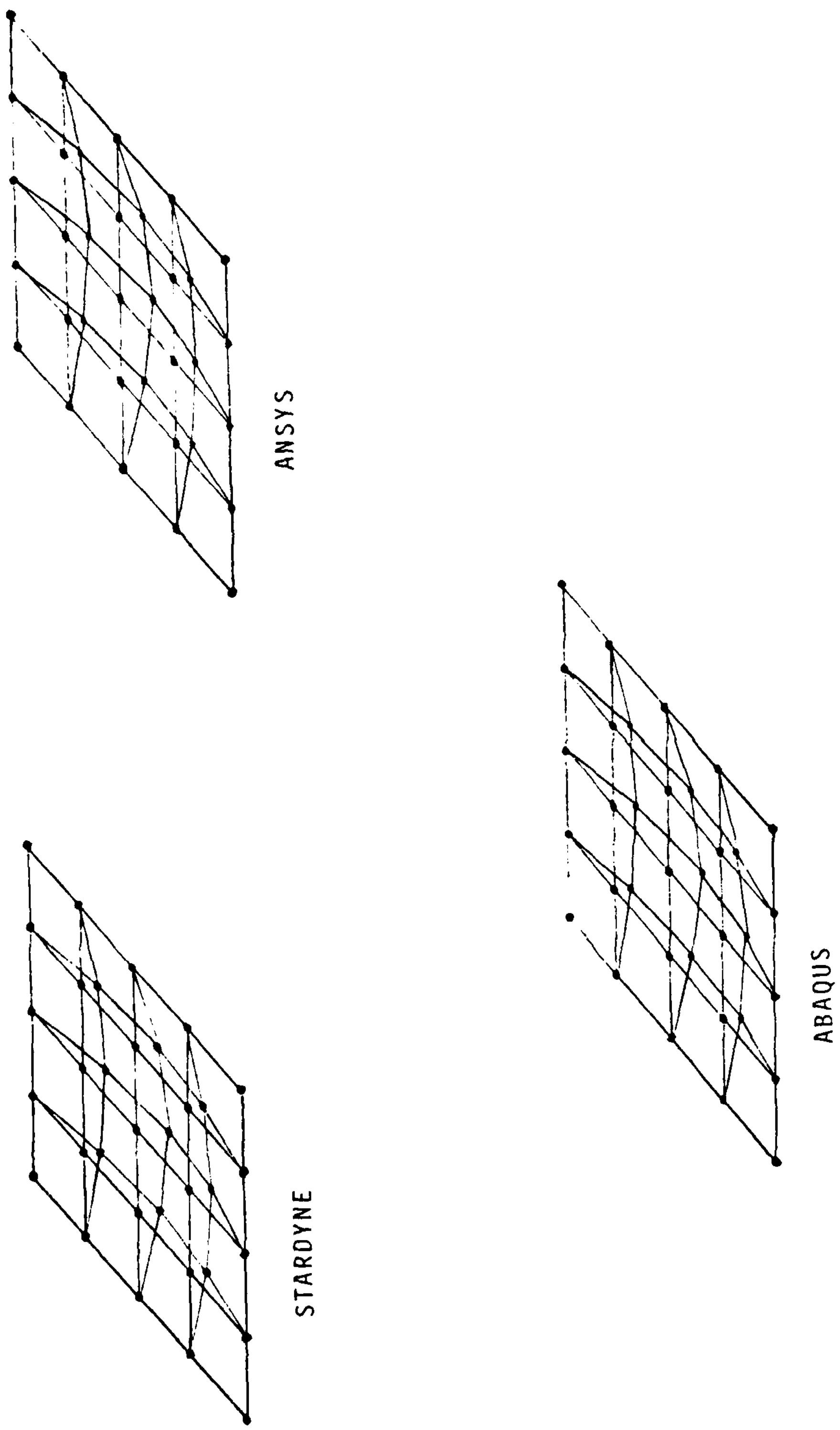

Figure 24. PC Board, Mode 1

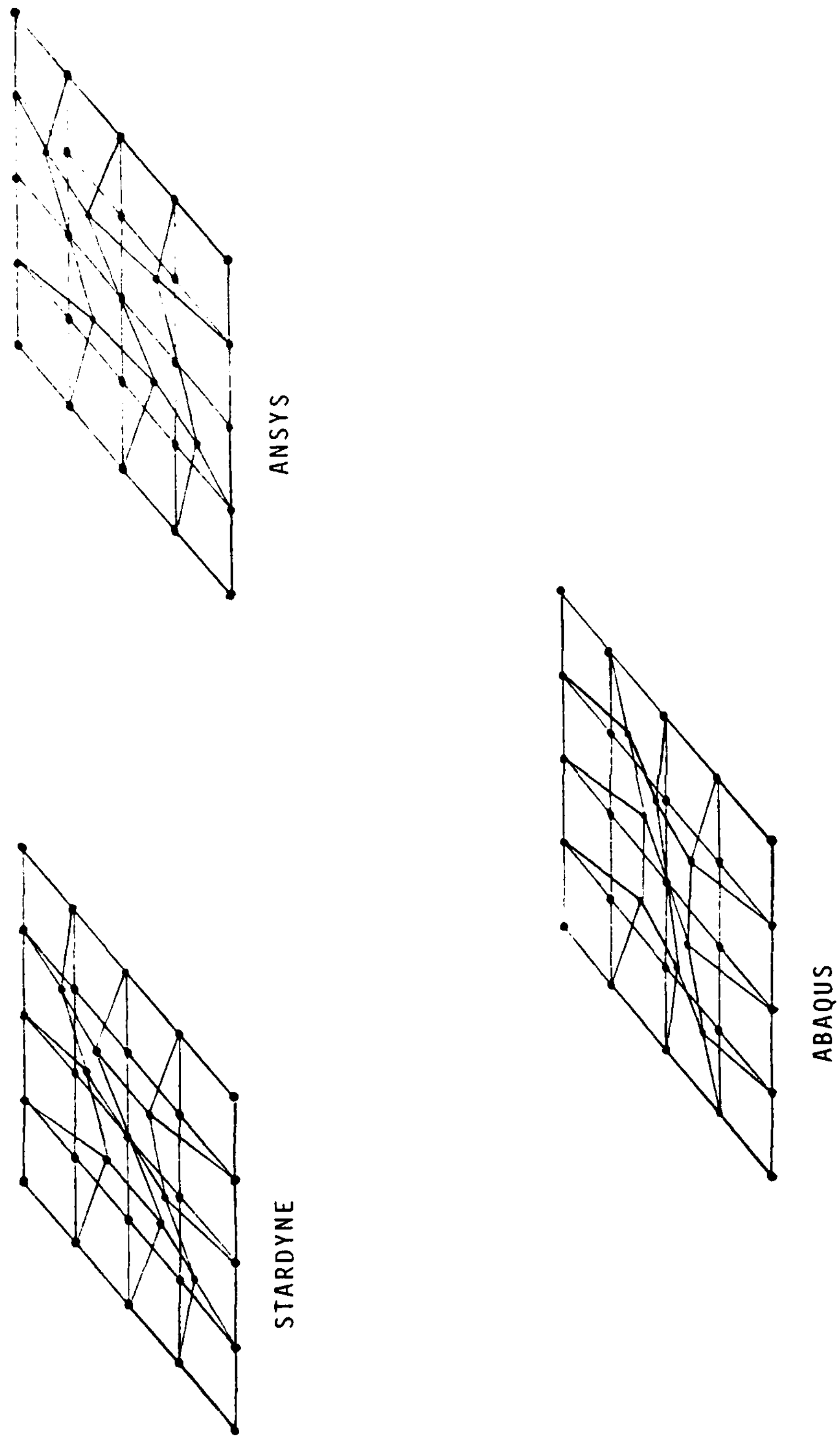

Figure 25. PC Board, Mode 2

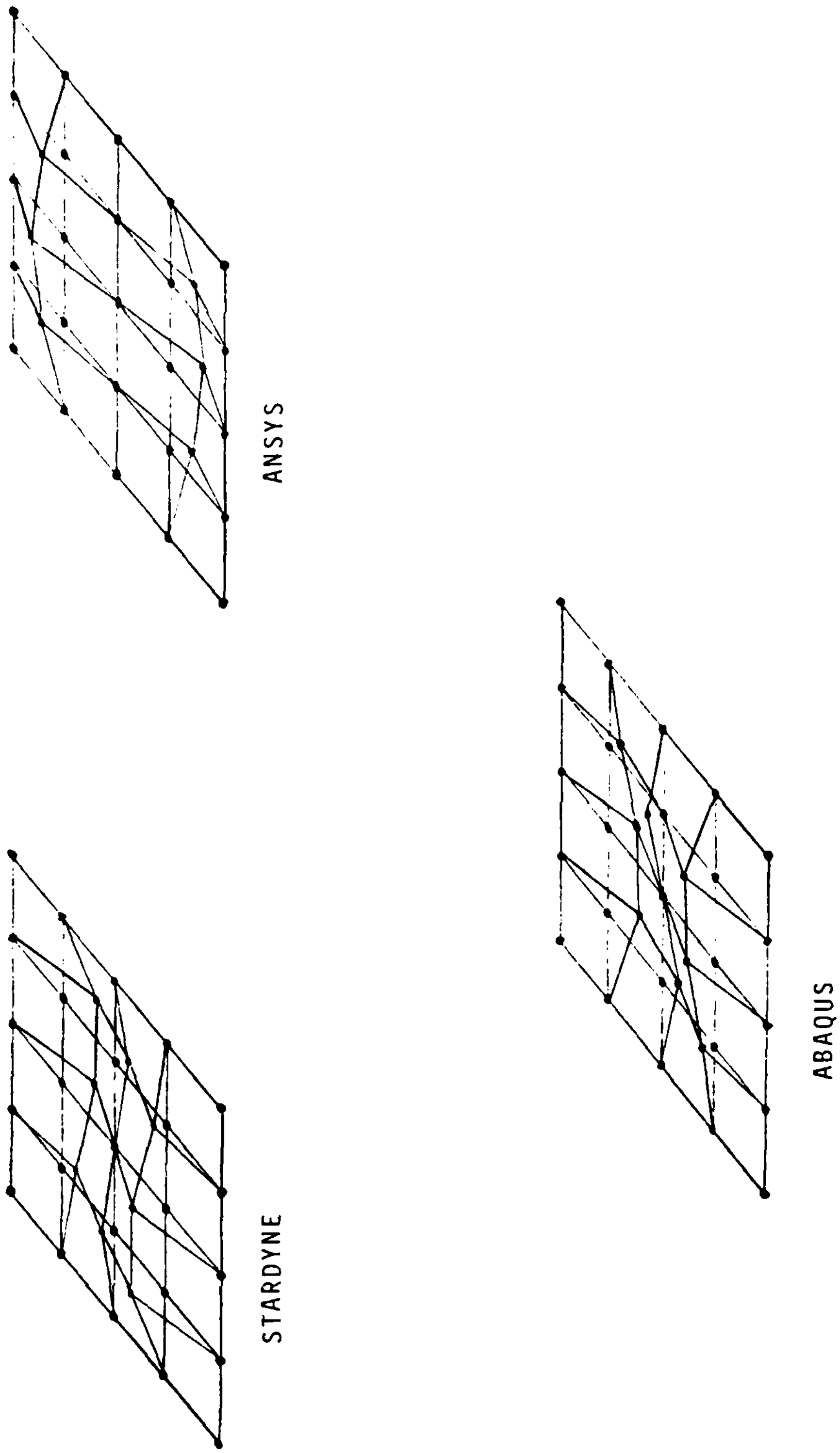

Figure 26. PC Board, Mode 3

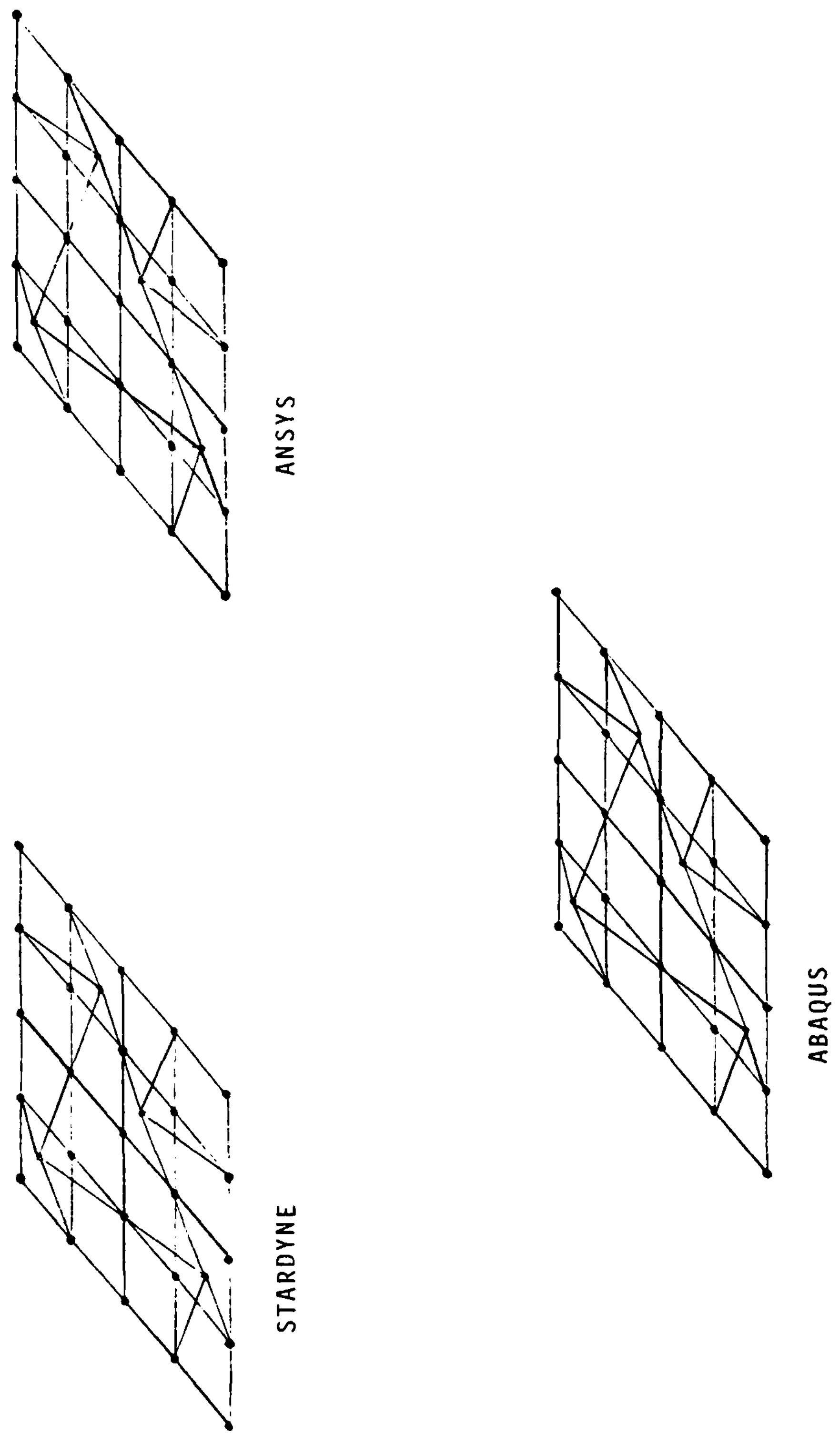

Figure 27. PC Board, Mode 4

and the heat transfer coefficient between the fin and the surrounding air flow was assumed to have a constant value of 12.7 $Btu/hr \cdot ft^2 \cdot {}^oF$. Also, it was assumed that the temperature distribution was one-dimensional along the length of the fin; the temperature across any given cross-section was assumed to be constant.

It was originally planned to solve this problem using both ANSYS and ABAQUS (STARDYNE does not have any heat transfer elements). Unfortunately, ABAQUS did not lend itself well to solving this one-dimensional problem; the reasons will be discussed later in this section of the report. Therefore, only a comparison of the theoretical closed-form solution and the ANSYS numerical solution was made. The ANSYS finite element model of the pin fin is shown below in Figure 28.

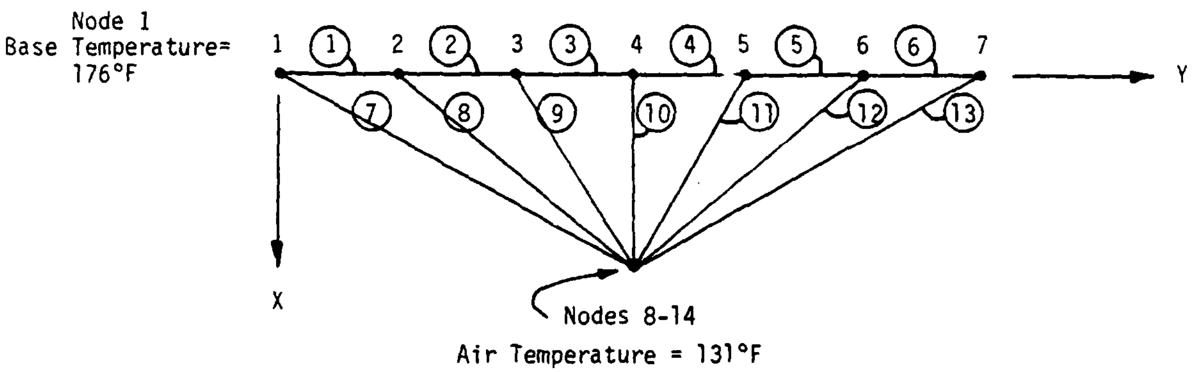

Figure 28. Pin Fin Finite Element Model

As shown in Figure 28, the pin fin finite element . del consisted of 14 nodes and 13 elements. Nodes 1-7 were used to define the pin fin structure, while nodes 8-14 were used to represent the ambient airflow "sink". It should be noted that nodes 8-14 could very easily be replaced by a single node to which the convective link elements 7-13 would be connected. At the time of the model creation, it was felt that having distinct ambient nodes would simplify the generation of the elements 7-13. However, this slight advantage in element generation was partially offset by the need to create the additional nodes 9-14.

Elements 1-6 are one-dimensional conduction elements having the conductivity of aluminum. Element 7 is a convective link element with a heat transfer coefficient of 12.7 Btu/hr ft^2 ^{o}F, and a heat transfer area ecual to the surface area of a 0.05" long by 0.1" diameter cylinder. Similarly, elements 8-12 are convective link elements, but their heat transfer areas are each ecual to the surface area of a 0.1" long by 0.1" diameter cylinder. Finally, the last convective link element, number 13, has a heat transfer area ecual to the sum of the surface area of a 0.05" long by 0.1" diameter cylinder and the surface area at the end of the pin fin.

As mentioned earlier, ABAQUS was not used to model the pin fin. The primary reason for the decision not to use ABAQUS was that ABAQUS did not provide a convective link element which could be used in conjunction with its one-dimensional conductive link element "DC1D2". Although ABAQUS does provide for convection heat transfer away from its one-dimensional conduction element, this convection occurs at each face of the element (a face being defined as the cross-sectional surface area at a node). As may be seen by referring to the previous paragraph, the cross-sectional area of the fin is not the convective heat transfer area recuired for this model.

A method of solution for this problem using ABAQUS was available using the program's 4-node, axisymmetric heat transfer element "DCAX4". However, this would have resulted in a two-dimensional solution to the problem, which would not have provided a totally valid comparison with the one-dimensional solution of ANSYS. Also, we felt that a problem of this simplicity did not warrant a second solution by ANSYS using two-dimensional heat transfer elements solely for the purpose of comparison with the two-dimensional ABAQUS solution. Therefore, only ANSYS was used to solve this thermal problem (a listing of the required ANSYS input is shown in Figure 29).

As indicated in the input data listing, the ANSYS "STIF32" element was used to represent the pin fin, and the ANSYS "STIF34" element was used to provide the convection link. One should not be confused by the fact that ANSYS labels its one-dimensional heat conducting bar (STIF32) as a two-dimensional element. By using the term "two-dimensional", ANSYS is referring to the fact that this element is used only in planar or axisymmetric analyses where each node is defined by two coordinates. ANSYS also has a one-dimensional heat conducting bar that is labeled as "three-dimensional": both of the elements' nodes are defined by a three-dimensional coordinate system.

5.5.1 Results for Sample Problem #3

As a basis of comparison for the ANSYS solution, the temperature distribution was also determined based on the theoretical solution. The closed-form solution was taken from the third edition of Principles of Heat Transfer by Frank Kreith [87], and is presented below:

```
*********** ANSYS INPUT DATA LISTING (TAPE18) ***********

     6     12    18    24    30    36    42    48    54    60    66    72    78
     V     V     V     V     V     V     V     V     V     V     V     V     V
RADC SAMPLE PROBLEM FOR THERMAL ANALYSIS ... PIN FIN
J.R. SOUTHLAND    0     0
   0 -1 00 0 0 1 1 0     099    1                                          0 1  0
                     173.                                       0            0 0 0
  1 32
  2 34  0  1
 -1
     1     2                                     1     1    0 0   6  1  1
54.541539E-6
     1     8                                     2     2    0 0
109.08308E-6            0           0
     2     9                                     2     2    0 0   5  1  1
218.16616E-6            0           0
     7    14                                     2     2    0 0
163.62462E-6            0           0
    -1
     1 0 0              0           0
     7 0 1              0         .05
     8 0 0              1         .02
    14 0 1              1         .03
    -1
  KXX    1   0       96.
 DENS    1   0   169.344
    C    1   0       .23
   HF    2   0      12.7
  END
   1  0  1  1           0
                                                                               1
           .01                                                                 0
     1 TEMP          176
     8 TEMP          131                14     1
    -1
    -1
    -1
END
FINISH
```

Figure 29. ANSYS Input Listing for Problem #3

$$\frac{T(y) - T_{air}}{T_{base} - T_{air}} = \frac{\cosh m(L-y) + (h/mk) \sinh m(L-y)}{\cosh (mL) + (h/mk) \sinh (mL)}$$

here:

$T(y)$ = temperature at distance "y" from the base (^{o}F)

T_{air} = air temperature ($131^{o}F$)

T_{base} = base temperature ($176^{o}F$)

m = $\sqrt{\frac{hP}{KA}}$

h = heat transfer coefficient (12.7 Btu/hr ft^2 ^{o}F)

P = pin fin perimeter (0.02618 ft)

K = Conductivity (96 Btu/hr ft ^{o}F)

A = pin fin cross-sectional area (54.54×10^{-6} ft^2)

L = pin fin length (0.05 ft)

In addition, the closed form solution for the heat transfer rate through the fin is again taken from Kreith:

$$c = \sqrt{PhAK}\left[T_{base} - T_{air}\right] \frac{\sinh (mL) + (h/mK) \cosh (mL)}{\cosh (mL) + (h/mK) \sinh (mL)}$$

Table 23 summarizes the temperature distribution along the fin at 0.1" intervals (and also indicates the heat flow rate) as determined by ANSYS and by the closed-form solution.

Table 23. Temperature Distribution and Heat Flow

Distance from Base	ANSYS	Theoretical
0.0"	176.00^{o} F	176.00^{o} F
0.1"	174.93^{o} F	174.92^{o} F
0.2"	174.04^{o} F	174.04^{o} F
0.3"	173.35^{o} F	173.35^{o} F
0.4"	172.85^{o} F	172.85^{o} F
0.5"	172.53^{o} F	172.53^{o} F
0.6"	172.39^{o} F	172.39^{o} F
Heat Flow Rate:	0.7377 Btu/Hr	0.7374 Btu/Hr

As shown in Table 23, the temperature distribution computed by ANSYS is virtually identical to the temperature distribution defined by the closed-form solution. Also, ANSYS' computed heat flow rate is within 0.04% of the theoretically correct value. Obviously, the one-dimensional heat transfer element of ANSYS is capable of sufficient accuracy for this type of analysis.

This concludes the discussion of the third sample problem. The next section of this report will deal with the last sample problem: a nonlinear statics problem.

5.6 Sample Problem #4 - Nonlinear Statics

As discussed in the sample problem "Introduction", the nonlinear statics problem involved the determination of the deflections for an electronic substrate. This substrate was assumed to be mounted in a module such that a 0.012" gap existed between the bottom surface of the substrate and the top surface of the module floor. The substrate was assumed to be mounted by screws at each of its four corners, and was subjected to constant accelerations of (+) and (-) 20,000 G's. The nonlinearity of this problem falls into a class of problems called "one-way structures". The substrate is free to deflect away from the module, but, when the acceleration is reversed, the substrate may only deflect freely until it encounters the module. At this point, further distortion of the substrate occurs until the restraining forces equal the applied load.

All of the following three programs are capable of solving this type of nonlinear problem: (1) STARDYNE, (2) ANSYS, and (3) ABAQUS. However, each program requires the analyst to go through different solution procedures. The finite element model shown in Figure 30 was used by each of the programs to solve for the substrate deflections.

As shown in Figure 30, the substrate finite element model consisted of 25 nodes and 16 elements. It should be noted that in addition to the nodes and elements shown in Figure 30, each of the three programs also required several other "gap" nodes and/or "gap" elements peculiar to each program; these will be described to a limited degree later in this section of the report (a complete description of the necessary gap elements and/or nodes for each program is given in the corresponding user manuals).

The following Table 24 summarizes the physical and material properties of the substrate required for this analysis.

Table 24. Physical and Material Properties

Physical Dimensions	1.0" x 1.0" x 0.020"
Plate Type	Bending and Membrane
Material	771 Alumina
Young's Modulus	43×10^6 psi
Poisson's Ratio	0.3
Weight	0.0028 lb
Restraints	Each corner fully restrained
Loading	20,000 G's

As shown in Table 24, the plates used for this analysis had both bending stiffness and membrane stiffness. In each case, the quadrilateral plate element which was used had four nodes per element. The element used for the STARDYNE analysis was the "QUAD" element, the element used for the ANSYS analysis was the "STIF43" element, and the element used for the ABAQUS analysis was the "S4R" element. Again, although both ANSYS and ABAQUS offer eight-node-per-element quadrilateral plates elements, the more simple four-node-per-element plate

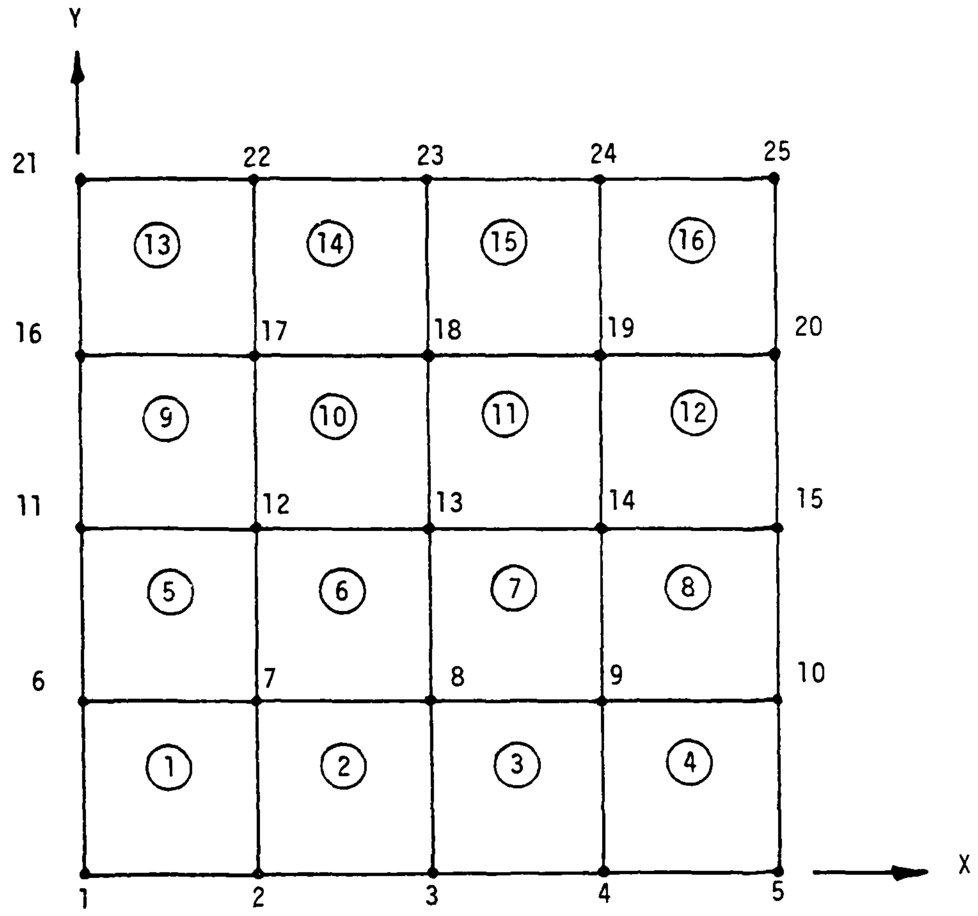

Figure 30. Substrate Finite Element Model

elements were used in order to provide a valid comparison with STARYDNE's four-node quadilateral element.

A listing of the required input for each of the three programs is shown in Figures 31 - 35. It should be noted that STARDYNE required a total of three different, sequential runs to solve this problem; hence, the three separate input listings. Also, the ANSYS input listing is only one of many different ANSYS runs which were required to determine the model's necessary "gap" element stiffness for the downward loading case. Finally, a representative ABAQUS input is shown.

5.6.1 Solution Techniques for Sample Problem #4

The first portion of this section of the report will be divided into three main topics, each will be devoted to a discussion of the solution procedure required by the different programs. It should be mentioned that a closed-form solution did not exist for this problem; therefore, the numerical solutions could not be compared with a theoretically correct solution.

5.6.1.1 STARDYNE Solution

STARDYNE's "NUBOP" program was used to solve for the deflections of the substrate when exposed to the acceleration loadings. NUBOP is used to obtain static solutions for models which have nonlinear connections, boundaries, or elements. Typical uses of NUBOP include "bottoming-out" or separation of adjacent structural members, or the analysis of tension-only or compression-only bar members.

In general terms, the following procedure was required to run the NUBOP program. First, the model of the substrate was examined for potential "bottom-out" points (referred to as a "BOP"). It was assumed that any of the following nodes might possibly bottom-out against the module

```
                               *** STARDYNE 3.0      INPUT ***
        /------------------------------ CARD  IMAGE  ------------------------------/
        1   4   8  12  16  20  24  28  32  36  40  44  48  52  56  60  64  68  72  76  80
        *   *   *   *   *   *   *   *   *   *   *   *   *   *   *   *   *   *   *   *   *
CARD NO ***************************************************************************  CARD TYPE
      2  RADC SAMPLE PROBLEM 4 ... SUBSTRATE MOUNTED ON STAND-OFFS      (STARDYNE)      RADC
      3 MATLG        1 771 ALUM      43.E6         .3       .140                       MATLG
      4              2 ALUMINUM      10.E6         .3          0                       MATLG
      5 END                                                                            END
      6 NODEGROl     1   5                                  1.0                        NODEG
      7 NODEGR02    21  25   5              1.0             1.0      1.0               NODEG
      8 END                                                                            END
      9 RESTG        1   5   4111111                                                   RESTG
     10             21  25   4111111                                                   RESTG
     11              2   4         1                                                   RESTG
     12              6  10         1                                                   RESTG
     13             11  15         1                                                   RESTG
     14             16  20         1                                                   RESTG
     15             22  24         1                                                   RESTG
     16 END                                                                            END
     17 QUADB        1   4   1       2       7       6       1   1   .020      2       QUADB
     18              5   8   6       7      12      11                                 QUADB
     19              9  12  11      12      17      16                                 QUADB
     20             13  16  16      17      22      21                                 QUADB
     21 END                                                                            END
     22 ENDGEOM                                                                        ENDGE
     23  LOAD CASES IN PREPARATION FOR USING NUBOP                                      LOAD
     24 STATIC               1          -1                                             STATI
     25  CASE ONE ... BOP POINT NO. 1    NODE 7 IN X3 DIRECTION                         CASE
     26 CONC         7                           1                                     CONC
     27 END                                                                            END
     28 END CASE                                                                       END C
     29  CASE TWO ... BOP POINT NO. 2    NODE 8 IN X3 DIRECTION                         CASE
     30 CONC         8                           1                                     CONC
     31 END                                                                            END
     32 END CASE                                                                       END C
     33  CASE THREE ... BOP POINT NO. 3    NODE 9 IN X3 DIRECTION                       CASE
     34 CONC         9                           1                                     CONC
     35 END                                                                            END
     36 END CASE                                                                       END C
```

Figure 31. First STARDYNE Input Listing for Problem #4

```
  CASE FJUR ... BOP POINT NO. 4     NODE 12 IN X3 DIRECTION                 CASE
CONC        12                           1                                 CONC
END                                                                        END
END CASE                                                                   END C
  CASE FIVE ... BOP POINT NO. 5     NODE 13 IN X3 DIRECTION                 CASE
CONC        13                           1                                 CONC
END                                                                        END
END CASE                                                                   END C
  CASE SIX ... BOP POINT NO. 6    NODE 14 IN X3 DIRECTION                   CASE
CONC        14                           1                                 CONC
END                                                                        END
END CASE                                                                   END C
  CASE SEVEN ... BOP POINT NO. 7    NODE 17 IN X3 DIRECTION                 CASE
CONC        17                           1                                 CONC
END                                                                        END
END CASE                                                                   END C
  CASE EIGHT ... BOP POINT NO. 8    NODE 18 IN X3 DIRECTION                 CASE
CONC        18                           1                                 CONC
```

Figure 31. First STARDYNE Input Listing for Problem #4 (continued)

```
                              *** STARDYNE 3.0      INPUT ***
        /----------------------------- CARD  IMAGE -----------------------------/
        1  4   8  12  16  20  24  28  32  36 * 40  44  48  52  56  60  64  68  72  76  80
        *  *   *   *   *   *   *   *   *   *    *   *   *   *   *   *   *   *   *   *   *
CARD NO ***************************************************************************** CARD TYP
    55  END                                                                            END
    56  END CASE                                                                       END C
    57   CASE NINE ... BOP POINT NO. 9    NODE 19 IN X3 DIRECTION                       CASE
    58  CONC        19                               1                                 CONC
    59  END                                                                            END
    60  END CASE                                                                       END C
    61   CASE TEN ... APPLIED LOAD (20,000 G'S) ON SUBSTRATE - DOWNWARD                 CASE
    62  ACCEL       -1                            20000                                ACCEL
    63  END                                                                            END
    64  END CASE                                                                       END C
    65   CASE ELEVEN ... APPLIED LOAD (20,000 G'S) ON SUBSTRATE - UPWARD                CASE
    66  ACCEL       -1                           -20000                                ACCEL
    67  END                                                                            END
    68  END CASE                                                                       END C
    69  ALL DONE                                                                       ALL D
    70  TAPE4G          1 9999                       1                                 TAPE4
    71  ENDMODEL                                                                       ENDMO
```

Figure 31. First STARDYNE Input Listing for Problem #4 (continued)

```
                                   *****  INPUT DATA CARDS  *****
            /------------------------------- CARD  IMAGE -----------------------------------/
            1    6    12   17   22   27   32   37   42   47   52   57   62   67   72       80
            *    *    *    *    *    *    *    *    *    *    *    *    *    *    *        *
CARD NO     ***********************************************************************************
      1     START     0         25        9         2         0         0         0
      2     BUP
      3               1         1         1        73
      4               1         2         2        83
      5               1         3         3        93
      6               1         4         4       123
      7               1         5         5       133
      8               1         6         6       143
      9               1         7         7       173
     10               1         8         8       183
     11               1         9         9       193
     12     END
     13     RHVECTOR
     14               1         1        10
     15               1         2        11
     16     END
     17     TOL
     18     -6        1    1000.0
     19     -6        1     -.012
     20     END
     21     ALL DONE

                      (END OF INPUT FOR MODEL NO.    1)
```

Figure 32. Second STARDYNE Input Listing for Problem #4

```
                                     *** STARDYNE 3.0      INPUT ***
            /------------------------------- CARD  IMAGE  --------------------------------/
            1  4    9  12  16  20  24  28  32  36  40  44  48  52  56  60  64  68  72  76  80
            *  *    *   *   *   *   *   *   *   *   *   *   *   *   *   *   *   *   *   *   *
  CARD NO   ****************************************************************************  CARD TYPE
        2    RADC SAMPLE PROBLEM 4 ... SUBSTRATE MOUNTED ON STAND-OFFS    (STARDYNE)          RADC
        3   MATLG       1 771 ALUM      43.E6       .3      .140                              MATLG
        4               2 ALUMINUM      10.E6       .3        0                               MATLG
        5   END                                                                               END
        6   NODEGRD1    1   5                                1.0                              NODEG
        7   NODEGRD2   21  25   5           1.0              1.0       1.0                    NODEG
        8   END                                                                               END
        9   RESTG       1   5   4111111                                                       RESTG
       10              21  25   4111111                                                       RESTG
       11               2   4         1                                                       RESTG
       12               6  10         1                                                       RESTG
       13              11  15         1                                                       RESTG
       14              16  20         1                                                       RESTG
       15              22  24         1                                                       RESTG
       16   END                                                                               END
       17   QUADB       1   4   1       2       7       6        1   1    .020        2       QUADB
       18               5   8   6       7      12      11                                     QUADB
       19               9  12  11      12      17      16                                     QUADB
       20              13  16  16      17      22      21                                     QUADB
       21   END                                                                               END
       22   ENDGEOM                                                                           ENDGE
       23    COMBINE BOP FACTORS WITH THE TWO APPLIED LOAD CASES                                COMB
       24   STATIC      0       1   0       1                                                 STATI
       25    CASE ONE ... DOWNWARD LOAD DUE TO 20,000 G'S COMBINED WITH BOP LOADS                CASE
       26   ACCEL      -1                          20000                                      ACCEL
       27   END                                                                               END
       28   CONCHEAD   14                                                                     CONCH
       29   END                                                                               END
       30   END CASE                                                                          END C
       31    CASE TWO ... UPWARD LOAD DUE TO 20,000 G'S COMBINED WITH BOP LOADS                  CASE
       32   ACCEL      -1                         -20000                                      ACCEL
       33   END                                                                               END
       34   CONCHEAD   14                                                                     CONCH
       35   END                                                                               END
       36   END CASE                                                                          END C
       37   ALL DONE                                                                          ALL D
       38   OUTPUT          1 9999222   2          2                                          OUTPU
       39   ENDMODEL                                                                          ENDMO
```

Figure 33. Third STARDYNE Input Listing for Problem #4

```
    ***********  ANSYS INPUT DATA LISTING (TAPE18)  ***********

       6     12     18     24     30     36     42     48     54     60     66     72     78
       V      V      V      V      V      V      V      V      V      V      V      V      V
RADC SAMPLE PROBLEM 4 ... SUBSTRATE MOUNTED ON BOSSES   (ANSYS)
J.R. SOUTHLAND    0     0
   0  0 00 0 0 0 1 0 0   099          0   0                                    0 0  0
          70           70                                              0        0 0 0
  1 43010  0
  2 52 01  0
 -1
    -2                                                                     4  5  4
     1     2     7     6                                1     1    0 0    4  1  1
         .02                                                  0
    26     7                                            2     2    0 0    9  1  1
       1.E8       .012        0.0
    -1
     5-2 5 5         0        .25  *        0
     1 0 0           0         0            0
     5 0 1           1.        0            0
     3-2 3 3         0        .25           0
    26 0 0         .25        .25       -.012
    28 0 1         .75        .25       -.012
    -1
  EX    1   0     43.E6
NUXY    1   0        .3
ALPX    1   0        0
DENS    1   0      .14
  MU    2   0        0
 END
  1  0-10  1                              20000
                                                                                  0
     1  ALL          0.
     5  ALL          0.
    21  ALL          0.
    25  ALL          0.
    26  ALL          0.               34     1
    -1
    -1
    -1
END
FINISH
```

Figure 34. ANSYS Input Listing for Problem #4

A B A Q U S   I N P U T   E C H O

P A G E   1

```
    5    10    15    20    25    30    35    40    45    50    55    60    65    70    75
-----------------------------------------------------------------------------------------
*HEADING
 RADC SAMPLE PROBLEM 4 ... SUBSTRATE MOUNTED ON BOSSES
*NODE, NSET=CORN
1,0,0,0
5,1,0,0
21,0,1,0
25,1,1,0
*NGEN, NSET=REST
1,5,1
21,25,1
1,21,5
2,22,5
3,23,5
4,24,5
5,25,5
*NODE, NSET=BASE
26,.25,.25,-.012
28,.75,.25,-.012
32,.25,.75,-.012
34,.75,.75,-.012
*NGEN, NSET=BASE
26,28,1
32,34,1
26,32,3
27,33,3
28,34,3
*ELEMENT,TYPE=S4R
1,1,2,7,6
*ELGEN, ELSET=ALL
1,4,1,1
1,4,5,4
2,4,5,4
3,4,5,4
4,4,5,4
*SHELL SECTION, ELSET=ALL
.020
*MATERIAL, ELSET=ALL
*DENSITY
3.62319E-4
*ELASTIC,TYPE=ISO
43.E6,.3
*BOUNDARY
CORN,1,6
BASE,1,6
*GAP, TYPE=UNI
7,26,.012
8,27,.012
9,28,.012
12,29,.012
13,30,.012
-----------------------------------------------------------------------------------------
    5    10    15    20    25    30    35    40    45    50    55    60    65    70    75
```

Figure 35. ABAQUS Input Listing for Problem #4

P A G E 2

```
    5   10   15   20   25   30   35   40   45   50   55   60   65   70   75
-----------------------------------------------------------------------------
14,31,.012
17,32,.012
18,33,.012
19,34,.012
*STEP
 LOAD OF 20,000 G'S APPLIED DOWNWARD
*STATIC, PTOL=.14,CUTMAX=10
*DLOAD , OP=NEW
ALL,BZ,-2800.
*PRINT
*EL PRINT
*NODE PRINT
*END STEP
*STEP, LINEAR=NEW
 LOAD OF 20000 G'S APPLIED UPWARD
*STATIC, PTOL=0.14
*DLOAD
ALL,BZ,2800.
*PRINT
*EL PRINT
*NODE PRINT
*END STEP
-----------------------------------------------------------------------------
    5   10   15   20   25   30   35   40   45   50   55   60   65   70   75
-----------------------------------------------------------------------------
```

Figure 35 ABAQUS Input Listing for Problem #4 (continued) surface: nodes 7-9, 12-14, and 17-19. Therefore, each of these nodes was defined as a "BOP".

Next, static load cases were run for the substrate model with upward unit loads applied separately to each of the BOP nodes (it was known that the module surface would resist the downward deflection of the substrate with an upward force). These unit static load cases, referred to as BOP cases, were then used by the NUBOP program to create a flexibility matrix for the substrate. In addition, a pair of load cases were run in which the two accelerations of interest ($\pm$20,000 G's) were applied to the structure. This resulted in the creation of a pair of vectors representing the relative displacements at each BOP node due to the two accelerations.

The third step in the NUBOP procedure was to set the displacement bounds for each BOP node in the displacement vectors. For our substrate problem, each BOP node was restricted to a maximum downward travel of 0.012".

Finally, to determine the deflection shapes of the substrate when exposed to the $\pm$20,000 G accelerations, a static load case was run which combined the applied acceleration loads with the necessary BOP loads. It should be noted that when the substrate deflected under the -20,000 G acceleration (which is equivalent to an upward load on the substrate), the displacement bound was not crossed, and no BOP loads were allowed to contribute to the final load vector.

5.6.1.2 ANSYS Solution

ANSYS did not require the series of procedural runs necessary for the STARDYNE solution, but ANSYS did require that nine additional nodes and elements be added to the finite element model. The additional elements (ANSYS "STIF52" elements) were nonlinear interface elements capable of supporting only compression in the direction normal to the surfaces and shear in the tangential directions. This element may be given a gap specification, and a specified stiffness acts in the normal and tangential directions when the gap is closed.

The STIF52 elements required for this analysis were each defined by a unique pair of nodes. The upper node for each of these elements was already in existence (nodes 7-9, 12-14, and 17-19); however, nine additional nodes were required to represent the module surface (these nodes were fully restrained).

Once the gap elements had been defined, it was necessary to specify a gap interface stiffness. The manual suggested that for most problems the local surface deformation is not of importance, and that the stiffness of the interface may be estimated as an order of magnitude or two greater than the adjacent element stiffness. However, it also warned against the use of unreasonably high stiffness values due to large increases in the iterative solution time. Ideally, we would have liked the interface stiffness to be infinite so that the solution could be compared directly with STARDYNE's solution (in which the BOP's were infinitely stiff when they encountered the transverse deflection limit of -0.012"). Therefore, after running the program several times, an interface stiffness of 1×10^8 lb/in was finally decided upon as a value approaching the maximum stiffness that would still allow static convergence of the solution.

5.6.1.3 ABAQUS Solution

The ABAQUS solution procedure is probably the simplest of the three programs' methods. Nine additional nodes were defined 0.012" below the nine potential bottom-out nodes on the substrate. Next, while specifying the boundary conditions, the gap condition was defined between the nine pairs of potential interface nodes. At this point, all that remained was to indicate to ABAQUS that a nonlinear statics run was to be initiated (several iteration and convergence parameters were required by the program).

Unfortunately, the ABAQUS runs were consistently aborted from the system. Finally, the ABAQUS Customer Service analysts were consulted with our problem. After several telephone conversations, it was concluded that the S4R quadrilateral plate elements which had been used to model the substrate could not be used for this model without resulting in nodal singularities. The S4R element could not handle the boundary condition restraints imposed upon the substrate (all four corners fully restrained) even for a linear static load case. If we wished to run this model, it would have been necessary to change the elements to "S8R" elements (quadrilateral plate elements with mid-side nodes). However, we decided that these higher order elements would not have provided a valid comparison with the four-node-per-element plate elements used by both STARDYNE and ANSYS. Therefore, no solution was found using ABAQUS for the nonlinear statics problem.

5.6.2 Results from Sample Problem #4

The following Table 25 summarizes the deflections due to both the -20,000 G acceleration and the +20,000 G acceleration, as determined by STARDYNE and ANSYS.

As shown in Table 25, the STARDYNE and ANSYS solutions differ by a considerable amount (it should be noted that only one-quarter of the model is represented in Table 25, due to the symmetry of the substrate). Unfortunately, even the linear part of the solution ("OPEN GAP" column) differs between the programs. A clue to which of the "linear" solutions is the more accurate might lie in the fact that the deflections for the symmetric node pairs (6 & 2, 11 & 3, and 12 & 8) of the ANSYS model are not identical, as they are for the STARDYNE model.

Table 25. Transverse Deflections of Nonlinear Substrate Model (inches)

	STARDYNE		ANSYS	
Node	Open Gap	Close Gap*	Open Gap	Close Gap*
2	0.00476	-0.00403	0.00626	-0.00595
3	0.00852	-0.00718	0.01055	-0.01001
6	0.00476	-0.00403	0.00625	-0.00526
7	0.01025	-0.00825	0.01313	-0.01167
8	0.01320	-0.01048	0.01621	-0.01451
11	0.00852	-0.00718	0.01054	-0.00875
12	0.01320	-0.01048	0.01626	-0.01413**
13	0.01566	-0.01200	0.01885	-0.01650**

* Refers to the case where the acceleration attempts to close the initial gap (+20,000 G)

** Exceeds initial gap clearance

This could indicate that the ANSYS solution had not fully converged for this particular run. Further iterations with various convergence criteria might possibly correct this discrepancy. However, based on the solutions presented in Table 25, it is believed that the STARDYNE solution is probably the more reliable of the two.

When comparing the "closed gap" solutions, it was immediately obvious that, in the ANSYS solution, the maximum deflection was not limited to -0.012 inches. This was due to the fact that the interface element did not have infinite stiffness; when the substrate encountered the module surface nodes, it actually deformed the module surface to some degree. However, we had hoped that the large stiffness that had been given to the interface elements would have prevented this from happening. It might be possible to increase the interface stiffness (and then increase the maximum number of iterations to allow the solution to converge) in order to more closely model the real world situation.

The STARDYNE "closed gap" solution appears to be a very believeable solution: the maximum deflection is -0.012 inches, and the symmetric node pairs have identical deflections. In addition to being the more believable solution, it must be noted that the STARDYNE solution was very straightforward. The STARDYNE solution worked the first time that it was run, and there was no uncertainty about interface stiffness or convergence criteria. STARDYNE appears to have the most user-oriented nonlinear "gap" routine of the three programs that were considered. This concludes the discussion of the nonlinear statics sample problem. The next section of this report will present a summary of the program capabilities and idiosyncrasies which became apparent during the sample problem analyses.

5.7 General Summary for Sample Problems Analysis(Phase2)

This summary will explain the major conclusions from each of the sample problem analyses, and it will also list the more general observations of program idiosyncrasies and/or useful features which were discovered during the sample problem analysis.

5.7.1 Linear Statics Problem

(1) ABAQUS most closely approximated the theoretical maximum deflection at the center of the lid. However, it should be noted that all solutions (STARDYNE, ANSYS, and ABAQUS) were within 3% of the theoretical answer.

(2) ABAQUS also came nearest to approximately the theoretical maximum stress in the center of the simply supported lid, followed closely by ANSYS

and STARDYNE. All stresses were within 8% of the theoretical answer; this error is partially a function of the coarse nodal gridwork used in our model.

(3) The deflection shapes calculated by STARDYNE and ANSYS compare well with each other. The deflection shape calculated by ABAQUS deviates slightly from the other two.

5.7.2 Linear Dynamics Problem

(1) STARDYNE most accurately predicted the first four natural frequencies of the circuit board (average deviation of 1.9%), followed by ANSYS (average deviation of 4.1%), and lagged considerably by ABAQUS (average deviation of 20.5%).

(2) STARDYNE's Lanczos routine was the most user-oriented modal analysis routine of the three programs; it accurately calculated the desired number of natural frequencies and mode shapes, and estimated several natural frequencies beyond those requested.

(3) ANSYS calculated a natural frequency for every "Master-DOF" in the structure. However, it provided mode shapes only for the first four requested natural frequencies. It should be noted that we did not reduce the number of DOF in this model to a few select DOF, as suggested by the ANSYS manual. Instead, we allowed all the structural DOF to contribute in the modal extraction process in order to remain consistent with the STARDYNE and ABAQUS solutions.

(4) ABAQUS Initially appeared to have a very straightforward modal analysis routine. However, ABAQUS recuired the user to recuest more natural frequencies and mode shapes then the four of interest to insure the accuracy of the higher modes. Unfortunately, this is not discussed in the manual; large errors were evident until this idiosyncrasy was discovered. Yet, even the best modal solution by ABAQUS did not approach the accuracy of STARDYNE or ANSYS.

(5) It should be mentioned that STARDYNE provides three other modal extraction methods in addition to Lanczos. These are "Householder-QR," "Inverse Iteration," and "Householder-QR with Guyan Mass Condensation." The "H-QR with Guyan Mass Condensation" method is somewhat similar to the method used by ANSYS in that it artificially reduces the number of DOF in the structural model to a few, select "master-DOF." For a complete understanding of these extraction methods, refer to the STARDYNE User Information Manual.[82]

5.7.3 Heat Transfer Problem

(1) ANSYS provided an accurate solution for the temperature distribution and the heat flux using relatively simply one-dimensional heat conducting elements. The model creation was very straightforward.

(2) ABAQUS did not provide an obvious method of including the convective heat transfer effects from the sides of the pin fin -- at least not using its one-dimensional heat conducting bar

element. The problem could have been solved with its two-dimensional element but this would not have provided a valid comparison with the ANSYS solution.

(3) STARDYNE has no heat transfer elements in its element library, and, therefore, could not be used to solve this problem.

5.7.4 Nonlinear Statics Problem

(1) The STARDYNE solution method was relatively user-oriented. It did require three separate procedural computer runs, and the storage and retrieval of data on files. However, the program required no knowledge of convergence criteria, the program ran properly the first time it was attempted, and the solution appears to be more accurate than the ANSYS solution (considering the symmetry of the calculated deflections, and the maximum downward deflection of 0.012").

(2) The ANSYS solution was not difficult; however, it did expect the first-time user to have some knowledge of the proper relation between gap-stiffness and convergence criteria. The program required several iterative runs before it appeared to converge; further runs could result in an even more accurate solution. The solution presented in this report does not display the expected deflection symmetry, nor does it limit the maximum downward travel of the module to 0.012". Also, a comparison of the upward deflection shape calculated by STARDYNE and ANSYS shows a considerable deviation for the

linear portion of this problem. It is believed that the ANSYS solution would require further manipulation before it approaches the results of the STARDYNE solution.

(3) The ABAQUS solution outlined in the user manual appeared to be very user-oriented. However, it became evident that the S4R element used to model the substrate was not capable of solving even the linear portion of this problem without aborting from the CDC system, due to nodal singularities. A discussion with ABAQUS' customer service indicates that the S8R quadrilaterial plate element (8 nodes per plate) should be able to solve this problem; it was not used because it would not have provided a valid comparison with the 4-node elements of STARDYNE and ANSYS.

5.7.5 General Observations

(1) STARDYNE offers only a 4 node quadrilateral element; both ANSYS and ABAQUS offer 8 node quadrilateral elements.

(2) STARDYNE and ANSYS require a fixed format input; ABAQUS offers a free format option.

(3) ANSYS offers third level element and node generation; STARDYNE offers first level element generation and second level node generation; ABAQUS provides first level element and node generation only.

(4) For modal analyses, STARDYNE requires a weight density while ANSYS and ABAQUS require a mass density.

(5) For plate elements, ANSYS allows the user to specify a small rotational stiffness about an axis perpendicular to the plate. The plate elements of STARDYNE and ABAQUS do not have any rotational stiffness in this direction; the corresponding DOF must be restrained.

6.0 CRITICAL PROBLEM ANALYSIS AND CORRELATION TO TEST DATA (PHASE 3)

6.1 Introduction

Throughout this study, we were searching for a critical problem that would be of current interest to the microelectronic industry, and yet one with existing closed-form and test results. From the survey results of Section 3.0, it was seen that lid seal of large hybrid packages seemed to be the problem which concerned most respondents. Fortunately, reference [88] contains the closed-form solution and test results for this type of problem. Libove [88] provides formulas for the maximum tensile stress in the lid-to-wall seal, the maximum lid deflection, and the lid collapsing pressure for a rectangular flat-pack under external pressure.

Two separate problems were considered. First, finite element analysis was applied to the flat-pack lid problem described in "Example 1" of Libove's report [88]. Basically, this example involved a wide-seal, uniform-wall, constant-thickness-lid flat-pack which was exposed to an external pressure of 30 psi; it was necessary to solve for both the maximum seal stress and the maximum deflection of the lid.

Second, an available Isotronics/Device Closures package was analyzed using the finite element method to solve for the stresses and deflections due to several loading conditions: (1) external pressure, (2) discrete point loads, and (3) thermal loads.

The hybrid which was considered was a uniform-wall package with a welded, stepped-thickness lid. Our numerical results for the external pressure load cases were compared to the values predicted by Libove, while our results for the discrete point load case and the thermal load case were compared to experimentally-derived results using this particular package.

6.2 Critical Problem #1

Critical problem #1 concerned a Kovar flat-pack which was exposed to an external pressure of 30 psi. In order to easily make a comparison between our analysis and the work of Libove, the flat-pack that was chosen was the same wide-seal, uniform-wall, constant-thickness-lid Kovar package described by Libove in his "Example 1" of RADC-TR-79-138. This package is further described in Figure 36.

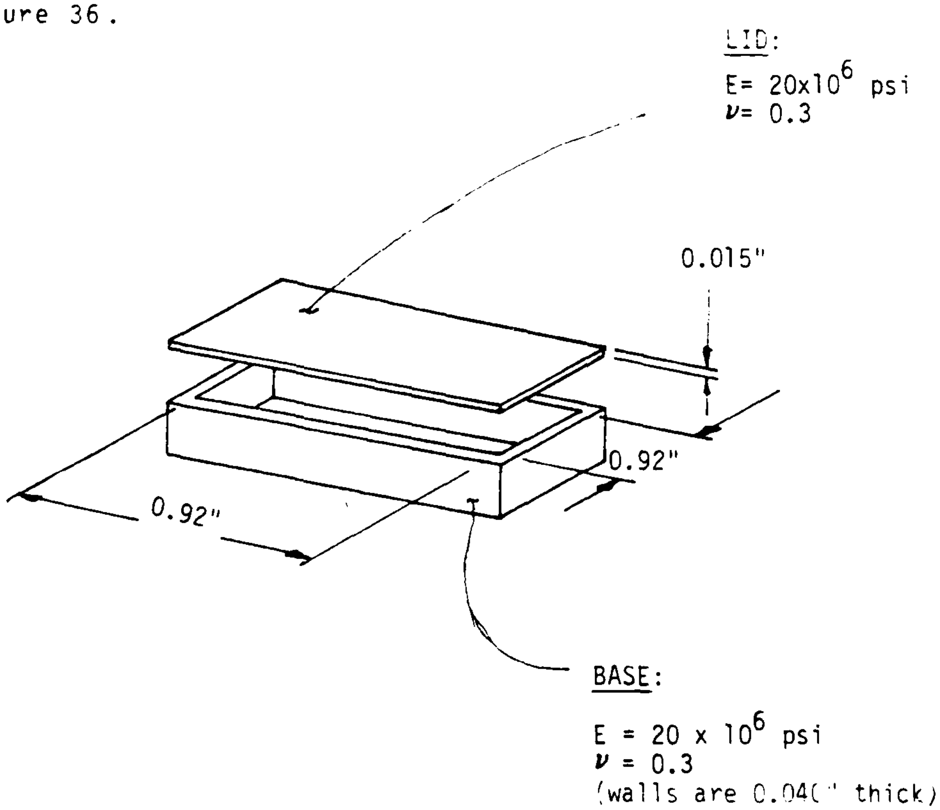

Figure 36. Critical Problem #1 Flatpack Configuration

6.2.1 "First-Cut" Finite Element Model

To begin our analysis of this problem, we decided to generate a preliminary "first-cut" finite element model which could be used to calculate the flat-pack lid deflections. We wished to demonstrate that a simple, inexpensive model could be used to determine the maximum lid deflection, and that this numerical solution would compare well with Libove's analytical results. In all of the following analyses, it should be noted that the STARDYNE finite element program was used to determine the required solutions.

The initial finite element model is shown in Figures 37 and 38. It should be noted that all finite element model views shown in this critical analysis section were generated with the Unistruc preprocessor. The model was a "quarter model" which took advantage of both the structural symmetry and the load symmetry to simplify the analysis. As shown, this model consisted of 34 nodes and 24 quadrilateral plate elements; it required only about one hour to generate this model and obtain the results.

It should be mentioned again that the purpose of this model was to obtain the maximum lid deflection; we were not looking for seal stresses at this time. Therefore, the model included only the package walls and the lid; no elements were included to represent the lid seal between the walls and the lid. The lid was connected to the package walls through the use of common nodes.

The model was fully restrained at the nodes along the bottom edges of the walls. This was a realistic assumption since the walls are effectively cantilevered from the bottom of the flat-pack (assuming a flat-pack bottom thickness of at least 0.040" thick, the rotational stiffness of the wall/bottom junction is considerably greater than the rotational stiffness of the wall/lid junction).

The next section of this discussion will explain our results, and will compare them with the solution presented by Libove.

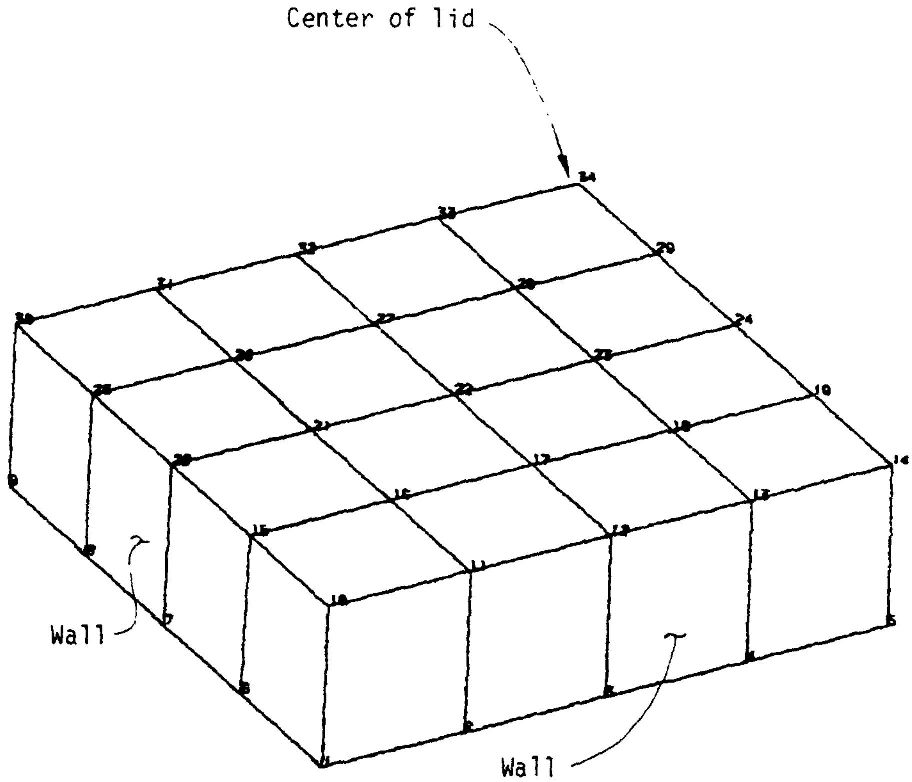

Figure 37. "First-Cut" Finite Element Model
(Node Numbers Shown)

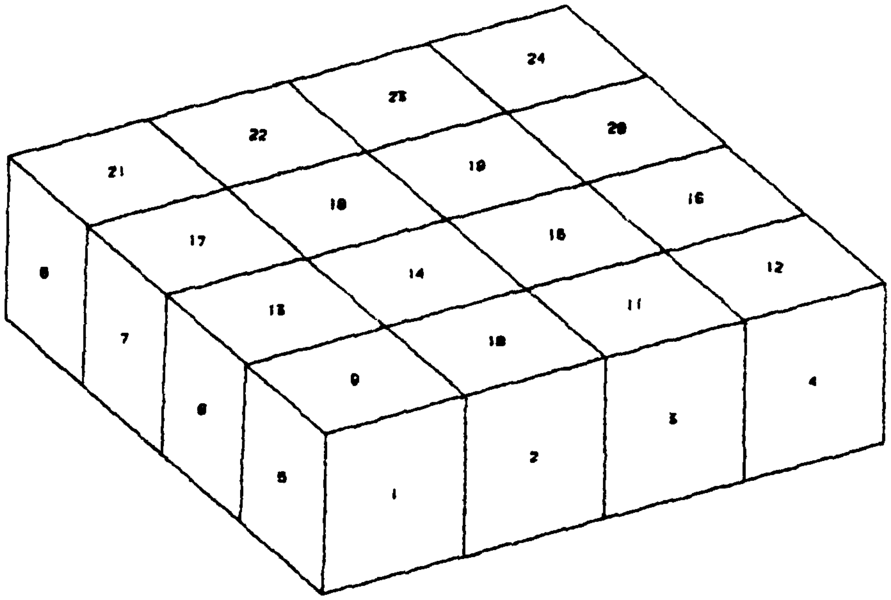

Figure 38. "First-Cut" Finite Element Model
(Element Numbers Shown)

6.2.1.1 "First-Cut" Results

The maximum lid deflection and lid stress calculated by our finite element analysis are compared to the deflection and stress predicted by Libove [88] in Table 26. In addition, the maximum lid deflection and the maximum lid stress determined by our finite element analysis are compared to the corresponding values calculated with the formulas provided by Roark for a clamped rectangular plate under external pressure [85]. The deflection and stress calculations using the methods of Libove and Roark are shown below:

(1) Libove (refer to "Example 1" of RADC-TR-79-138, page 30)

(a) Deflection

$$\delta_{max} = 12\ (1-V^2)\ \frac{P}{E} \left(\frac{a}{t}\right)^3\ (a)\ (n_4)\ (n_5)$$

where:

δ_{max} = maximum lid deflection

V = Poisson's ratio = 0.3

P = pressure = 30 psi

E = Young's Modulus = 20×10^6 psi

a = lid width = 0.92"

t = lid thickness = 0.015"

n_4 = function of K and b/a = 0.00125

K = ratio of wall's to lid's flexural stiffness = 113

b = lid length = 0.92"

n_5 = large deflection theory correction factor=0.981

δ_{max} = 0.00426"

(b) Stress

$$\sigma_{max} = \frac{6\ n_1\ P\ a^2}{t^2} \quad \text{(page 21 of Libove)}$$

where: σ_{max} = maximum lid stress at middle of long edge

n_1 = function of K and b/a = 0.051

p = pressure = 30 psi

a = lid width = 0.92"

t = lid thickness = 0.015"

σ_{max} = 34,533 psi

(2) Roark (refer to Formulas for Stress and Strain, page 392)

(a) Deflection

$$y_{max} = \frac{\alpha c\ b^4}{ET^3}$$

where: y_{max} = maximum plate deflection

c = pressure = 30 psi

b = plate width = 0.92"

E = Young's modulus = 20×10^6 psi

t = plate thickness = 0.015"

α = function of a/b = 0.0138

y_{max} = 0.00439"

(b) Stress

$$\sigma_{max} = \frac{B_1\ c\ b^2}{t^2}$$

where: max = maximum plate stress at middle of long edge

q = pressure = 30 psi

b = plate width = 0.92"

t = plate thickness = 0.015"

B_1 = function of a/b = 0.3078

σ_{max} = 34,736 psi

Table 26. "First-Cut" Results for Critical Problem #1

Max Lid Deflection			Max Lid Stress		
Libove	STARDYNE	Roark	Libove	STARDYNE*	Roark
0.00426"	0.00442"	0.00439"	34,533	17,019 psi	34,736 psi

*Von Mises combined stress

As shown in Table 26, the maximum lid deflections as calculated by Libove, STARDYNE, and Roark correlate well; STARDYNE calculates a deflection which is only 3.7% greater than the value published by Libove. Interestingly enough, the solution by Roark also compares well with the other two solutions -- remember that the Roark solution was based on an analysis of a totally clamped rectangular plate. This tends to support the Libove proposal that the walls of this flat-pack are effectively clamping the edges of the lid.

Also shown in Table 26 is a comparison of the maximum lid stresses as calculated by Libove, STARDYNE, and Roark. As indicated, Roark and Libove agree within 0.6%; this small difference could be due to the fact that Roark's solution assumes completely clamped edges, while Libove's solution considers the edges as something just slightly less than fully clamped.

However, both Libove and Roark disagree with the STARDYNE solution. The primary reason for this discrepancy is that the finite element program calculates the outer-surface plate stresses at the centroid of each element. Therefore, although it is known that the maximum stresses in the lid will occur at the midpoints of the lid's edges, STARDYNE considered the maximum stress to occur at the centroid of elements 12 and 21 (the elements nearest the edge midpoints). It would be necessary to generate a finer element grid near the edge midpoints (nodes 14 and 30) to approach the actual stress value as predicted by Libove and Roark. (It should be remembered that the primary purpose of this model was to calculate deflections.)

One advantage of the STARDYNE model is that it can consider the effect of the pressure applied to the package walls as well as the package lid. However, our analysis indicated that there was no significant difference in the calculated lid deflections when the pressure on the walls was included in this model.

The next section of this discussion will describe a more detailed finite element model of the flat-pack which includes elements that represent the lid seal.

6.2.2 Finite Element Model with Lid Seal

To continue our analysis of Critical Problem #1, we felt that it was necessary that we consider a finite element model of the flat-pack which included the lid seal. This would allow us to determine the maximum seal stress in addition to the maximum lid deflection and the maximum lid stress. Also, we were interested in determining the effect of different seal materials on the deflection and stress values.

This finite element model is shown in Figure 39. Again, the model is a "quarter model" which took advantage of both the structural and the loading symmetry. As indicated, the model consisted of 112 nodes, 43 cube elements, and 43 quadrilateral plate elements. The cube elements were used to model the package walls, the lid, and the lid seal. The 43 thin membrane plate elements (0.00001" thick) were applied to the top and bottom surfaces of the lid's cube elements, and to the outside surfaces of the wall elements. These plate elements were necessary for two reasons: (1) to determine the maximum lid bending stresses on the top and bottom surfaces of the lid (the stresses calculated for the cube elements are calculated at the cube centroids, not on the exterior faces), and (2) to allow a pressure to be applied to the top surface of the lid elements and to the exterior surface of the wall elements (the STARDYNE program does not allow a pressure to be applied to a cube element).

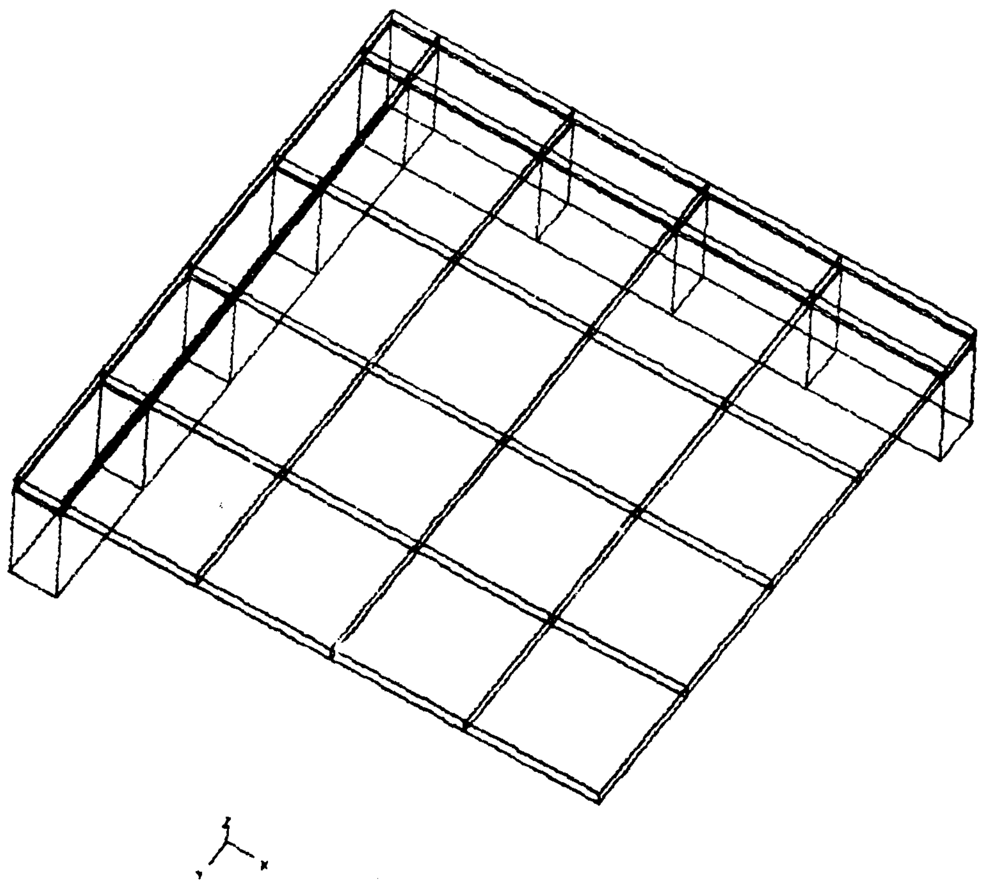

Figure 39. Finite Element Model with Lid Seal

As previously mentioned, cube elements were used to model the lid seal; it was not possible to accurately model the structural geometry with plate elements. The seal was assumed to be 0.005" thick, and as wide as the top of the wall. Three different seal materials were considered: Kovar, solder, and glass. The necessary properties of these materials are listed in Table 27.

Table 27. Seal Material Properties

Seal Material	Young's Modulus(E)	Poisson's Ratio(V)
Kovar	20×10^6 psi	0.3
Solder (62% Sn, 36% Pb, 2% Ag)	6.4×10^6 psi	0.4
Glass (Corning "9010")	9.8×10^6 psi	0.22

This flat-pack model, as in the previous "first-cut" model, was fully restrained at the nodes along the edges of the bottom of the walls. However, in this case, the cubical seal elements were used to connect the flat-pack walls to the lid elements.

The next section of this discussion will explain the results obtained with this model, and will compare them with the solution presented by Libove.

6.2.2.1 Results of Model with Lid Seal

The maximum lid deflections and stresses obtained with each of the three seal materials are compared to the value predicted by Libove in Table 28.

As shown in Table 28, the maximum lid deflections as calculated by Libove and STARDYNE correlate fairly well. Note that Libove's solution makes no allowance for variations in seal material, and he predicts a single lid deflection regardless of seal material. However, as shown by the STARDYNE solution, Libove's neglect of seal material effects might be appropriate:

the lid deflection variation due to the three different seal materials analyzed with this model may be considered insignificant.

Also, in regard to the maximum lid deflections, the deflection calculated by STARDYNE for each of the three seal materials is less than the deflection calculated by STARDYNE for the previous "first-cut" analysis. This is not what was expected, especially for the glass and the solder cases. The addition of the seal to the model should have increased the maximum lid deflections. An explanation for this apparent discrepancy is that different elements were used in the generation of the two models. Any variation in the stiffness formulations for the cube elements and the quadrilateral plate elements could result in different calculated deflections for the same flat-pack lid (remember that the quadrilateral plate elements are 5 D.O.F. per node, and that the cube elements are 3 D.O.F. per node).

When considering the maximum lid stresses in Table 28, it appears that there is a substantial disagreement between Libove's value and the STARDYNE values. However, as in the "first-cut" analysis, the stress calculated by Libove is located at the midpoints of the lid edges; the stresses computed by STARDYNE are located at the centroids of the two plate elements closest to the mid-side nodes. A finer element grid would be required for STARDYNE to predict a stress closer to the mid-side node locations. For this reason, the lid stress comparison of Table 28 is not completely valid. Yet, it is interesting to note that the effect of varying seal materials is almost insignificant as far as the lid stress is concerned.

Table 28. Results of Model with Lid Seal

Parameter	Seal Material: Kovar	Solder	Glass
Maximum Lid Deflections:			
Libove	0.00426"	0.00426"	0.00426"
STARDYNE	0.00391"	0.00399"	0.00397"
% diff.	-8.2%	-6.3%	-6.8%
Maximum Lid Stresses:			
Libove	34,533 psi	34,533 psi	34,533 psi
STARDYNE*	13,943 psi	13,790 psi	13,829 psi
% diff.	-59.6%	-60.1%	-60.0%
Maximum Seal Stresses:			
Libove Vertical Stress	5,443 psi	5,443 psi	5,443 psi
STARDYNE:			
(a) Von Mises Stress	4,888 psi	2,185 psi	2,820 psi
(b) Lateral Stress	-5,737 psi	-2,662 psi	-3,244 psi
(c) Longitudinal Stress	-1,903 psi	1,222 psi	-828 psi
(d) Vertical Stress	-335 psi	-332 psi	-333 psi

* Von Mises Stress

Finally, Table 28 compares the maximum seal stresses as predicted by Libove and by STARDYNE. For the STARDYNE solution, four different stress quantities are tabulated: (1) the Von Mises combined stress which should be used to predict seal failure, (2) the lateral normal stress across the width of the seal, (3) the longitudinal normal stress down the length of the seal, and (4) the vertical normal stress across the thickness of the seal. Although the STARDYNE vertical stresses vary insignificantly with seal material, they do not compare well with Libove's calculated vertical tensile stress of 5,443 psi. However, once again, we are not able to compare stresses at a common point. The STARDYNE stresses are all calculated at the centroid of the seal elements nearest the midpoints of the lid's edges, while Libove's maximum stress is calculated along the most outward edge of the seal at the midpoints of each of the lid's edges. It is very possible that the seal stress distribution across the width of the seal is such that the vertical stress at the outside edge of the seal is about 5,000 psi (corresponding to Libove's value) and the vertical stress in the center of the seal is about -300 psi (corresponding to STARDYNE's value). Figure 40 compares Libove's assumed stress distribution with STARDYNE's central vertical seal stress; note that it would recuire a more complicated seal model, one with several elements placed across the seal width, to determine the actual stress distribution.

Continuing with the discussion of the STARDYNE seal stresses, it can be seen that the lateral and longitudinal stresses at the center of the seal are larger than the vertical stresses. These stresses cannot be ignored, and therefore, they were combined with the vertical stress to compute the Von Mises combined stress at the center of the seal (experience has shown that the Von Mises combined stress is usually a better method of predicting structural failure than by relying on only a single component of the overall stress state). Libove's analysis appears to suggest that the only significant stress at the outside edge of the seal is the vertical tensile stress; therefore, the Von Mises combined stress for Libove's analytical stress state is probably very close to the value indicated in the table for his vertical stress component. Again, however, the STARDYNE Von Mises stress should probably not be expected to compare with the Libove stress since they are not calculated at the same location in the seal.

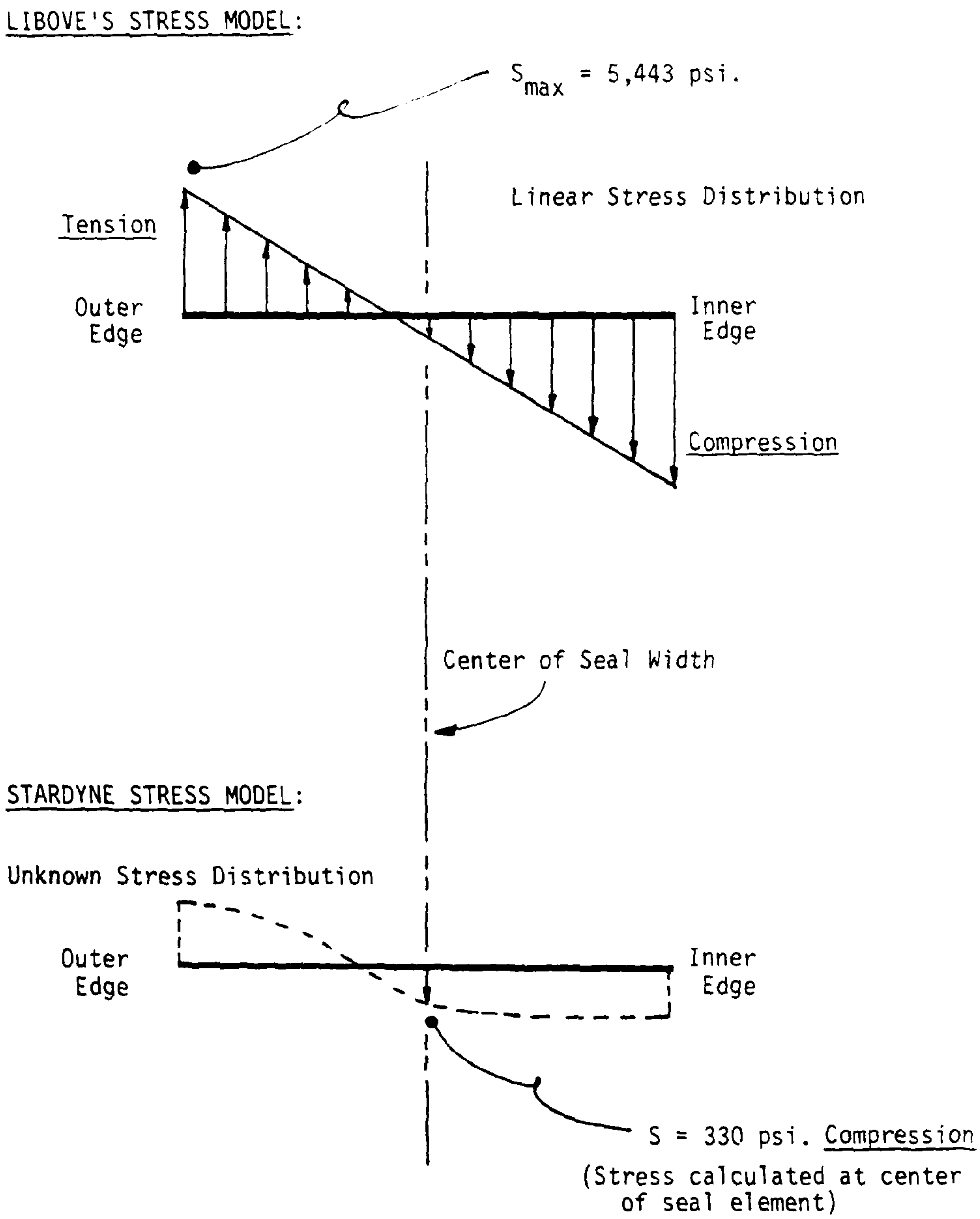

Figure 40. Comparison of Libove's and STARDYNE's Vertical Seal Stresses

The next and final analysis which was performed with regard to Critical Problem #1 concerned a model of a single section of the lid seal. The purpose of this final analysis was to obtain some idea of the vertical stress distribution across the width of the seal.

6.2.3 Local Seal Model

In order to more accurately determine the vertical stress distribution across the seal width, we decided to take a closer look at a single section of the lid seal. Obviously, from an analytical viewpoint, it would have been desirable to simply modify our previous work by incorporating a more detailed seal model into the finite element model of the flat-pack. However, the seal had to be modeled with several elements located across the seal width in order to more accurately predict the stresses along the interior and exterior wall surfaces, and also to give a more meaningful distribution of stress values across the width of the seal. To do so for the entire flat-pack model would have resulted in a complex and relatively expensive finite element model. Therefore, it was decided to take a quick and easy look at the problem by analyzing only a small portion of the total seal.

In effect, a single "strip" was removed from the most highly stressed seal area of our previous "quarter-model"; this strip of elements included lid elements, seal elements, and wall elements. It was then attempted, through several methods, to force this strip of the original lid into the deflection shape which this particular group of lid elements had assumed during our prior analysis. By doing so, we hope to apply the same forcing function as originally seen by our chosen seal elements to the more detailed model of this section of the seal. Figure 41 describes the seal model and shows its relationship to the previous flat-pack model.

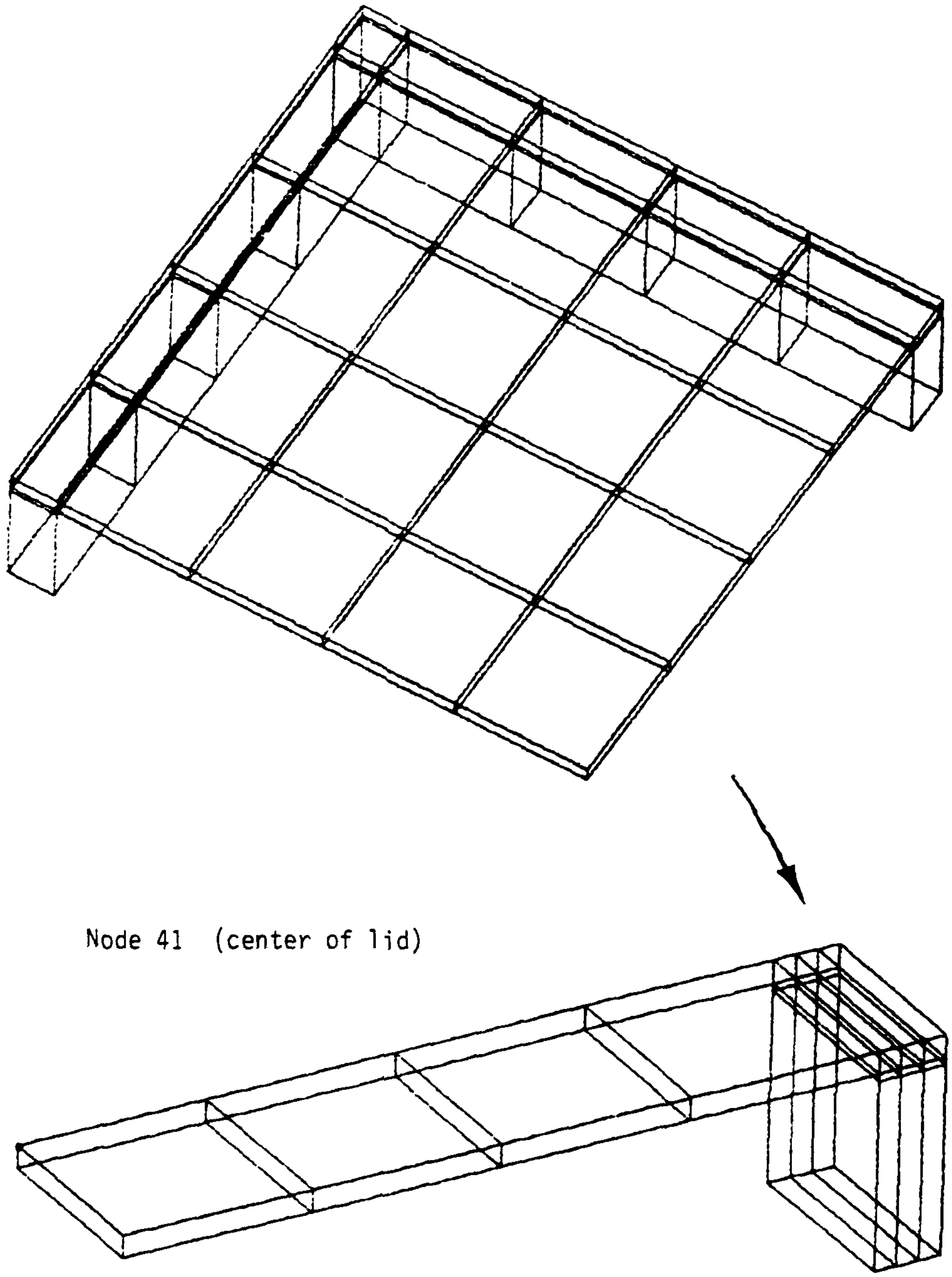

Figure 41. Detailed Seal Model

As shown in Figure 41, the seal was modeled using three rows of cube elements across its width. To better determine the vertical stress distribution across the seal's width, four thin (.0001") membrane plate elements were added to the vertical faces of the three seal cube elements. These elements were located at the inner and outer walls of the seal and at the two adjoining vertical faces of the interior seal cube elements. This method, in effect, allowed us to use seven elements to determine the vertical stress distribution across the seal's width. To provide the required element connectivity, it was necessary to also subdivide the lid and wall elements in the immediate vicinity of the seal. With the above modifications, our local seal model consisted of 48 nodes, 13 cube elements, and 14 quadrilateral plate elements (10 of these plate elements were added to the exterior surfaces of the lid, seal, and wall elements so that pressure could be applied to our cube-element structure). Also, it should be mentioned that Kovar was considered to be the seal material for this analysis.

To recreate the state of stress present in the seal of our previous model, it was necessary to recreate the overall forcing function which caused the original stress state. Several potential methods were considered, but time did not allow all methods to be investigated. Therefore, two loading conditions were considered for this dislocated portion of the flat-pack model.

Both of the loading conditions which we considered were based on the assumption that the lid's center deflection was the prime influence on the stress state of the seal. The first loading condition, therefore, was to simply force the node representing the center of the flat-pack (node 41) to deflect the same amount as discovered in our previous lid analysis (0.00391"). We felt that the remainder of the nodes would then deflect in a manner similar to the deflection shape previously determined, the majority of any difference probably being due to the different stiffness formulation of the seal elements with the new gridwork modification in effect.

The second loading condition was identical to the first except that the 30 psi pressure loading was applied to the top surface of the lid and to the exterior surfaces of the wall and the side. It was hoped that the addition of this pressure would help recreate the original deflection shape even more accurately than for the first loading case.

Another possible, seemingly obvious, loading case should be discussed. It would be possible to force every node common to both this model and our original model to deflect the amount that was calculated in the original analysis of the model with the seal. This would seem to be an obvious solution method, except for one consideration. The previously calculated nodal deflections were based on the seal stiffness formulation of the original model. However, by changing the gridwork of the seal elements, the effective seal stiffness has been modified somewhat. Therefore, in a region close to the revised seal elements, the previously calculated deflections might not truly represent the deflection shape which the lid would assume with the modified seal elements. In effect, we would be forcing a deflection shape which might not ever be realized had the 30 psi pressure been applied to a complete lid model with our modified seal elements. This explains the reason why our forcing loading conditions were concerned with the central deflection only: we assumed that the modified seal elements would not have significantly affected the central deflection, but that their different stiffness formulation would have only affected nodes in the local region. Therefore, we forced the central deflection to be the same as for our previous analysis, but we allowed the deflections of nodes near the seal to assume a deflection consistent with the revised seal element stiffness.

6.2.3.1 <u>Results of Local Seal Model</u>

The stresses which were calculated for the elements across the width of the seal are summarized in Table 29 for both loading cases. As shown in the table, the vertical seal stresses vary significantly across the width of the seal.

Table 29. Seal Stress Across Seal Width

	Seal Stress Location		Seal Stress (psi)			
Loading Description	Element	Location	Vert.	Long.	Lat.	Von Mises
Forced Center	Plate 24	Inside	-4,488	-1,170	-	4,191
Displacement	Cube 11		-3,961	-2,486	-1,833	4,471
(load case 1)	Plate 25		2,912	898	-	2,591
	Cube 12	Middle	445	1,612	605	2,155
	Plate 26		-69	-69	-	192
	Cube 13		191	633	170	1,273
	Plate 27	Outside	1,171	245	-	1,095
Forced Center	Plate 24	Inside	-8,207	-2,125	-	7,462
Displacement	Cube 11		-6,788	-4,567	-3,173	7,778
Plus Pressure	Plate 25		4,890	1,598	-	4,329
(load case 2)	Cube 12	Middle	749	2,680	1,094	3,600
	Plate 26		-172	-52	-	310
	Cube 13		287	1,049	349	2,159
	Plate 27	Outside	2,025	503	-	1,849

Figure 42 shows the vertical stress distribution across the seal width. Along the inside edge of the seal there are large compressive stresses; along the outside edge of the seal, the stresses are smaller in magnitude, and they are tensile instead of compressive. For both load cases, it is obvious that the vertical stress distribution is not linear. To better understand this

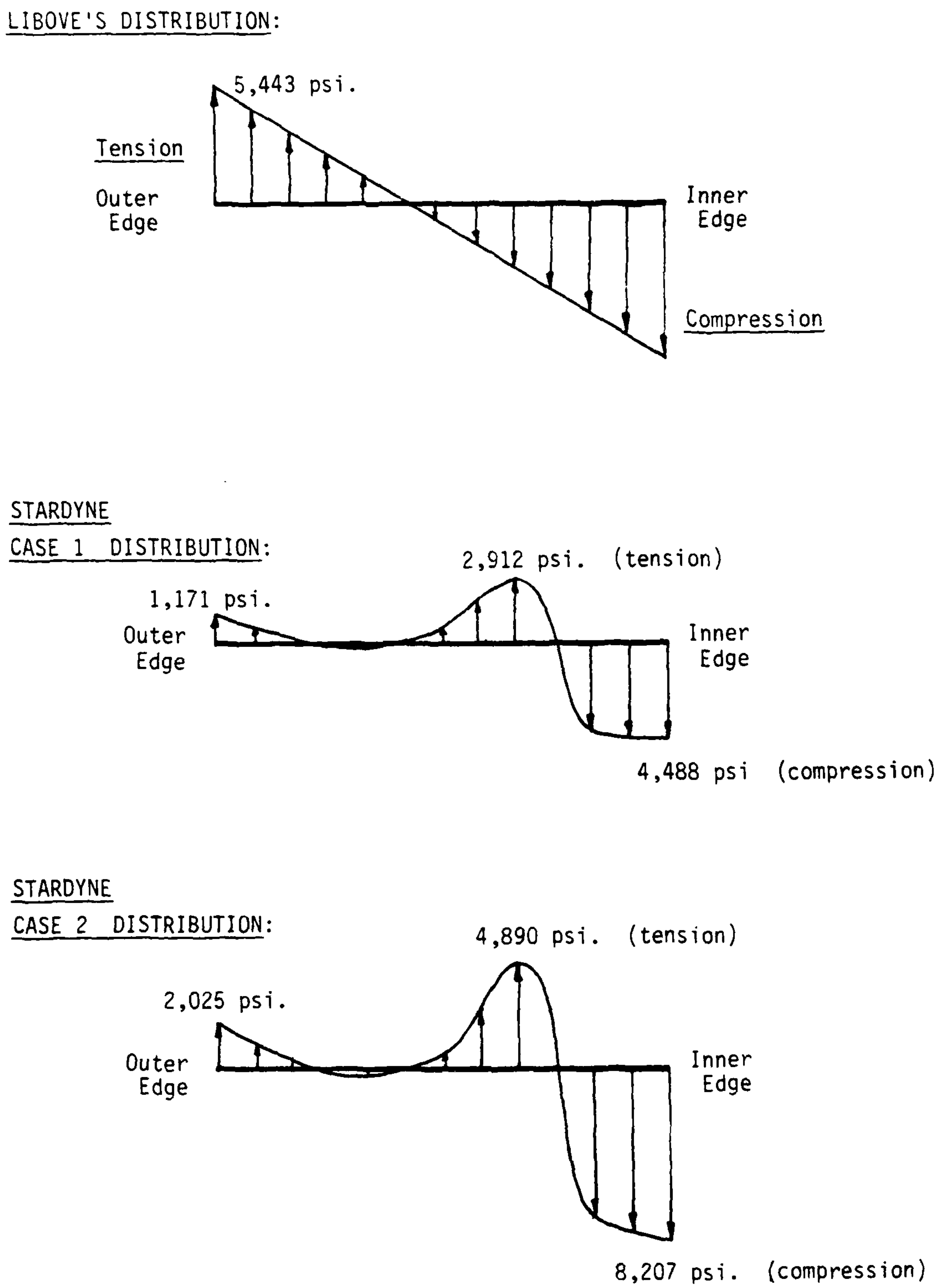

Figure 42. Vertical Stress across Seal Width

phenomena, one must consider the differences between Libove's closed-form solution and the finite element solution. First, Libove assumes a stress distribution as shown on Page 62 of his report [88]. Examination of this distribution and Libove's formulas for the maximum seal stress appears to indicate that he assumes equal maximum tensile and compressive stresses. However, the reactive forces applied to the seal appear to be concentrated towards the inner wall, indicating that these maximum stresses should really not be equal. The force distribution seems to imply that the inner compressive stress should be greater than the outer tensile stresses.

Second, the finite element solution considered the flexibility of the wall underneath the seal. Libove's solution appears to have ignored this effect. This wall flexibility may have contributed somewhat to the seal stress distribution determined by our finite element model. The distribution indicates that the effect of the applied moment is dominant, and is reacted by the inner half of the seal. Note that the maximum tensile and compressive stresses in the inner half of the seal width are on the same order of magnitude, but the compressive stresses are larger. Also, note that there is a tensile lifting of the seal at the outer edge of the lid. Figure 42 also shows that STARDYNE's calculated stress distribution varies depending on the load case. It is not immediately obvious which load case results in the more accurate stresses, although it seems reasonable that load case #2 might be the better of the two.

In summary, the maximum seal stress magnitudes as predicted by Libove's closed-form solution and our finite element models are in the same "ballpark." However, the vertical stress distributions predicted by these two methods are markedly different.

Basically, what we have shown with this local seal analysis is that the vertical seal stress distribution is not likely to be linear. However, this has only been an initial look at the problem; more analysis would be required to accurately determine the seal stress distribution.

The next section describes the second critical problem.

6.3 Critical Problem #2

Critical Problem #2 was concerned with a hybrid package consisting of an Isotronics base and a Device Closures lid. The dimensions of the base and the lid are shown in Figure 43.

In the following two analyses, the hybrid package will be analyzed to determine its response to a pressure load of 30 psi, a series of concentrated loads of 3 lb, and a thermal load induced by a 180^{o} F temperature differential. The first analysis will be a relatively simple analysis of the hybrid lid; the walls will be neglected for this first analysis. Also, this analysis will take advantage of the symmetry of the lid and its loads, and we will, therefore, use a "quarter" finite element model.

The second analysis of this package will use a "full" finite element model of the hybrid's base, walls, and lid. A full model was used so that we could determine deflections caused by asymmetrical point loads. These calculated deflections were then compared to the actual measured deflections induced by the various point loads which were applied to the hybrid lid. In addition, the analytical thermal strains were compared to the thermal strains measured in the laboratory.

6.3.1 "First-Cut" Finite Element Model

To begin the analysis of Critical Problem #2, we decided to perform a relatively simple analysis of the hybrid lid neglecting the effects of the walls and the hybrid base. Due to our use of a "quarter" model for this analysis, we were limited to only investigating symmetrical load cases.

The model used for this analysis is shown in Figure 44; as shown, it consists of 161 nodes, 72 cube elements, and 72

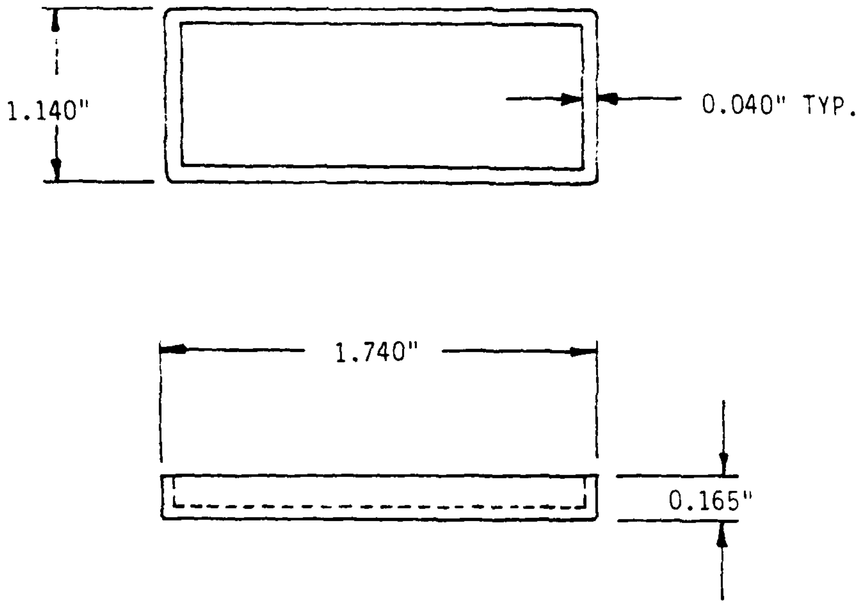

KOVAR LID (Welded to base)

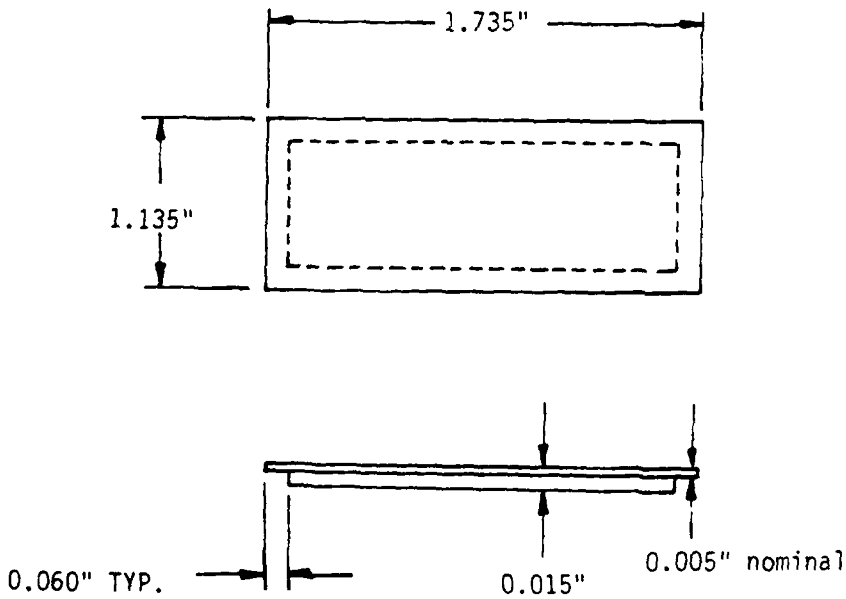

Figure 43. Critical Problem #2 Package Configuration

ISOMETRIC VIEW:

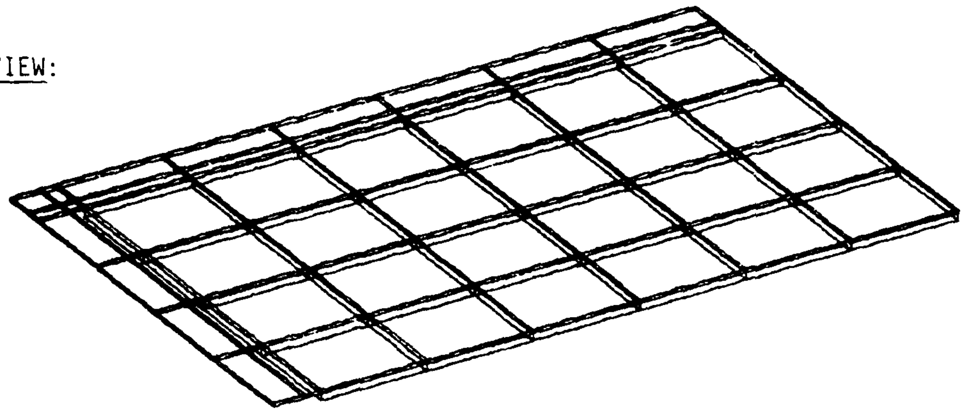

TOP VIEW:

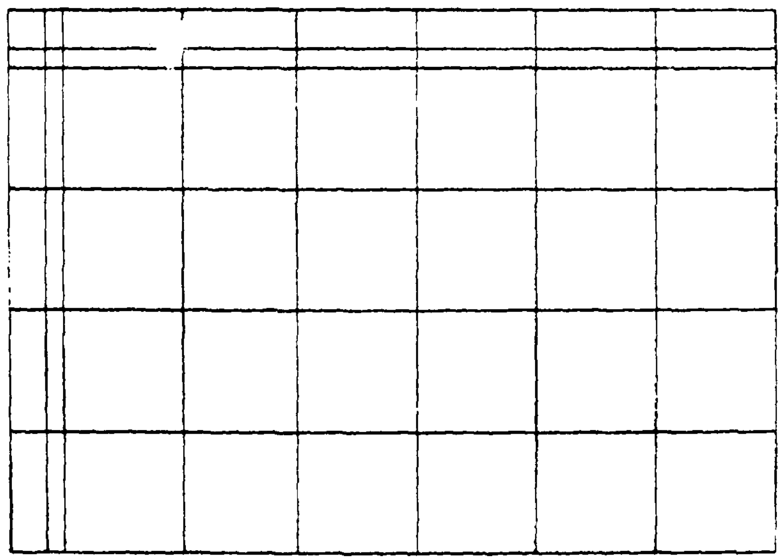

EDGE VIEW:

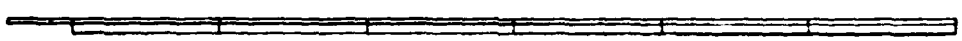

Figure 44. Quarter Model of Hybrid Lid

cuadrilateral elements. The lid structure was modeled with cube elements, and the model included the stepped-thickness feature of the actual lid. Also, the quadrilateral plate elements (0.0001" thick) were applied to the top and bottom surfaces of the lid to incorporate the effect of the nickel plating used on the real lid. In addition, these elements allowed us to apply an external pressure to the upper surface of the lid (remember that STARDYNE's cube elements may not be directly loaded with a pressure).

The thin outer perimeter of the lid was assumed to have a thickness of 0.005" (average of the dimensioned values), and the central portion of the lid was assumed to be 0.015" thick. The lid model was fully restrained at the nodes along the bottom surface of the lid perimeter; in a more complete model these nodes would have connected the lid to the hybrid walls. Also, the nodes along the axes of symmetry were restrained consistent with the necessary boundary conditions (note that it was not necessary to restrain the various rotations since this is a 3-DOF cube element model, and all nodal rotations are identically zero).

It should be mentioned that the above restraints apply to the pressure loading case and the point loading case only. For the thermal strain analysis, all boundary restraints were removed, one node was full restrained, and the lid was allowed to expand freely (the base is also Kovar, and will expand very nearly the same as the lid).

6.3.1.1 "First-Cut" Results

The maximum deflections and stresses for both of the force load cases are summarized in Table 30 below.

Table 30. "First-Cut" Results for Critical Problem #2

Load Case	Center Deflection	Lid Stress (element)
30 psi Pressure	0.02325"	28,700 psi (cube 32)
3 lb Central	0.00513"	6,647 psi (cube 72)

As shown in Table 30, the 30 psi external pressure produces a central lid deflection of 0.02325", and a maximum Von Mises combined stress of 28,700 psi in cube 32 (cube 32 is located adjacent to the midpoint of the long side of the hybrid, and it is one of the 0.005" thick perimeter elements, this stress is less than the yield strength of 50,000 psi).

The equations presented in Roark's Formulas for Stress and Strain [85] may be used to show that a 0.015" thick, clamped rectangular Kovar plate (1.66" x 1.06") would have a central deflection of 0.01386" under a 30 psi load. This is less than our calculated lid deflection because Roark does not consider the effect of the variable thickness lid (refer to Appendix A).

Also, the calculated central lid deflection of 0.02325" due to the pressure loading falls into the range of deflections calculated by Libove; Libove suggests that the deflection will fall between 0.0138" and 0.0402" depending upon the extent of plastic flow which is initiated in the lid (refer to Appendix B, and Libove pp. 23-26).

Table 30 also shows that the center of the lid will deflect approximately 0.005" when subjected to a 3 lb central load. The corresponding maximum Von Mises stress occurs in the center of lid, and has a value of about 6,650 psi. Note that these stress values were used in determining maximum loads for use in our laboratory investigations. (This lid deflection may be compared with actual measured deflection discussed later in this report).

The final portion of this analysis consisted of the 180^{o}F differential temperature loading. The lid was assumed to be at an initial temperature of 77^{o}F, and the thermal strains were calculated for the lid after it was raised to a temperature of 257^{o}F. A coefficient of thermal expansion (CTE) of 3.05 x 10^{-6} in./in.^{o}F was used for the Kovar lid, and a CTE of 8.40 x 10^{-6} in./in.^{o}F was used for the thin nickel plating. The resulting in-plane thermal strain was calculated to be 5.70 x 10^{-4} in/in. Again, this strain will later be compared to experimental data.

6.3.2 Second Finite Element Model

To continue our analysis of critical problem #2, we decided to model the hybrid with a somewhat more detailed finite element model which would allow us to calculate deflections for asymmetrical loads. This model included elements which represented the hybrid lid, walls, and base, and would be used to compare calculated deflections and thermal strains to laboratory values.

The finite element model is shown in Figure 45. As shown, the model was constructed entirely of plate elements (122 nodes, 116 quadrilaterals, and 4 tri-plates). For the pressure and point force loads, all of the nodes along the bottom of the hybrid were fully restrained. However, for the thermal load, only a single corner node was restrained so that the hybrid would be free to expand as dictated by its CTE.

6.3.2.1 Pressure Loading Results

The following Table 31 summarizes the results of the pressure loading case.

Table 31. Pressure Loading of Hybrid Model

Load Case	F.E.M Lid Deflection	Libove Lid Deflection		Lid Stress 0.015" Central Section	Lid Stress 0.005" Edge Section
30 psi Pressure	0.03240"	0.0138"	0.0402"	43,900 psi (Quad 96)	210,300 psi (Quad 71)

As shown in Table 31, the calculated lid deflection is approximately 0.0324" which is greater than our previous calculated value of 0.0233". The difference is due to the different stiffness formulations of the cube elements from the previous model and the plate elements of the present model.

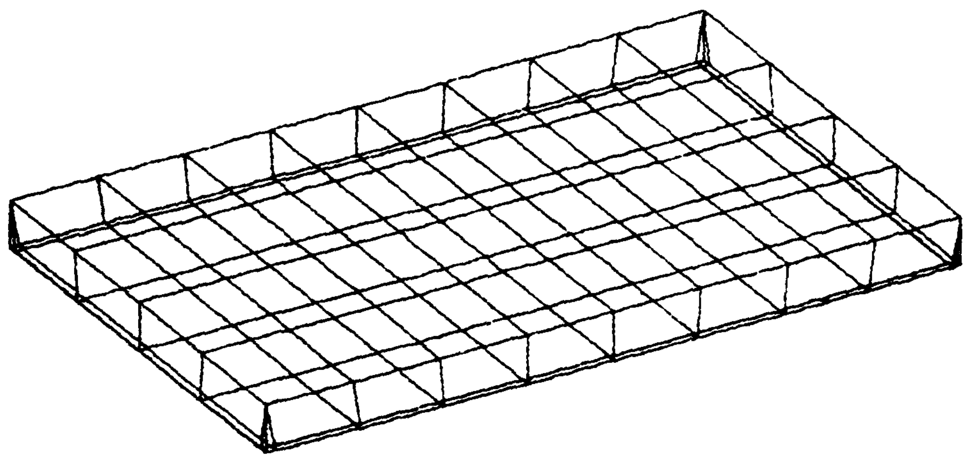

Figure 45. Complete Hybrid Model

Also, from the table, it appears that the maximum stress in the thick (0.015") portion of the lid is reasonable, and this stress occurs in the elements adjacent to the center of the lid. However, the maximum stress calculated for the thin perimeter of the lid (0.005") is not reasonable. This stress occurs at the midpoints of the long edges of the lid, but its magnitude is adversely affected by our use of excessively large aspect ratio quadrilateral plates in this region. (Ideally, aspect ratios for plate would be kept between 1 and 3 for the most accurate results.) If we desired to obtain a better stress in this area, a different gridwork would be required for our model.

It should be noted that no laboratory results were available to correlate with our calculated deflections for the pressure loading case. However, for both the point load cases and the thermal load case, experimental data was collected and used for correlation purposes.

6.3.2.2 Point Loading Results

As shown in Figure 46, five different point load cases were considered in the laboratory; in each case a load of 3 lb was applied to the lid. Figure 46 shows the points of application of these loads. Appendix C presents the test plan which was followed during the laboratory investigations.

Table 32 indicates both our measured deflections and our calculated deflections for each point of load application. Note that there are two sets of calculated deflections. The first corresponds to the deflections based on an assumed central lid thickness of 0.015" and an assumed edge thickness of 0.005". However, after the deflection tests were complete, the hybrid lid was sectioned, and actual thickness measurements were made. It was found that the center portion of the lid varied between 0.0140" 0.0145". Therefore, the second set of calculated deflections

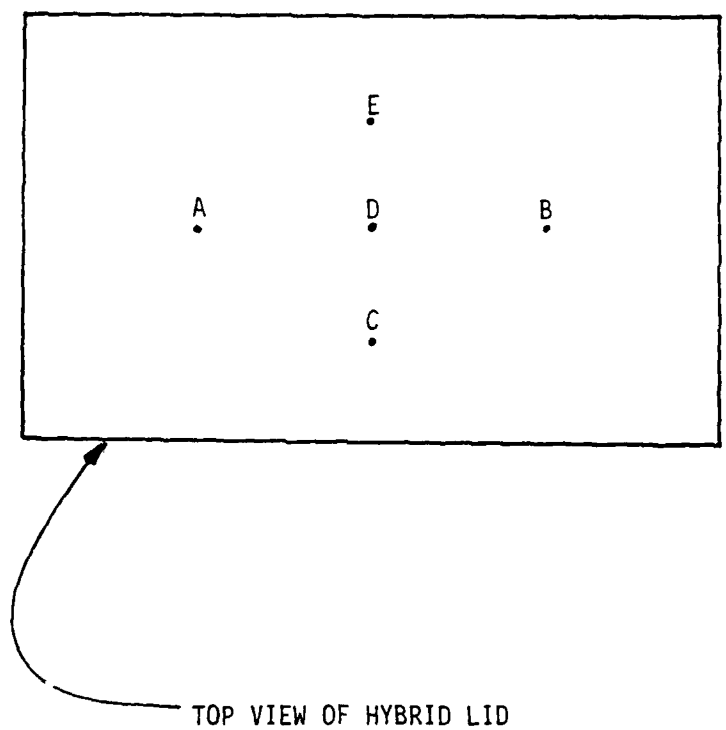

Figure 46. Points of Concentrated Load Application

represents the deflections after the above thickness changes were included in the lid model.

Table 32. Point Loading of Hybrid Model

Point of Application	Measured Deflections	Calculated Deflections Nominal Thick for Lid	Calculated Deflections Actual Thick for Lid	% Difference*
A	0.00575"	0.00551"	.00614"	+6.8%
B	0.00625"	0.00551"	.00624"	-0.2%
C	0.00456"	0.00444"	.00493"	+8.1%
D	0.00775"	0.00693"	.00785"	+1.3%
E	0.00562	0.00444"	.00518	-7.8%

*Percent difference between our "best" calculated deflections and the measured deflections

As shown in Table 32, the measured lid deflections correlate very well (within 8%) with the calculated lid deflections which were based on the actual lid thickness. The error would have been significantly greater had we not reiterated our calculated lid deflections once the actual lid thicknesses were known. This is just one example of how the analyst may use a combination of analysis and test data to more fully understand what may seem initially to be significant deviations between his analysis and the test results.

6.3.2.3 Thermal Loading Results

As previously done in our "first-cut" analysis, we thermally loaded the hybrid with an increase in temperature of $180^{o}F$, and calculated the resulting thermal strains. Using a CTE of 3.05×10^{-6} in./in.^{o}F for the hybrid, we determined in-plane strains of 5.49×10^{-4} in/in. However, it should be noted that this calculation did not include the effects of the nickel plating on the thermal expansion of the lid. Therefore, assuming a plating thickness of 0.0001", an effective CTE of 3.16 in/in/^{o}F may be found from our previous analysis which results in a thermal strain of 5.69×10^{-4} in/in for this model.

To experimentally determine the lid strain due to a 180°F temperature change, it was decided to instrument the hybrid lid with a pair of strain gages. Unfortunately, we did not have available the required gages for this experiment (i.e., no gages of the proper size and with a CTE of 3×10^{-6} in./in.$^{\circ}$F). However, we did decide to go ahead with the test using the gage that we had available, realizing that we were introducing some error into our measurements.

Basically, we were required to adjust our measured strain data to consider the following four aspects:

1. Mismatched CTE between gage and lid
2. Apparent strain due to temperature/resistivity effects (higher temperature increases resistance of gage)
3. Gage factor variation with large temperature differentials
4. Transverse strain effects on each gage

At the conclusion of our strain gage testing, and after correcting the data for the above effects, it was obvious that our data was not sufficiently accurate to correlate with our analysis. Three factors had combined to invalidate our results: (1) the relatively large temperature differential exaggerated the effect of the CTE mismatch between the gage and the lid, (2) the relatively high test temperatures produced apparent strains of the same order of magnitude as the strains we were trying to measure, and (3) we relied on the published average "correction-data" for this particular type of gage; for better accuracy, the gage in use would need to be tested to obtain its individual correction factors. (Time constraints did not allow us to continue with this effort.)

Since our strain gage data did not prove to be usable, we dedicated to use a dilatometer to measure the thermal strain in the hybrid lid (refer to Figure 47 for a sketch of a dilatometer). The following data was collected and is presented as Table 33.

Table 33. Dilatometer Strain Measurements (zero strain @ $74^{o}F$)

T	Dial Gage	Avg. Strain	Effective CTE
$183^{o}F$	+0.0335 mm	7.60×10^{-4}	$4.15 \times 10^{-6}/^{o}F$
$93^{o}F$	+0.0180 mm	4.08×10^{-4}	$4.39 \times 10^{-6}/^{o}F$
$-42^{o}F$	-0.0080 mm	-1.82×10^{-4}	$4.32 \times 10^{-6}/^{o}F$
$-142^{o}F$	-0.0290 mm	-6.58×10^{-4}	$4.63 \times 10^{-6}/^{o}F$
		Average CTE =	$4.37 \times 10^{-6}/^{o}F$

As shown in Table 33, the average thermal strain due to a temperature differential of $180^{o}F$ is measured to be about 7.6×10^{-4} in/in. This does not correlate well with our calculated strain of 5.69×10^{-4} in/in.

Two possible explanations of this discrepancy are apparent. First, there may be more than a 0.0001" thick layer of nickel plating on the Kovar lid (0.0001" was only an assumed value). If this is true, our effective CTE would increase slightly from the calculated value of 3.16×10^{-6} in/in.^{o}F, and the calculated thermal strain would correspondingly increase. (Note that the measured effective CTE of this hybrid is 4.37×10^{-6} in/in^{o}F). Figure 48 plots the variation of thermal strain with temperature, and shows the results of both our test secuence, and some Westinghouse test data [92]. Note that the slope of the curves indicates the CTE for Kovar. Although there is some deviation between the two sets of data, it is not excessive.

Second, we are relying on statistical "average" data for our values of the CTE for Kovar. This does not consider the variation in properties from lot to lot of the material (i.e., it is possible that our hybrid is made of Kovar which may be several

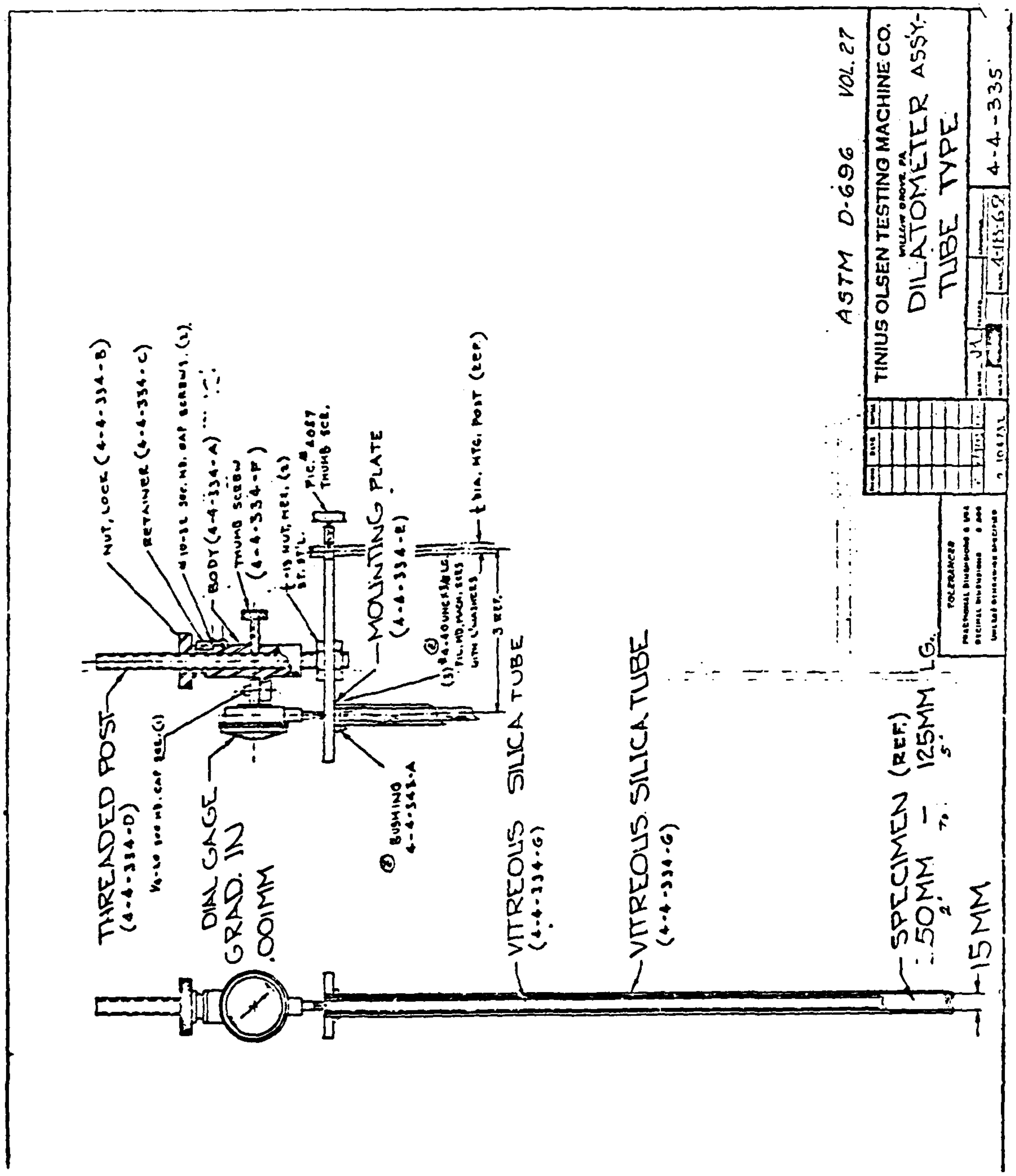

Figure 47. Dilatometer Drawing

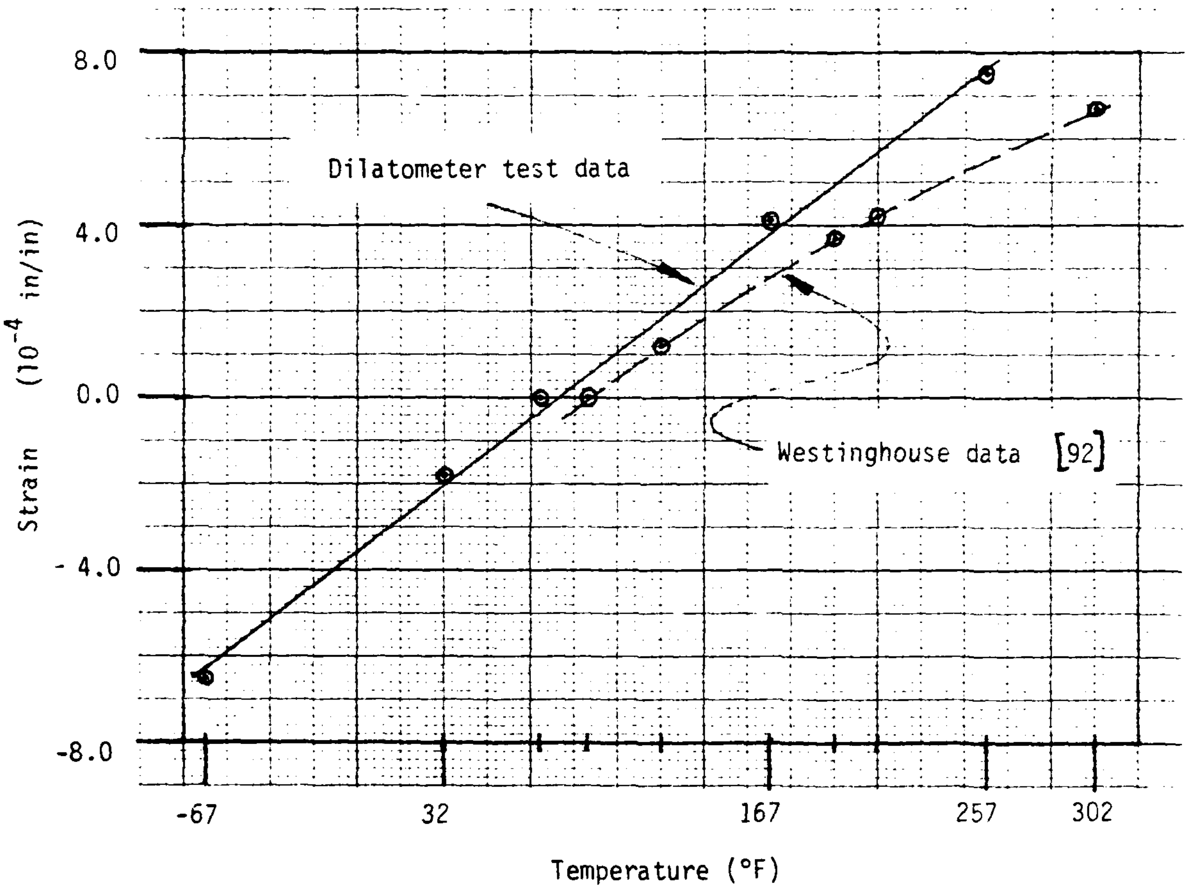

Figure 48. KOVAR Thermal Strain Data

standard deviations removed from the "average" Kovar sample). Also, the Kovar CTE used in our analysis does not include any effects which may be caused by the different working processes our sample has seen during the production of the hybrid.

In summary of the thermal strain analysis, it is obvious that our measured and calculated strains did not correlate well. However, this appears to be due to an error in assuming an effective CTE for the hybrid model (had we used a CTE of 4.37 x 10^{-6} in/in^{o}F in our analysis, our calculated strain for a temperature differential of 180^{o}F would have been 7.87 x 10^{-4} in/in -- much closer to the measured strain).

It should be mentioned that two control tests were run with the dilatometer. First, the empty dilatometer was cycled over temperature extremes to measure its strain over this temperature range -- its measured strain was "zero". This means that the dilatometer was not exaggerating the strain of any sample being tested. Second, a sample of 6061-T651 aluminum was tested; its measured CTE was approximately 7.5% lower than published values. Therefore, we concluded that the dilatometer was not producing consistently higher values of CTE than published.

The next section summarizes the results of the critical problem analyses.

6.4 General Summary of Critical Problem Analysis and Correlation to Test Data (Phase 3)

The following is a summary of the findings of the two critical problem analyses.

6.4.1 Critical Problem #1

1. Good correlation (3.7%) was found between the lid deflections calculated by Libove and our "first-cut" finite element model. This model was purposely kept simple; it required approximately one hour to generate the model and to obtain the

results. However, due to the simplicity of this model, no elements were included to represent the lid seal, and therefore, no seal stresses were obtained with this model.

2. Good correlation was also found between the lid deflections calculated by Libove and those calculated by our second, more detailed finite element model. This included a 0.005" thick lid seal, and three different analyses were performed based on three possible seal materials. It should be noted that the calculated lid deflections and stresses varied only slightly with the seal material.
3. The Von Mises seal stresses calculated by our second finite element model vary significantly depending upon the seal material. However, it should be noted that the vertical stress component at the center of the seal did not vary much with seal material, and this stress is low (as predicted by Libove's vertical stress distribution).
4. A relatively simple finite element model of the most highly stressed seal area was generated to better determine seal stresses and the seal stress distribution across the seal width. Results confirmed that the seal experienced large compressive stresses nearest the package cavity; however, these preliminary results also indicated that the seal stress distribution is most likely not linear across the seal width. A more detailed finite element analysis would be required to investigate this subject in greater depth. It is recommended that an investigation of the seal

stress distribution be included in the work of a future study.

6.4.2 Critical Problem #2

1) A simple "cuarter" finite element model of the lid may be used to approximate lid deflections and stresses for symmetrical loads. This model confirmed that a stepped lid will experience greater deflections for any given load than would a constant thickness lid. The maximum lid deflection calculated by this model fell inside the deflection range predicted by Libove.

2) A more complex finite element model was generated in order to handle asymmetric load cases. Calculated deflections for various point load cases correlated well (within 8%) with experimental data once the actual lid thickness had been measured. For these calculations, it was not sufficiently accurate to rely on the nominal lid dimensions.

3) It is recommended that future design analyses consider lid thickness tolerances -- minimum lid thickness values should be used in design analyses.

4) The thermal strains calculated by the two finite element models were virtually identical, and were constant at all points on the hybrid lid. The predicted thermal strains occurring over a wide temperature range did correlate well with our measured strain values. However, CTE values did not correlate well--this may be caused by a difference between the published value and the real value of the effective CTE for the hybrid.

7.0 ANALYSIS GUIDELINES (PHASE 4)

7.1 Introduction

"The whole concept of the finite element technique can be compared with that of a jigsaw puzzle. A jigsaw is usually a complete picture which is broken down into small irregular-shaped pieces. The problem is then to reconstruct the picture by assembling the individual parts. Obviously, the pieces cannot be assembled arbitrarily, but have to be assembled according to certain rules."[89] The above quote is an accurate description of finite element modeling. It also infers that finite element modeling can sometimes become more of an "art" than a "science".

The purpose of this guidelines section is to provide the mechanical engineer with general procedures which can be applied to microelectronics packaging analysis. Simply stated, the finite element process can be divided into three tasks: (1) understanding the problem, (2) developing the model, and (3) interpreting the results. These three tasks will now be discussed in detail.

7.2 Understanding the Problem

This step sets the tone for the entire analysis, and is oftentimes not considered in sufficient detail. It is imperative that the analyst understand the problem from both a physical as well as an analytical standpoint.

A complete understanding of the problem requires the analyst to: (1) know what's required, (2) consider program choices, (3) perform simple hand calculations, and (4) recognize typical microelectronics problems.

a. Know What's Required

When an analyst is assigned to a problem, he needs to understand the entire scope of the problem. Parameters that influence the problem's scope are those engineering and project constraints that are imposed at the outset. For microelectronics packaging, typical engineering constraints include environmental definition, system/subsystem relationship, device physical description, and specific design concerns based on past experience. Project constraints include cost, schedule, workload, availability of analysts, etc.

Before the analyst proceeds, he must answer the following questions: (1) what am I analyzing, (2) why am I analyzing it, (3) who am I analyzing it for, and (4) when am I expected to produce results? When the above questions are answered, the analyst can proceed in selecting a suitable finite element program.

b. Consider Program Choices

The topic of program selection has been previously discussed in Section 4.0 of this report - Analysis Methods. For microelectronics analysis, the choice of programs is usually dictated by the imposed environmental requirements. For instance, if random vibration were considered the most important environment, the analyst would not choose a program such as ANSYS, since it cannot provide random vibration analysis. A choice such as STARDYNE or NISA would be more appropriate.

A secondary consideration would be the availability of elements necessary to analytically represent the device being modeled. For instance, modeling a thin membrane plate structure with plate elements capable of resisting bending forces would produce erroneously large stresses and lead to an overdesign. However, this is not considered a problem, since the recommended programs have sufficiently adequate element libraries to describe the myriad of micorelectronic devices.

Each program has its own idiosyncrasies. This was illustrated in Sample Problems 2 through 4. Sample Problem #2 showed ANSYS and ABAQUS to have less efficient methods for calculating natural frequencies than STARDYNE. Sample Problem #3 pointed out how differently ABAQUS and ANSYS treat convection. Finally, Sample Problem #4 showed how differently ABAQUS, ANSYS, and STARDYNE all solved the same nonlinear problem. The analyst must try to be aware of program idiosyncrasies before choosing a program.

c. Perform Simple Hand Calculations

Hand calculations can provide the analyst with a "feel" for the problem, as well as a check on results obtained from the finite element model. Depending on the problem complexity, this step may or may not be difficult. Regardless of problem complexity, the analyst must make some assessment of the problem before he starts modeling.

This process was illustrated in Section 5.0 of this report - Sample Problems. The first three sample problems showed how finite element results can be compared to hand calculations. However, the fourth sample problem had no closed-form solution available. The analyst was then recuired to interpret results based on a physical interpretation of the problem.

d. Recognize Typical Microelectronics Problems

What are the typical microelectronics problems? Based on this writer's experience, the following list is provided: (1) hybrids, DIPS, flatpacks, or discrete components mounted on printed circuit boards, (2) microware integrated circuits and stripline modules, and (3) printed circuit boards in general including connectors, solder joints, copper runs, component leads, and acceleration-sensitive components.

A list of common microelectronic failures was presented in Section 3.0 of this report - Technical Assessment. This list is reproduced here to help the analyst identify more specifically microelectronic problem areas that need to be considered.

- o Lack of hermeticity
- o Die bond failure
- o Broken external lead
- o External lead corrosion
- o Wirebond and wire failures
- o Microwave package failures
- o Leadless chip carrier solder joint failure
- o Air wound inductor breakage
- o Connector wear or lead breakage

Knowing from past experience what typically causes real-world failures will help the analyst to concentrate on solving meaningful problems, which will help to identify potential failures and increase device reliability.

Once the analyst has completed the above steps, he is ready to develop the finite element model.

7.3 Model Development

Since the finite element model is a mathematical idealization of the actual structure, the modeling process is critical to the analysis' success. Once the model is defined, it will form the basis for analyses which may consider a dozen environmental or loading conditions. The finite element modeling procedure involves the following: (1) grid optimization, (2) proper element selection, (3) restraints, (4) material properties, (5) types of analyses, (6) reouired input data, and (7) submitting the job to the computer. These seven steps will now be described in detail.

a. Grid Optimization

The process of defining a grid (nodes) is that part of the finite element process which can be described as an "art". The general rule-of-thumb is to use as many nodes as you can afford. Generally speaking, the more nodes a model has, the more accurate it becomes. However, the strength of the finite element method is that the model will converge an acceptable answer quickly when on an "appropriate" number of nodes is used.

There are two physical constraints that require nodes. The first is physical interfaces. Examples include where two planes of a component intersect, where a hybrid lead attaches to a circuit board, or where a ciruit board attaches to an electronic chassis. The second constraint is boundary conditions. Examples include the edges of a circuit board, the ends of a component lead, or the attachment surface of an MIC module.

The real "art" of finite element modeling is the spacing of nodes when their presence is not required by physical constraints. In static analysis, highly stressed regions will have a higher concentration of nodes than elsewhere. Dynamic analysis requires that regions where higher order vibration modes need to be determined will also have a higher concentration of nodes than elsewhere. The key to this step is the analyst's preparation - in particular, his hand calculations and experience will describe where regions of high stress or higher order vibration modes are expected.

When static loading is symmetrical, device symmetry can be used to, in effect, decrease the model complexity by only modeling a portion of the device that exhibits symmetry. For instance, Sample Problem #1 used a quarter model, as did Critical Problem #1 - Models 1 and 2 and Critical Problem #2 - Model 1. The analyst is cautioned that symmetrical models should only be used when the modeled device possesses symmetry and the loading is static and symmetrical.

When the static loading is asymmetrical or vibration modes are needed, the entire device should be modeled. This technique is especially important in dynamic modeling since few, if any, vibration modes are symmetric. Sample Problem #2 used this technique for dynamics analysis, whereas Critical Problem #2 - Model 2 needed this modeling method, due to asymmetrical static loading.

Another aspect of grid optimization is the effect of a program which generates several nodes and/or elements at one time. The analyst must be constantly aware of this program feature, since it can save him a lot of time. A discussion of this technique is presented in Sample Problem #1.

A commonly used technique is that of creating a "first-cut" model. This model is designed to be simple and fast, but still provides the analyst with an "idea" of what to expect with a more complicated model. This technique was used in "Critical Problem #1 - Model 1. The purpose of this model was to obtain hybrid lid deflections, and good correlation with closed-form results was obtained.

As the analysis progresses, the analyst learns about device behavior and then concentrates on areas that may indicate potential failures. this was illustrated in Critical Problem #2 - Model 2, when the seal was introduced into the model and in Critical Problem #2 - Model 3, where a highly stressed region of the seal was analyzed with a local model.

b. Proper Element Selection

The most common finite elements are shown in Figures 49 and 50. Choosing the proper elements requires the analyst to have some preconception as to the expected structural behavior of the device being modeled. For instance, beam/bar elements are typically used to model component leads, plate elements are used to model circuit boards, and solid elements are used to model component bodies.

Many elements are able to resist different types of loading. The most general beam element can resist all three types of loading shown in Figure 49. However, if only axial loads were expected, then the general element should be limited to resisting only axial bar loads. If in-plane membrane forces are expected, then the membrane plate element should be used, etc. Refer to Appendix D for a glossary of finite element terms.

Optimal element usage can be enhanced by understanding element behavior and element limitations. Standard tests [57] have been developed and limitations of elements [57,90] have been published in the literature. Since each element is a stand-alone structure, the analyst needs to understand the element's theoretical makeup. When this is done, optimal use of the elements will be achieved. No element is theoretically perfect for all types

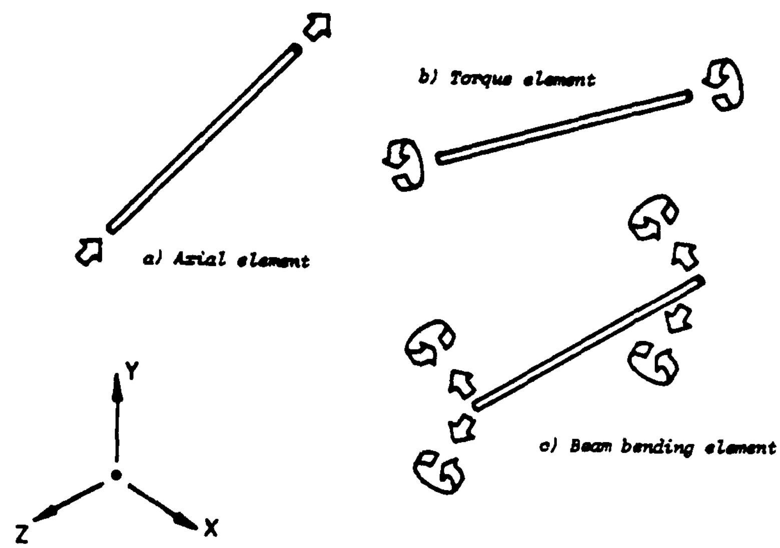

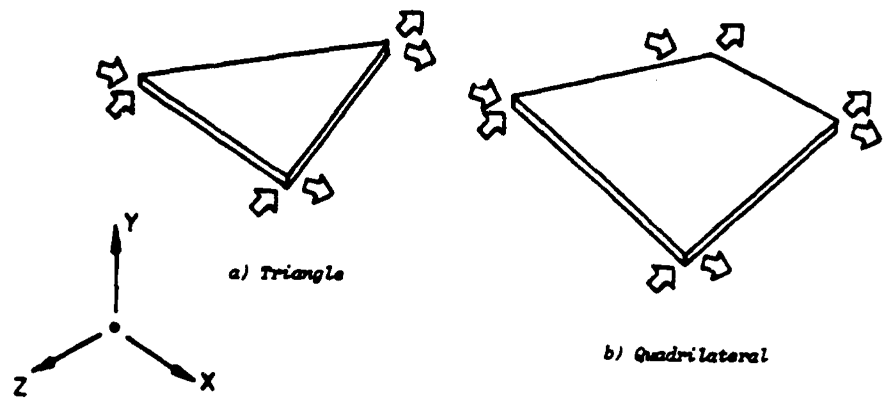

Figure 49. Beam and Plate Elements

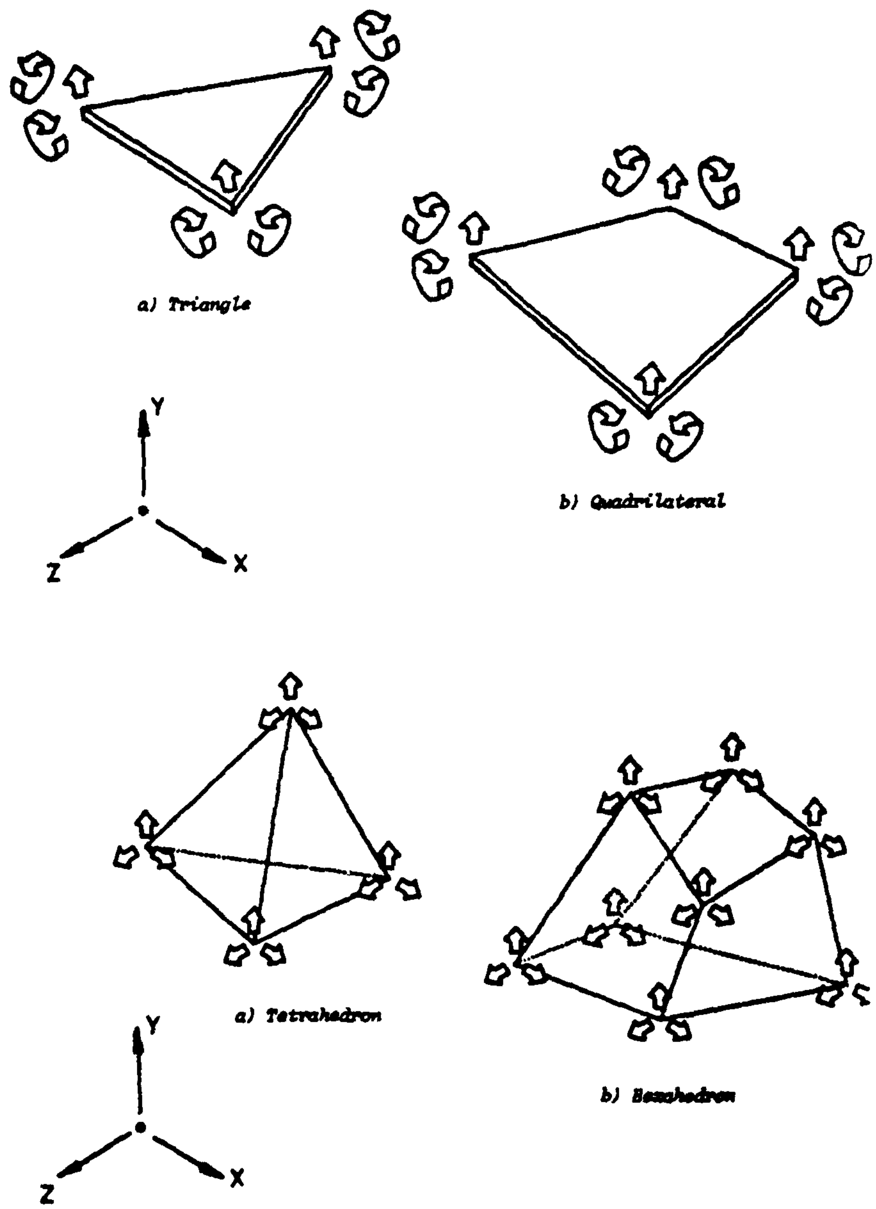

Figure 50. Plate and Solid Elements

of usage. However, if the theory is understood, then an element's strengths can be best utilized in model development.

It is common to mix element types within a finite element model. For example, a model of a hybrid attached to a circuit board would include beam, plate, and solid elements. All three of these elements resist different types of forces. The analyst must exercise care when connecting elements of different types, since force-compatibility does not necessarily exist. The analyst's knowledge of what's expected physically at these interfaces determines that restraints are to be applied to assure transfer of load.

For example, consider a beam element attached at one common node to a plate element. Assume that the beam's axis is perpendicular to the plane of the plate. The beam element can resist forces in the three translational and three rotational directions (six degrees of freedom (DOF)). However, the plate element can resist all forces <u>except</u> rotation about an axis perpendicular to its plane (5 DOF). Assume, now, that a twisting load about the beam's axis is applied at the beam's end opposite where it is attached to the plate. This load will get transferred to the beam-plate common node where the plate has no stiffness to resist this load. The result will be a theoretically infinite rotation about the beam's axis and the program will produce a warning message. This problem can be alleviated by restraining the rotation about the beam's axis at the common beam-plate node, and is discussed in detail in Sample Problem #1. Restraints will be further discussed in the next portion of this section.

Throughout the critical problem analysis cubes and/or plates were used to model the hybrid walls, lids, and seals. When considering plate bending, either element type may be used. Plate elements are more commonly used because they have typically half as many nodes (four, compared to eight) as a cube element. However, plate elements do have more DOF per node (five compared to three) than cube elements. Therefore, the total DOF per element would be 20 for a plate and 24 for a cube. The general rule-of-thumb is to use plate elements. Cubes are to be used when they are needed to physically describe the device's geometry. For example, plates were used in Critical Problem #1 - Model 1 and Critical Problem #2 - Model 2. Cubes were used in Critical Problem #1 - Models 2 and 3 and Critical Problem #2 - Model 1.

The critical problem analysis also used cubes and membrane plates. The STARDYNE program does not allow direct application of pressure loading to its cube elements, and cube stresses are only available at the element's C.G. Therefore, attaching thin (.0001 in) membrane plates to these cube elements allowed the analyst to apply pressure loading and to obtain stresses at the cube's faces.

c. Restraints

Restraints are one area of modeling that is critical and not necessarily straight-forward. Basically, a restraint is a boundary condition that is an imposed zero displacement at the node. Since each node has six degrees of freedom (three translations and three rotations), a maximum of six displacements can be restrained at any node. Once again, knowledge of what happens physically determines what restraints are to be applied.

For example, connectors on circuit boards are usually assumed clamped (all six displacements restrained), bolted electronic chassis attachment points are usually assumed ball-and-socket joints (all three translations restrained, all three rotations unrestrained), and circuit board edges supported by rubber are assumed simply supported (two translations restrained, and two rotations restrained). Test data can be very beneficial in determining difficult-to-describe restraints.

The sample problem and critical problem analyses provides two additional restraint examples. Sample Problem #1 illustrates the procedure for applying restraints along an axis of symmetry when using a symmetrical model. Critical Problem #2 - Model 1 shows how only one node need be fully restrained for free-expansion thermal stress models.

d. Material Properties

Typical material properties required for a dynamic analysis include Young's modulus, Poisson's ratio and density. Static analyses require Young's modulus, Poisson's ratio, coefficient of expansion (for thermal stresses), and density (if weight loading is involved). Depending on the program, properties may be linear, nonlinear, isotropic, anisotropic, or orthotropic.

When modeling a circuit board, the copper circuitry stiffens the board and its effect must be included in the Young's modulus value used in the model. An "equivalent" modulus is calculated in this case, which now represents the composite effect of the copper and board material. This calculation is aptly described in Steinberg's book, "Vibration Analysis for Electronics Equipment" [91]. Sample Problem #2 also illustrates how the total suspended weight of a circuit board is used in computing an appropriate density. This problem also pointed out the program idiosyncrasies that STARDYNE required a <u>weight</u> density input, whereas ABAQUS and ANSYS required a <u>mass</u> density input. Finally, Critical Problem #2 - Model 1 showed how an equivalent CTE can be calculated. This shows how a simple model can be used to determine properties necessary for a more detailed model.

e. Types of Analyses

The two types of microelectronic analyses are static and dynamic. The purpose of static analysis is to apply a load and obtain deflections and stresses. Typical loads include point loads, distributed loads, applied temperatures (thermal stress analysis), applied displacements, and accelerations. Dynamic analysis first involves obtaining a number of natural frequencies (eigenvalues) and mode shapes (eigenvectors). Then, the response to a particular dynamic environment is computed. Dynamic environments commonly found in microelectronic analysis include sinusoidal vibration, random vibration, shock pulse, shock spectrum, and transient waveforms. Finally, the dynamic response can be used to calculate dynamic stresses. These dynamic stresses can, in turn, be used to assess a device's fatigue life.

Referring to the typical causes of microelectronic failures, the following list is provided to show which types of analysis can be performed to prevent these types of failures.

- Lack of hermeticity - static, thermal stress, dynamic
- Die bond failure - static, thermal stress, dynamic
- Broken external lead - static, dynamic
- External lead corrosion - usually prevented by proper plating
- Wirebond and wire failures - static, dynamic

AD-A117 979 HARRIS CORP MELBOURNE FL GOVERNMENT INFORMATION SYST--ETC F/G 9/5
FINITE ELEMENT ANALYSIS OF MICROELECTRONIC PACKAGES.(U)
MAY 82 J R SOUTHLAND, V R BEATTY F30602-81-C-0083
UNCLASSIFIED RADC-TR-82-133 NL

3 OF 3
AD A
117979

END
DATE
FILMED
09-82
DTIC

- o Microwave package failures - static, thermal stress
- o Leadless chip carrier solder joint failure - nonlinear statics, thermal stress
- o Air wound inductor breakage - dynamic
- o Conductor wear or lead breakage - thermal stress, dynamic

f. Required Input Data

The required input information is dependent on the type of analysis and the program being used. Each program has a specific format for inputting data. The user's manual provides this format which must be followed. The input data is usually recorded on computer coding sheets which are used to create a deck of punched cards. Examples of this are shown in the four sample problems. However, recent advances in graphics terminal capabilities have improved these procedures.

There are an excellent number of preprocessors available which allow the analyst to create and check a model graphically. Examples of the procedures are documented in the literature and substantial savings can be realized by using a preprocessor [57]. The basic strength of a preprocessor is that the analyst can see his model displayed, correct any errors, and submit it to the computer error-free. This is shown in the critical problems analyses where the Unistruc preprocessor was used to generate isometric views of the finite element models. The advent of color graphics [57] and a seemingly endless number of improvements makes this topic one of great promise and should form the basis for future work. Future work would include a study comparing various pre-post processors, their capabilities, speed, cost, and accuracy.

g. Submitting the Job to the Computer

If a preprocessor were used, then the model will be debugged. All that's required is to then submit the job to the computer, calling on the appropriate finite element program to perform the analysis. If a preprocessor were not used, then a number of geometry runs will be needed until the model is debugged. Then, the analysis can be accomplished using the appropriate program.

7.4 Interpreting Results

For a static analysis, expected results include deflection shapes and stresses. Dynamic analysis results include natural frequencies, mode shapes, plots of dynamic response, and dynamic stresses. A graphics postprocessor is an invaluable tool for interpreting deflection shapes, stress contours, mode shapes, and dynamic responses. Since much of finite element analysis results are graphical, displayed results are nearly a necessity.

The analyst must ask the question, "Are the results reasonable?" Simply stated, do the results reflect what's expected and reasonable? Are the deflections, stresses, natural frequencies, or mode shapes consistent with those found by hand calculations or experience? Is there continuity of deflections and stresses? Do the applied loads equal the reactions? All of the above cuestions must be considered by the analyst once results are obtained.

The following is a synopsis of how the results of the sample problem and critical problem analyses were interpreted.

- o Sample Problem #1 - The maximum stresses and deflections compared very well with the hand calculations, considering the coarseness of the model's grid.
- o Sample Problem #2 - The natural frequencies compared well with the hand calculations. The mode shapes also compared well, but care was needed when interpreting (visually) the mode shapes.
- o Sample Problem #3 - The ANSYS results agreed closely with the closed-form solution. The ANSYS and ABAQUS programs had different ways of handling convection.
- o Sample Problem #4 - No closed-form solutions were available. Therefore, STARDYNE's solution method and corresponding answers appeared most valid when considering a physical assessment of the problem.
- o Critical Problem #1 - Model 1 - Good deflection correlation was obtained with a simple "first-cut" model. Poor stress correlation resulted because of a coarse grid occurring in the region of maximum stress.
- o Critical Problem #1 - Model 2 - Different seal materials resulted in varying seal stresses. A more detailed model of the seal is needed to assess the vertical stress distribution across the seal's width.

- Critical Problem #1 - Model 3 - The seal vertical stress distribution appears reasonable when considering the physical aspects of the problem. The resulting moment appears to be reacted by the inner half of the hybrid wall. A more complicated model is needed to further assess seal stresses.
- Critical Problem #2 - Model 1 - The quarter model provided stresses for establishing static loading for hybrid testing. Nickel plating has little effect on lid CTE.
- Critical Problem #2 - Model 2 - Good correlation was obtained between analysis and test lid deflections under static loading. Test and analysis CTE at room temperatures did not compare well, but thermal strains did compare reasonably over a range of temperatures. Closer scrutiny of published manufacturer's CTE values is needed. Lid thickness tolerance effects are sizeable when considering lid deflections. Worst case (thinnest) lid dimensions should be used in design analysis.

8.0 CONCLUSIONS AND RECOMMENDATIONS

8.1 Summary

The conclusions and recommendations will be presented according to each section in this report. The conclusions represent a summary of the information gained through the technical assessment and the various analyses performed on microelectronic packages. The conclusions presented here are abbreviated versions of those presented at the end of each section. Refer to each section for a complete wording of appropriate conclusions.

The recommendations will be directed toward the need for additional work. This work must be accomplished with respect to information gained through the technical assessment, more detailed analysis, analysis substitution for testing, and an indepth study of pre and postprocessor programs in conjunction with CAD/CAM activities.

8.2 Conclusions

8.2.1 Technical Assessment (Phase 1)

- o Although FEA is primarily a tool for designers of large complex structures a great potential exists if applied to microelectronic packages.
- o By using FEA for early warnings of potential failures the mechanical engineer can play a significant role in assuring or improving the reliability of microelectronic systems.
- o The survey showed that the areas giving microelectronic packages the most problems were hermeticity, broken or corroded internal wires, and broken wirebonds.
- o FEA can provide accurate answers if proper assumptions are made and if one understands the finite element theory.
- o Commercial hybrid houses claim lower cost and higher reliability than similar products produced at military hybrid houses.
- o Most companies do not use FEA to assess the structural and thermal integrity of microelectronic packages.
- o The "full blown" screening in MIL-STD-883 is not recommended by most of the companies polled. Instead, an abbreviated version that works for them is utilized.

- Closed-form solutions can result in accurate, cost-effective solutions.
- Considerable cost savings can be realized by substituting FEA for MIL-STD-883 screening tests. An example, showed a cost savings from $25,000 to $50,200 for a lot of 1,000 hybrids with 11 hybrid types.

8.2.2 Analysis Methods (Phase 2)

- Five programs-ADINA, FINITE, MARC-CDC, NASTRAN, and SAP IV were rated "very good" and have specific solution methods that were rated "excellent". However, these programs should only be used for analyzing unique, specific microelectronic problems that address the program's strengths.
- The four programs recommended for microelectronic analysis are ABAQUS, ANSYS, NISA, and STARDYNE. These programs will best be utilized when analyzing the following types of microelectronic problems:
  a. ABAQUS - nonlinear statics and dynamics
  b. ANSYS - heat transfer and thermal stress
  c. NISA - composite and sandwich structures
  d. STARDYNE - linear statics and dynamics
- STARDYNE is the best program for analyzing the majority of microelectronic problems.

8.2.3 Sample Problems Analysis (Phase 2)

8.2.3.1 Linear Statics Problem

- ABAQUS, ANSYS, and STARDYNE had good correlation with theoretically determined maximum lid deflections (within 3%) and stresses (within 8%) with a relatively coarse grid.
- ANSYS and STARDYNE deflection shapes compared well with each other - ABAQUS results were slightly different.

8.2.3.2 Linear Dynamics Problem

- STARDYNE has the most accurate, user-oriented methods for obtaining natural frequencies and mode shapes.
- ANSYS obtained accurate values of natural frequencies and mode shapes--however, its method is not efficient and is therefore more expensive than STARDYNE's.
- ABAQUS provided inaccurate values of natural frequencies and mode shapes - its method is not user-oriented.

8.2.3.3 Heat Transfer Problem

- ANSYS provided an accurate, straight-forward solution to this problem.
- ABAQUS did not have an obvious method for handling convection for this simplified problem.
- STARDYNE does not have heat transfer analysis capability.

8.2.3.4 Nonlinear Statics Problem

- STARDYNE provided the most user-oriented, accurate solution.
- ANSYS provided a user-oriented, yet somewhat inaccurate solution.
- ABAQUS could not solve this problem with its four node plate element.

8.2.4 Critical Problem Analysis and Correlation to Test Data (Phase 3)

8.2.4.1 Critical Problem #1

- Lid deflections obtained with a simple finite element model correlated well (within 3.7%) with Libove's closed-form solution.
- Different seal materials result in different seal stresses.
- The vertical stress distribution across the seal width is probably not linear and needs a more in-depth model to better determine this distribution.

8.2.4.2 Critical Problem #2

- Lid deflections computed with a simple quarter model fell within the range predicted by Libove's closed-form solution.
- Good correlation (within 8%) between finite element model results and experimentally determined hybrid lid deflections under point loading was achieved.

- Design analyses should use minimum hybrid lid thickness values.
- Good correlation was not obtained between predicted and measured hybrid CTE at room temperature--however, reasonable correlation of thermal strains was observed over a wide temperature range.

8.2.5 Analysis Guidelines (Phase 4)

The guidelines section was, in itself, a set of "conclusions and recommendations". Therefore, the end of the guidelines section did not include a set of conclusions and recommendations. The following are provided as general recommended procedures for performing microelectronic finite element analysis.

1. The finite element process involves understanding the problem, developing the model, and interpreting results.
2. Understanding the problem requires the analyst to:
   - Know what's recuired
   - Consider program choices
   - Perform simple hand calculations
   - Recognize typical microelectronic problems
3. Developing the model recuires the analysis to understand:
   - Grid optimization
   - Proper element selection
   - Restraints
   - Material properties
   - Types of analysis
   - Required input data
   - Submitting the job to the computer

4. Interpreting results requires the analyst to answer the following questions:
   - o Do the results reflect what's reasonable and expected?
   - o Are the deflections, stresses, natural frequencies, and mode shapes consistent with those found by hand calculations?
   - o Is there continuity of stresses and deflections?
   - o Do the applied loads equal the reactions?

8.3 Recommendations

As in any study, many interesting problems were discovered that were beyond the scope of this effort but should form the basis for future studies. Below is a list of recommendations for future work:

1. Sealing of large custom packages should be investigated to gain more knowledge on fracture failures of brittle materials used in packages such as glasses and ceramics.
2. There is a need to develop a criteria for inspecting mounted hermetic chip carriers (leaded and leadless).
3. Military specifications should include provisions for selective qualification by analysis. To fully utilize this approach more work is needed in the test-analysis correlation area.
4. The area of nonlinear analysis - particularly solder material effects - is a promising area for future work and should be investigated.

5. More work is required in the area of hybrid lid seal analysis to more accurately determine the stress distribution - this will provide more insight to design criteria for sealing large custom packages.

6. Pre and postprocessor computer program studies should be performed, similar to the present studies on FEA, to determine the optimum programs for microelectronic package analysis. Combined with CAD/CAM activities, this will enable designers to improve their productivity.

APPENDIX A

HAND CALCULATIONS - ROARK - CRITICAL PROBLEM #2

From Roark [85], page 392, Case 8, the expression for maximum deflection is:

$$y_{max} = \frac{\alpha q b^4}{E t^3}$$

where:

y_{max} = maximum lid deflection

α = .0247 for a/b = 1.66/1.06 = 1.566

q = pressure = 30 psi

b = plate width = 1.06"

E = Young's modulus = 20×10^6 psi

t = lid thickness = 0.015"

y_{max} = 0.01386"

APPENDIX B

HAND CALCULATIONS - LIBOVE - CRITICAL PROBLEM #2

Referring to Libove [88], page 23, ecuation 34, the lower bound for the maximum lid deflection is:

$$\delta_{max1} = 10.92 \frac{P}{E} \left(\frac{a}{t}\right)^3 an_4$$

where:

δ_{max1} = maximum lid deflection

P = pressure = 30 psi

E = Young's modulus = 20 x 10^6 psi

a = lid width = 1.06"

t = lid thickness = .015"

n_4 = .00225

δ_{max1} = 0.01379"

Referring to Libove [85], page 25, ecuation 38, the upper bound for the maximum lid deflection is:

$$\delta_{max2} = \frac{12\ (1-v^2)a^2}{Et^3}\ (pa^2\ n_4\ (0) - m_e n_9)$$

where:

δ_{max2}	=	maximum lid deflection
v	=	Poisson's ratio = 0.317
p	=	Pressure = 30 psi
a	=	lid width = 1.06"
E	=	Young's modulus = 20×10^6 psi
t	=	lid thickness = .015"
$n_4(0)$	=	.008
m_e	=	.446
n9	=	.103
δ_{max2}	=	0.04020"

APPENDIX C

TEST PLAN

FOR

HYBRID LID TEST

(CRITICAL PROBLEM #2)

1.0 INTRODUCTION

This test is necessary in order to obtain correlation between the finite element analysis on a hybrid lid and test data. Two tests will be performed: 1) A concentrated load with deflection measurements, and 2) a high and low temperature test with strain gages mounted to the top of the lid for correlation to thermal stress analysis.

2.0 TEST PROCEDURE

2.1 Test Sample

The test sample is a large hybrid (1.74" x 1.14") shown in Figure 2.1-1. The lid, shown in Figure 2.1-2, is a stepped lid, .015 inches thick. The lid is welded to the hybrid package.

2.2 Test Conditions and Measurements

The first test to be performed shall be a concentrated load at the locations shown in Figure 2.2-1 with deflection measurements being made at the point of load application. The base of the hybrid shall be supported with a solid piece of aluminum so that a fixed support can be assumed in the analysis. Loads shall be applied continuously from 0.0 to 3.0 pounds at the defined locations. Deflections shall be recorded for the maximum load as shown in Table 2.2-1.

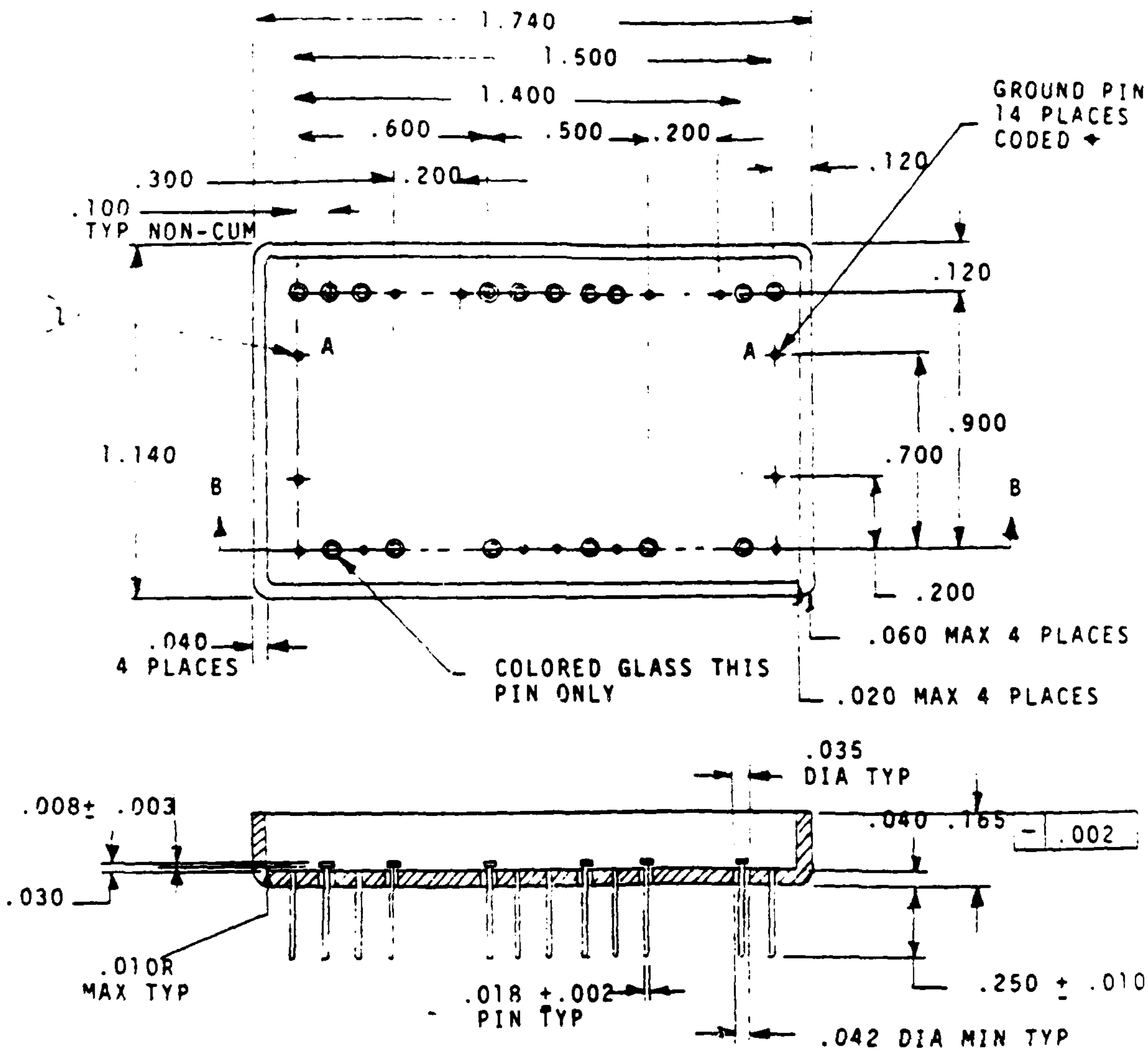

SECTION B-B

4 ground pins marked "A" to be flush, or underflush with inside surface of case.

OUTLINE AND DIMENSIONS (-401)

Figure 2.1-1

A=1.735
B=1.135
C=1.615
D=1.015
E=0.060
F=0.060
G=0.015
H= .004/.006
R1=0.060
R2=0.020

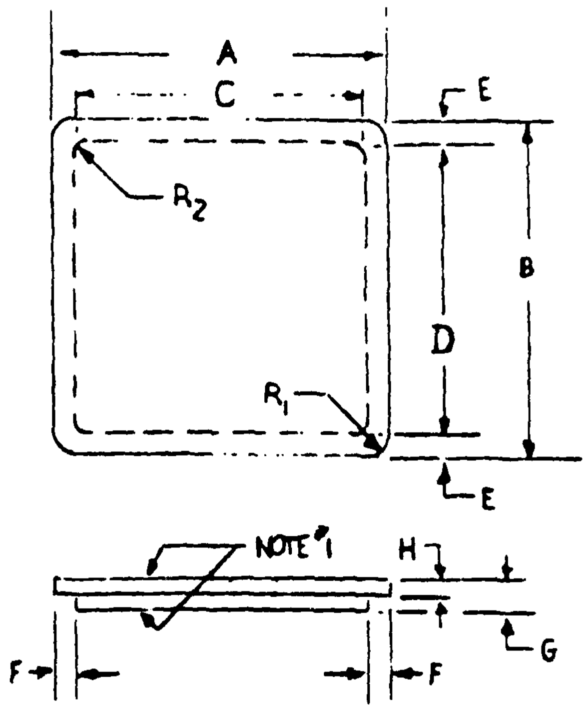

Figure 2.1-2. Stepped Lid Nickel Plated Kovar or Alloy 42

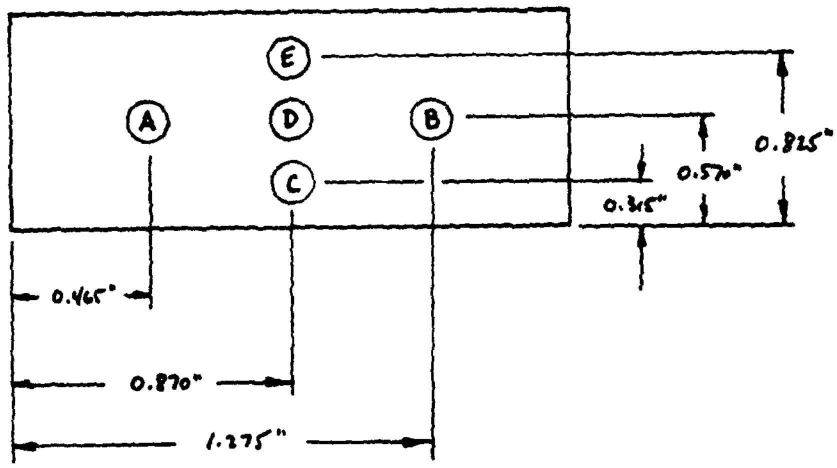

Figure 2.2-1. Hybrid Load and Deflection Locations

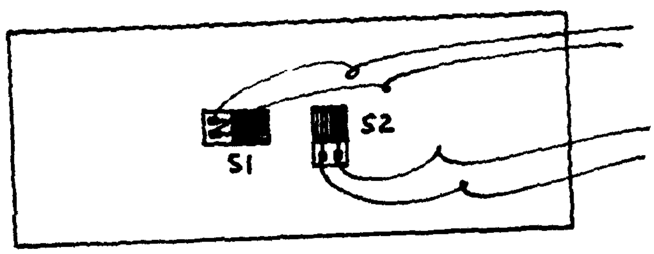

Figure 2.2-2. Strain Gage Locations

Table 2.2-1. Deflection Measurements

Load, lb.	Deflection measurement for points A - E, inches				
	A	B	C	D	E
3.0					

Table 2.2-2. Strain Gage Measurements*, PSI

Strain gage location	Temperature				
	$25^{o}C$	$-55^{o}C$	$25^{o}C$	125^{o}	25^{o}
S1					
S2					

* Measurements taken after 30 minutes at each temperature for stabilitation.

The second test will be a high and low temperature test with strain gages mounted as shown in Figure 2.2-2. Strain gage measurements shall be taken at -55°C, 25°C and 125°C as shown in Table 2.2-2.

3.0 RESULTS

A short report will be generated to document this test, the results and equipment used for correlation to the finite element analysis.

APPENDIX D

GLOSSARY OF FINITE ELEMENT TERMS

1. Linear Statics - statics problems that can be solved without an iterative process

2. Thermal Stress - stresses caused by temperature-only loading

3. Nonlinear Statics - statics problems involving an iterative solution

4. Geometric nonlinearity - nonlinearity caused by gaps, bottoming out of adjacent structures, one-way springs, tension-only and compression-only members

5. Material Nonlinearity - nonlinearity caused by materials which exhibit nonlinear behavior such as elastic-plastic, viscoelastic, creep, or swelling

6. Large Deflection Nonlinearity - nonlinearity which exceeds the bounds of small deflection theory engineering mechanics

7. Linear Dynamics - dynamics not involving geometric, material, or large deflection nonlinearities

8. Modal Extraction - the process of obtaining eigenvalues (natural frequencies) and eigenvectors (mode shapes)

9. Transient Response - dynamic response to transients such as shock pulses, step changes, etc.

10. Harmonic Response - dynamic response to sinusoidal vibration excitation

11. Random Vibration Response - dynamic response to random vibration excitation

12. Shock Spectra Response - dynamic response to shock spectrum excitation

13. Nonlinear Dynamics - dynamics involving geometric, material, or large deflection nonlinearities

14. Linear Heat Transfer - heat transfer involving only linear phenomena such as conduction

15. Nonlinear Heat Transfer - heat transfer involving nonlinear phenomena such as convection or radiation

16. Bar Element - element capable of resisting axial-only forces

17. Beam Element - element capable of resisting axial, torsional, and bending forces

18. Membrane Plate Element - element which can resist in-plane forces

19. Bending Plate Element - element which can resist bending forces

20. Thin Plate/Shell Element - element that conforms to loading via thin plate/shell theory only

21. Thick Plate/Shell Element - element that is sensitive to variations in stress through its thickness

22. Isoparametric Solid Element - element whose displacement function is identical to its shape function which produces better accuracy within the element and, therefore, requires less elements for modeling

23. Axisymmetric Element - an element used to model structures which have circular symmetry about an axis such as a cylinder

24. Pipe Element - a beam element capable of resisting fluid flow loading

25. Gap Element - one dimensional element used for sensing gaps or bottoming out of adjacent structures

26. Friction Element - one dimensional element used to introduce friction

27. Spring, Mass, Damper Elements - one dimensional dynamics elements used to introduce stiffness, mass, or damping at a node

28. Node - a point within a model which defines an element's boundaries or a point where element(s) intersect

29. Node Generation - the process of automatically generating a series of equally-spaced nodes

30. Element - a finite continuum defined by nodes

31. Element Generation - the process of automatically generating a group of elements

32. Load Generation - the process of automatically generating a series of loads

33. Restart Capability - the ability to use stored model information for multiple load cases

34. Free Format Input - input that has no rigid format, such as information needing to be only input in certain columns of a field

35. Data Input Check - a capability checking for correctness of input data prior to making a complete computer run with loads, etc.

36. Substructuring - the process of dividing an element into a detailed model within itself (a substructure) and then assembling the substructures into a large model

37. Equivalent Stiffness Properties - replacing the composite stiffness of a layered section with an equivalently stiff uniform section

38. Isotropic - having properties which are equal in all directions

39. Anisotropic - having unequal properties in all directions

40. Orothotropic - having material properties which vary in three orthogonal directions

41. Visoelastic - having properties that cause behavior like a thick fluid and/or a solid material

42. Composite - a layered structure that has predominately planar properties which can vary according to direction

43. Sandwich - a layered structure with two outer bending layers and one inner core which transmits shear and is very strong transversely

44. Deflection Coupling - the process of forcing deflections from two adjacent elements to be equal at a common node

45. Degree of Freedom Releasing - the process of not restraining a specific degree of freedom

46. Closed Form Solution - an analytical approximation (usually in the form of equations) to the solution of a physical problem.

REFERENCES

1. Curtis, C.M., R.H. Messier, B.E. Sandman, and R. Brown, "Characterization of Torpedo Structural Modes and Resonant Frequencies," The Shock and Vibration Bulletin, Part 1, 1978.

2. Ewins, D.J., J.M.M. Silva, and G. Maleci, "Vibration Analysis of a Helicopter Plus an Externally - Attached Structure," The Shock and Vibration Bulletin, Part 2, 1980.

3. Giltrud and D.S. Lucas, "A Numerical Comparison With an Exact Solution for the Transient Response of a Cylinder Immersed in a Fluid," The Shock and Vibration Bulletin, Part 3, 1979.

4. Gran, J.K., L.E. Schwen, J.D. Colton, and H.E. Lindberg, "Finite Element Analysis of Multicomponent Structures in Rigid Barrier Impacts," The Shock and Vibration Bulletin, Part 2, 1978.

5. Harari, A. and B.E. Sandman, "Experimental and Theoretical Dynamic Analysis of Carbon - Graphite Composite Shells," Part 3, 1978.

6. P.W. Whaley, "Calculation of Natural Frequencies and Mode Shapes of Mass Loaded Aircraft Structures," The Shock and Vibration Bulletin, Part 3, 1978.

7. Johnson, C.D., P.A. Kienholy, and L.C. Rogers, "Finite Element Prediction of Damping," The Shock and Vibration Bulletin, Part 1, 1981.

8. Dunham, R.S., R.J. James, A.S. Kushner, and D.E. Ranta, "Fluid-Structure Interaction, and Evaluation of: Doubly Asymptotic Approximation; Staggered Solution Schemes; USA - STAGS," The Shock and Vibration Bulletin, Part 1, 1981.

9. Compiled by A.H. Agajanian, "Microelectronic Packaging, a Bibliography," IFI/Plenum, 1979, New York.

10. LIE AN-TUN, "Linear Elastic and Elasto-Plastic Stress Analysis for Adhesive Lap Joints," University Microfilms International, Ann Arbor, Michigan, 1981.

11. Journal of Thermal Stress, Volume 4, No. 1, January 1981.

12. IVAR HOLAND and KOLBEIN BELL, "Finite Element Methods in Stress Analysis," TAPIR, NORWAY, 1969.

13. Doughertz, W.E., "Control of Thermal Coefficient of Expansion of Substrate Materials," IBM Technical Disclosure Bulletin, Volume 19, No. 18, January 1977.

14. Howard, R.T., "Semiconductor Device Package having a Substrtae with a Coefficient of Expansion Matching Silicon," IBM Technical Disclosure Bulletin, Volume 20, No. 7, December 1977.

15. Amijima, S., T. Fujii, and A. Yoshida, "Two Dimensional Stress Analysis on Adhesive Bonded Joints," 20th Japan Congress on Materials Research, March 1977.

16. Allman, P.J., "A Theory for Elastic Stresses in Adhesive Bonded Lap Joints," Journal of Applied Math, Volume XXX, Part 4, 1977.

17. Kinniment, D.J. and D.A. Edwards, "Thermal Design in a Hybrid System with High Packaging Density," IEEE Transactions on Components, Hybrids, and Manufacturing Technology, Volume CHMT-1, No. 2, June 1978.

18. Newell, W.E., "Transient Thermal Analysis of Solid-State Power Device, Making a Dreaded Process Easy," PESC 75 Record.

19. Ritchie, K, "Application of Thermal Analysis to the Semiconductor Plastic Package Thermal Shock Testing Reliability," Microelectronics and Reliability, Volume 15, Pages 489 to 490, 1976, Pergamen Press, Great Britain.

20. Buckley, R.G., "Considerations for Selecting and Evaluating Glass-to-Metal Seals," Insulation/Circuits, Page 19, November 1978.

21. Buckley, R.G., "Understanding Glass-to-Metal Seals," Electronic Packaging and Production, Page 74, October 1978.

22. Fresh, D.L., "Reliability of Interconnections on Microcircuits," Proceedings of 1975 Reliability and Maintainability Symposium.

23. George, A.H., "The Reliability, Testing, and Evaluation of Hybrid Microcircuits," Electrocomponent Science and Technology, 1977, Volume 4, Pages 213-217.

24. Matheson, R., "Designing Glass-to-Metal Seals," Electronic Packaging and Production, Page 197, July 1977.

25. Relchson, S.M. and O.V. Mazurin, "Stress Relaxation in Glass-to-Metal Seals," Glass Technology, Volume 18, No. 1, February 1977.

26. Hagy, H.E., "Thermal Expansion Mismatch and Stress in Seals," Electronic Packaging and Production, Page 182, July 1978.

27. Hanley, L.D. and J.H. Martin, "A Test of Parylene as a Protective System for Microcircuitry," Published at the Charles Stark Draper Laboratory Inc.

28. Kale, V.S., "Interaction of Parylene and Moisture in Hermetically Sealed Hybrids," Published by Teledyne Microelectronics Division.

29. Proceedings of the Army Symposium on Solid Mechanics, 1974, The Role of Mechanics in Design of Structural Joints.

30. Szipe, F., "Strength of Adhesive - Bonded Lap Joints with Respect to Change of Temperature and Fatigue," Experimental Mechanics, 1966.

31. La Bruyne, N.A., "The Strength of Glued Joints," Aircraft Engineering, 1944.

32. Lockheed Missiles and Space Company, "Adhesive Bonding of Passive Components to Substrates (Hybrids) Requirements for, General Specification for" 1974.

33. Dickson, J.N., T.M. Hsu, and J.M. McKinney, "Development of an Understanding of the Fatigue Phenomena of Bonded and Bolted Joints in Advanced Filamentary Composite Materials, Volume i, Analysis Methods," Lockheed-Georgia Company, for AFFDL, WPAF, 1972.

34. Corvelli, N. and E. Saleme, "Analysis of Bonded Joints," by Grumman Aerospace Corporation, 1970.

35. Galand, M. and E. Rerssner, "The Stresses in Cemented Joints," Journal of Applied Mechanics, 1944.

36. Hart-Smith, L.J., "Adhesive-Bonded Single - Lap Joints," McDonnell Douglas Aircraft Company for NASA, 1973.

37. Renton, W. James, "The Analysis and Design of Composite Material Bonded Joints under Static and Fatigue Loadings," Delaware University for the Air Force Office of Scientific Research, 1973.

38. Renton, W.J. and J.R. Vinson, "Analysis of Adhesively Bonded Joints Between Panels of Composite Materials, Journal of Applied Mechanics, 1977.

39. Allman, D.J., "A Theory of Elastic Stresses in Adhesive Bonded Lap Joints, Journal of Applied Mathematics, 1977.

40. Humphreys, E.A. and C.T. Herakovich, "Nonlinear Analysis of Bonded Joints with Thermal Effects," by Virginia Polytechnic Institute and State University for NASA, 1977.

41. Renton, W.J., "The Analysis and Design of Anisotropic Bonded Joints," Delaware University for the Air Force Office of Scientific Research, 1974.

42. Hybrid Technology Cost Reduction Improvement Study Program, Volume 1, Results of Literature Search and Questionnaire Survey, Final Report, 1978 for Naval Avionics Center by Rockwell Internal.

43. Hybrid Technology Cost Reduction Improvement Study Program, Volume II, Abstracts of Articles on Hybrid Microcircuits, 1978 for Naval Avionics Center by Rockwell International.

44. Hybrid Technology Cost Reduction and Reliability Improvement Study, March 1978, for Naval Avionics Facility of Boeing Aerospace Company.

45. ER-YUNG YU, "Determination of Temperature of Integrated - Circuit Chips in Hybrid Packaging," IEEE Transactions on Parts, Hybrids, and Packaging, Volume PHP-12, No. 2, June 1976.

46. Weirick, L.J., "Prevention of Liquid - Metal Embrittlement and Stress - Corrosion Cracking in Kovar Leads," Solid State Technology, 1976.

47. Buhanan, D.C. and E.A. Wilson, "An Experimentally Verified Heat Transfer Model for Integrated Circuit Packages,"

48. Hugh, S.C., "Thermal Design Criteria for Porcelainized Steel vs. Alumina Substrates," Boeing Aerospace Company.

49. Wilson, E.A., "Thermal Characterization of Single Chip Integrated Circuit Packages,".

50. Pogson, J.T., "Electronics Temperature Control," Boeing Company, 1975.

51. Wilson, E.A., "Analysis of Heat Sinks with Multiple Heat Sources," Electronics Packaging and Production, April 1981.

52. Johnson, G.M. and L.K. Conaway, "Reliability Evaluation of Hermetic Dual In-Line and Flat Microcircuit Packages," Final Technical Report December 1977 by McDonnell Douglas Astronautics Company - St. Louis for NASA, MSFC.

53. Loafman, J.W. and R.D. Lowrey, Isoparametric Finite Element Structural Analysis Seminar, Sperry Rand, Copyright 1976.

54. Proceedings of the 1980 Hybrid Microcircuit Symposium, June 1980, ERADCOM, Fort Monmouth, N.J.

55. Althouse, L.P., "Methods for Surface Treating Metals, Ceramics, and Plastisc Before Adhesive Bonding," Lawrence Levermore Laboratory, February 1976.

56. Proceedings of the 31st Electronic Components Conference, May 1981, Atlanta, Georgia.

57. Robinson, J., "Finite Element Methods in the Commercial Environment," Volume 1, October 1978, Dorset, England.

58. The Shock and Vibration Information Center, "Shock and Vibration Computer Programs - Reviews and Summaries," SVM-10, 1975.

59. Control Data Corporation Information Bulletin 201113B, "EASE2," January 1977.

60. Information Systems Design Information Bulletin, "Structural Engineering Applications," April 1977.

61. Shipley, J.W., Private Communication, Harris Government Electronic Systems Division, Melbourne, Florida, June 1981.

62. Control Data Corporation Information Bulletin 201807, "STRUDL II," February 1979.

63. Control Data Corporation Information Bulletin 200520G, "NASTRAN," April 1978.

64. The Shock and Vibration Information Center, "An International Survey of Shock and Vibration Technology," March 1979.

65. Fox, H., Private Communication, Control Data Corporation, Miami, Florida, June 1981.

66. Information Systems Design Information Bulletin, "Structural Engineering Applications - MARC," April 1976.

67. Control Data Corporation Information Bulletin 200543F, "MARC-CDC," February 1979.

68. Chang, T.Y., Private Communication, University of Akron, Akron, Ohio, June 1981.

69. Robinson, J., "Finite Element Methods in the Commercial Environment," Volume II, October 1978, Dorset, England.

70. Dodds, R.H., Private Communication, University of Kansas, Lawrence, Kansas, June 1981.

71. Control Data Corporation Information Bulletin 201712A, "ADINA," December 1978.

72. Chang, T.Y. and Padovan, J., "Evaluation of ADINA: Part 1 - Theory and Programming Descriptions," June 1980.

73. Chang, T.Y. and Padovan, J., "Evaluation of ADINA: Part 2 - Operating Characteristics," June 1980.

74. Control Data Corporation Information Bulletin 202448, "ABAQUS," October 1980.

75. Control Data Corporation Information Bulletin 200703E, "ANSYS," April 1979.

76. Engineering Mechanics Research Corporation Information Brochure, "NISA."

77. Control Data Corporation Information Bulletin 100675G, "STARDYNE," April 1979.

78. Fredricksson, W. and Mackerle, J., "Overview and Evaluation of Some Versatile General Prupose Finite Element Computer Programs," October 1978.

79. Systems Architects, Inc., "Evaluation of Finite Element Structural Stress Analysis Packages for Design of Tactical Shelters," September 1981.

80. Lipeles, J.L., Private Communication, International Dynamics Corporation, Casselberry, Florida, February 1982.

81. Belgin, M.F., Mitchell, B.C., and Beatty, V.R., "Microwave Integrated Circuits Procedures Evaluation," RADC-TR-80-201, June 1980.

82. Control Data Corporation, "STARDYNE User Information Manual," April 1980.

83. Control Data Corporation, "ANSYS User Information Manual," November 1978.

84. Control Data Corporation, "ABAQUS User Information Manual."

85. Roark, R.J. and Young, W.C., "Formulas for Stress and Strain," Fifth Edition, McGraw-Hill, 1975.

86. Blevins, R.D., "Formulas for Natural Frequency and Mode Shape," Van Nostrand - Reinhold Company, 1979.

87. Kreith, F., "Principles of Heat Transfer," Third Edition, Harper and Row, Publishers, 1973.

88. Libove, C., "Rectangular Flat-Pack Lids Under External Pressure: Improved Formulas for Screening and Design (Revised)," RADC-TR-79-138, June 1979.

89. Robinson, J., "Understanding Finite Element Stress Analysis," 1981.

90. Robinson, J., "A Simple Temperature Study Using Major Finite Element Systems," June 1981.

91. Steinberg, D.S., "Vibration Analysis for Electronics Equipment," Wiley, 1973.

92. Westinghouse Electric Corporation, "Kovar Handbook-Including Information on 42 and 52 Nickel-Iron and other Hermetic Sealing Alloys".

MISSION
of
Rome Air Development Center

RADC plans and executes research, development, test and selected acquisition programs in support of Command, Control Communications and Intelligence (C^3I) activities. Technical and engineering support within areas of technical competence is provided to ESD Program Offices (POs) and other ESD elements. The principal technical mission areas are communications, electromagnetic guidance and control, surveillance of ground and aerospace objects, intelligence data collection and handling, information system technology, ionospheric propagation, solid state sciences, microwave physics and electronic reliability, maintainability and compatibility.